gear TECHNOLOGY®

MAR/APR 2015

Burning Questions

What Are the Hot Topics in Heat Treating?

How Do You Solve the Forgings Paradox?

PLUS: 3-D Printing is Going to the Final Frontier

www.geartechnology.com

THE JOURNAL OF GEAR MANUFACTURING



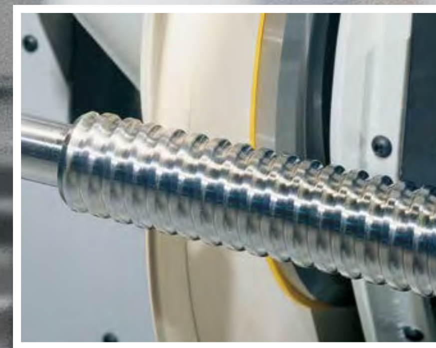
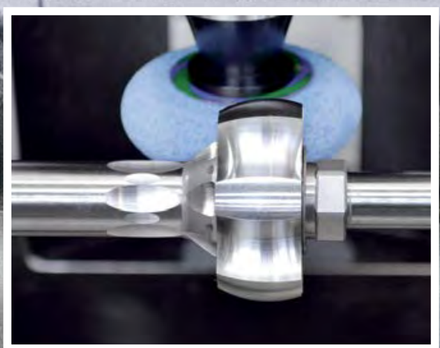
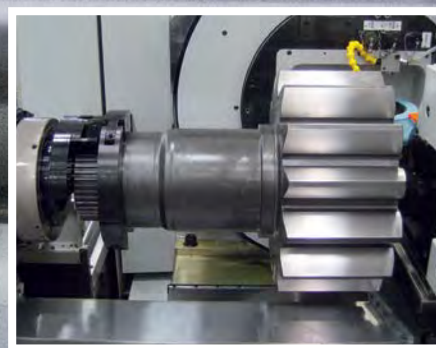


G 500 H
SAMPUTENSILI

gear TECHNOLOGY

MAR/APR 2015

30

features

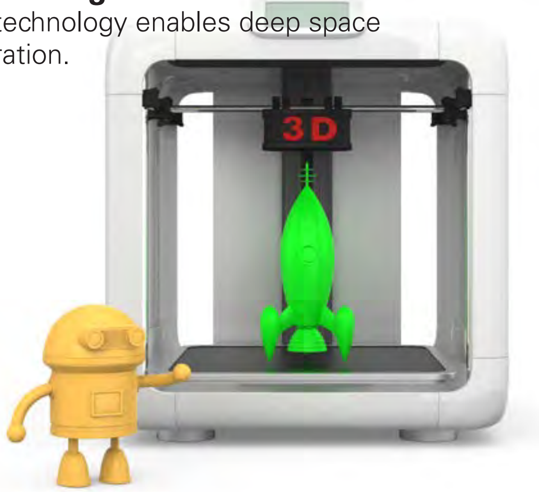

technical

Vol. 32, No. 2 GEAR TECHNOLOGY, The Journal of Gear Manufacturing (ISSN 0743-6858) is published monthly, except in February, April, October and December by Randall Publications LLC, 1840 Jarvis Avenue, Elk Grove Village, IL 60007, (847) 437-6604. Cover price $7.00 U.S. Periodical postage paid at Arlington Heights, IL, and at additional mailing office (USPS No. 749-290). Randall Publications makes every effort to ensure that the processes described in GEAR TECHNOLOGY conform to sound engineering practice. Neither the authors nor the publisher can be held responsible for injuries sustained while following the procedures described. Postmaster: Send address changes to GEAR TECHNOLOGY, The Journal of Gear Manufacturing, 1840 Jarvis Avenue, Elk Grove Village, IL, 60007.

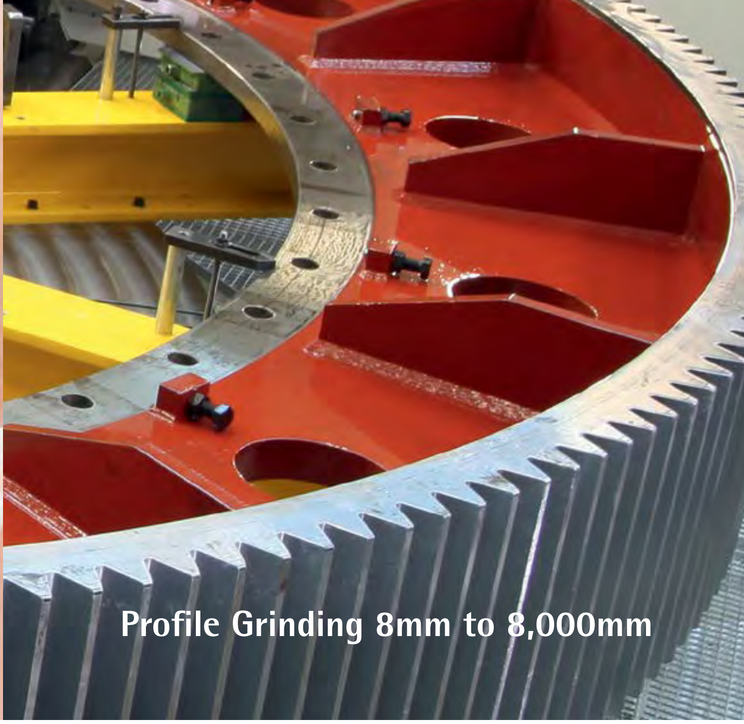

Handling all your grinding needs... the Smallest and the Largest.

KAPP
KX 100 DYNAMIC

A machine so small you could keep it in your garage (really)

NILES ZP 80

A machine so large you could park a Cessna Skyhawk in it. (really)

KAPP Technologies
2870 Wilderness Place Boulder, CO 80301
Phone: (303) 447-1130 Fax: (303) 447-1131

KAPP NILES

www.kapp-niles.com info-usa@kapp-niles.com

gear TECHNOLOGY

Vol. 32, No. 2

departments

Cover photo of gears undergoing case carburizing courtesy of TEAM Industries, Bagley, MN.

THE GEAR INDUSTRY'S INFORMATION SOURCE

www.geartechnology.com

Heat Treat and Induction Hardening of Industrial Gears

Horsburgh & Scott demonstrate the company's large gear and shaft heat treating capabilities in this online video. See how they carburize and induction harden large parts. Visit *www.geartechnology.com* to watch the video.

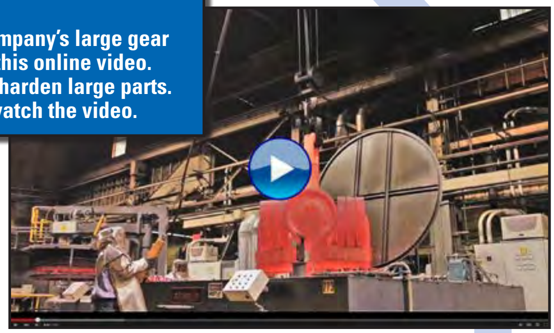

Heat Treating Treasure Trove

Did you know there are hundreds of online articles on gear heat treating at the *Gear Technology* website? Try some of these keywords in our search box to find the ones most relevant to you!

For Related Articles Search

heat treating
carburizing
induction hardening
vacuum treating
quenching

at **www.geartechnology.com**

Gear Milestones Needed

"The American Gear Manufacturers Association (*www.agma.org*) will be celebrating its centennial in 2016. In preparation for the big party, they are developing a timeline of major milestones of our trade, both technical and commercial. They need your help in making sure that the people and events that shaped the business are accurately remembered."

Read more about AGMA's upcoming anniversary and what you can do to help on Chuck Schultz's blog at *www.geartechnology.com/blog*

Buyers Guide: Recently Added

The following companies have recently upgraded to premium listings on *geart-echnology.com*. Now you can find out more about their products, and you can contact them quickly and easily, through the *Gear Technology* Buyers Guide:

American Chemical Technologies, Inc.

ZOLLER expect great measures

ZRIME

WILLMAN INDUSTRIES INC

Stay Connected

Follow us on Twitter
twitter.com/#!/Gear_Technology

Connect with us on LinkedIn
www.linkedin.com/groups/Gear-Technology-Magazine-3893880

Subscribe Online
www.geartechnology.com/subscribe.htm

gear TECHNOLOGY

RANDALL PUBLICATIONS LLC
1840 JARVIS AVENUE
ELK GROVE VILLAGE, IL 60007

(847) 437-6604
FAX: (847) 437-6618

Erosion of Knowledge

Publisher & Editor-in-Chief
Michael Goldstein

Have you ever stood on a beach at the edge of the water and felt the grains of sand dissolve from under your feet as the water recedes? No matter how hard you plant your feet or grip your toes, you can't hold on to the sand. It just flows away right from under you. In many ways that sand is like knowledge and experience of our graying manufacturing workforce. It seems inevitable that much of that knowledge is being washed away.

The reason I'm waxing poetic — and thinking about beaches — is that I had lunch with an old friend the other day. Throughout most of his career (and mine), he's been the chief executive at a major gear manufacturing company. Well respected throughout the industry, he's recognized as a champion of U.S. manufacturing, having worked with industry, academia and government to ensure that America's manufacturing base remains strong — all in addition to running a top-notch manufacturing company.

This man has a passion for manufacturing, for *American* manufacturing, and for American *gear* manufacturing.

Now that he's officially "retired" from the company where he spent most of his career, my friend is moving on to the next phase of his life. Although he's well past the age when most people retire, he's far from being done. Unlike many, who become burned out after spending their careers in a single industry, this man is energized, enthusiastic and hopeful that he can still make a meaningful contribution. I admire him for these qualities and wish our industry had more people like him.

Instead of moving to the South and living on a beach somewhere, he's working hard to develop a new business based on everything he's learned over the years. He's in the process of building a consulting business, one composed of like-minded, well-experienced individuals who share his motivation to help American manufacturing companies compete on a global scale. He's drawing on his many contacts to assemble a team of professionals with a wide variety of talents that complement his own.

My friend doesn't believe that his accumulation of knowledge and many years of experience should just wash away when the tide goes out. Rather, he believes that his expertise should be used to fuel the next generation of manufacturing successes.

I'm not here to endorse my friend's new business, nor to tell you where to seek the manufacturing expertise that will help you succeed. But I *am* here to endorse his attitude, his passion and his commitment to our industry. These are things we could all use a little bit more of.

I don't have to tell you that the gear industry — like most of American manufacturing — is a graying industry. Irreplaceable knowledge and experience disappear every day, as the "old-timers" leave the ranks of our employed. These are people who have already made the thousands of mistakes that rookies to the business are likely to repeat. When these experts leave us, they take with them all of the experience, wisdom and judgment that they've acquired over the years. And if we just let them go, it's gone forever.

When I was much younger, I used to build sandcastles. It was always a challenge to build close to the water. That's where the sand was wettest and best for building. But it's also where your structure was in danger of demolition. So I erected shield walls, built moats and engineered other ways to keep the water from washing away my work.

In many ways, that's what I've been trying to do for nearly 31 years with *Gear Technology* — to build a repository of knowledge that's proof against time, to collect the wisdom and experience of generations of gear manufacturing experts and preserve them for the future. *Gear Technology* is *my* shield wall against the inevitable erosion of information.

Although he's doing so in a different way, my friend is also doing his part to help preserve the knowledge. If you share the same kind of passion for manufacturing that we do, then you should too. Tell us what you're doing to preserve *your* company's expertise for the next generation (*publisher@geartechnology.com*).

Index

WILL DEMONSTRATE MODULAR 8-SPINDLE AUTOMATIC CNCTURNING MACHINE AT PMTS 2015

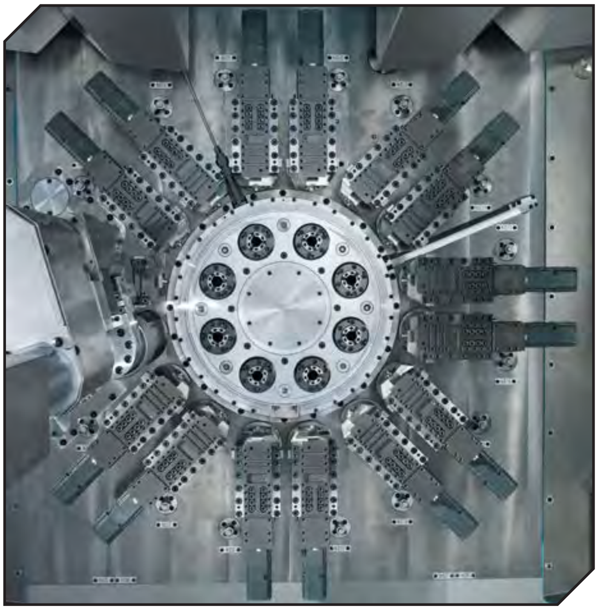

Index will demonstrate its MS22C-8, a modular eight-spindle automatic CNC turning machine, producing brass connector parts at PMTS 2015, Booth 400. The MS22-8 is designed for fast parts machining capability.

The Index MS22C-8 has many applications, from automotive to medical technology. It can be bar-fed or loaded with chucked parts.

The machine can be configured to operate as an 8-spindle machine, a double 4-spindle machine, dropping two complete parts at a time or a machine with double rear-end machining. The MS22C-8 in double 4-spindle mode runs as two machines working with one another simultaneously on a single base. Every second tool station always has simultaneous access to the same tools.

The MS22C-8 can accomplish turning, off-center drilling and thread cutting, inclined and cross-drilling, milling, multi-edge turning, hobbing, tooth milling, deep-hole drilling or slotting. Another benefit for the user is that all standard tool holders and tool holder system interfaces can be used with a range of adapters (Capto, HSK, VDI, INDEX systems).

Each of the eight spindles, arranged in the Index spindle drum, are assigned two cross-slides which can travel on the X-axis as well as the Z-axis. Each cross-slide can be additionally equipped with a Y-axis.

The speed of each of the eight liquid-cooled spindles can be controlled separately. The fluid-cooled spindle drum keeps the thermal growth in the spindle carrier to a minimum. The advantage compared to the previous air-cooling approach is the higher power density in the spindle drum and the capability of energy recovery from the heated cooling fluid. In addition, the spindle bearing temperature can be kept at a low level, which also prolongs its service life and improves thermal stability.

The cross slides with integrated drive have a low-mass design with hydrostatic bearing support. Their low moment of inertia and resulting high dynamics facilitates acceleration in operation.

When operated as an 8-spindle machine, the drum indexing angle from spindle to spindle is 45°; if the machine operates with two times four spindles, the drum indexing angle is 90°.

In double rear-end machining, there are six spindle positions available for front machining the workpiece and two spindle positions for rear end machining, and they all work simultaneously. With this approach, it is possible to machine the rear end of a workpiece during two drum indexing cycles.

After front machining, for which six spindle positions are available, workpieces are picked up by two rear machining units and machined simultaneously on the rear end. Because rear-end machining is done during two drum indexing cycles, up to six tools can be used for this simultaneously with the other spindles.

The advantage of hydrostatic sliding guide in the feed axis (Z) is their damping characteristic that prevents the transfer of the machining vibrations to the adjacent slide via the headstock. This helps to mitigate vibration and rattling while workpieces are being machined — even when the most diverse machining processes are being performed concurrently by the eight spindles.

For example, one spindle can be used for heavy-duty roughing while high-precision finishing takes place on another spindle without sacrificing surface quality. In addition, the hydrostatic bearing is wear-free — there is neither friction nor a stick-slip effect.

The swiveling synchronous spindles are locked into the end positions by three-part Hirth couplings. The high level of stiffness that this achieves also guarantees that even with bar diameters up to 24 mm, rear-end machining operations with very high cutting volumes and simultaneously high machining precision can be performed.

The Hirth coupling also means it is no longer necessary to electronically compensate at the end position. The mechanical lock ensures optimal stiffness and increases the positioning accuracy. This allows even highly complex components to be produced that require complex cut-off side machining. The swivel movement to the rear-end position occurs in less than 0.3 seconds.

The advantage of the front-opening design for the operator is the accessibility during setup and tooling. Moreover, there is the free chip flow down into the chip discharge chute. To save space, the Index engineers placed the control cabinet "on the machine." This principle of integrating the control cabinet into the machine roof has been applied to Index multi-spindle machines for almost 15 years.

Discharging workpieces damage-free from the work area and placed on pallets in the right position for later treatment, the MS22C-8 can include optional handling solutions: machine- integrated handling with external stacking unit that ensures both destruction-free removal of parts from the machine, including measuring operations for the workpieces if needed. Workpiece data can be fed back directly to the machine control so it can automatically correct its machining parameters.

For more information:
Index Corporation
Phone: (317) 770-6300
www.indextraub.com

Northfield Precision Instrument

INTRODUCES EXPANDED COLLET CHUCK

Northfield Precision Instrument Corporation, a designer and manufacturer of precision workholding chucks, recently introduced its newest expanding mandrel collet chuck.

This chuck was custom-designed for a customer to clamp the minor diameter of an internal spline. While clamped, the customer machines the internal counter bore, the outside profile, and the face of the workpiece. The chuck also includes air detect sensor holes, and provides positive air blowout to keep chips and slurry away from clamping and locating surfaces.

Northfield Precision Instrument designs and manufactures air chucks for any lathe, boring machine, grinder or VMC. Models include through-hole, high-speed and quick-change. Chucks are available in SAE or metric, in sizes from 76 mm to 457 mm.

For more information:
Northfield Precision Instrument Corporation,
Phone: (516) 431-1112
www.northfield.com

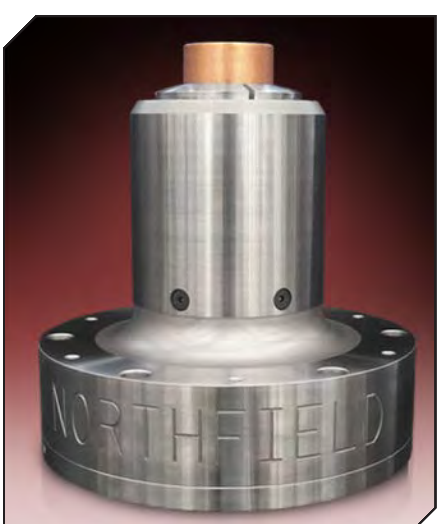

Dillon

NOW OFFERS 1018 STEEL JAWS FROM 1½ TO 10 INCHES TALL

DMI Series H extra-high chuck jaws from Dillon Manufacturing provide extended jaw lengths with heights available to 10-inches tall. The longer lengths can provide greater workpiece stability, plus multiple uses of the blank before it is consumed. The extra length also allows the machinist to avoid additional time and costs associated with the welding and bracing needed to lengthen a standard height top jaw.

Manufactured from 1018 steel, 4140 steel or 6061 aluminum, these extra high jaws are available in all standard chuck mounting styles. DMI Series H, extra high jaws are ideal for precision boring, tapping, drilling and finishing.

With production capabilities to produce large runs of jaws with the same speed and accuracy as small runs, Dillon is qualified to handle any jaw manufacturing request. Their applications department works with customers to modify jaws from an extensive catalog of existing designs, or manufacture custom jaws from supplied customer specs/drawings.

Dillon uses optical checking to check for more than just simple dimensions. Length and width measurements, for example, can be obtained from two separate measurements by using a micrometer. These superficial measurements, however, might not reveal burrs, scratches, indentations or undesirable machined characteristics of a part. Such imperfections are detected on the DMI comparator.

For more information:
Dillon Manufacturing, Inc.
Phone: (800) 428-1133
www.dillonmfg.com

Drake

DELIVERS DRUM GRINDER FOR THE TAPERED ROLLER BEARING INDUSTRY

Drake Manufacturing Services Co., LLC recently delivered a "drum" or "crown" grinder to an Asian manufacturer of tapered roller bearings. The drum is a threaded steel drive roll used in a centerless grinder to move the tapered rollers across the face of the grinding wheel. The rollers start on one end as rough blanks and emerge on the other as round rollers. The drums wear over time so the Drake grinder not only grinds threads on new drive rolls, but also regrinds the threads after they are worn.

This 8-axis precision CNC drum/roll grinder is also called a crown grinder because the outside diameter of the drive roll is actually shaped like a barrel. The B-axis of the Drake machine pivots during the grind to keep the grinding wheel tangent to the radius surface of the roll.

"It was rewarding to see another customer's eyes light up when cycle times on four different drums ground during runoff at Drake were reduced from 4 hours to just 30 minutes," said Stig Mowatt-Larssen, Drake's director of research and development. "Our machine design and hydrostatic spindle combination make aggressive grinding possible — even of hardened D2."

Drake's crown grinder is used by tapered roller bearing manufacturers in the USA and Asia to regrind drums/rolls used in their manufacturing process. The part holding fixture will accommodate most drive, feed, support and back-

Mitsui Seiki

LAUNCHES NEW VERTEX 55X II VERTICAL MACHINING CENTER

Mitsui Seiki recently evolved its "Vertex 550-5X" line of machines with new features and capabilities, and a broader range of options and configurations within the series. The new model series, comprising six distinct models, is now called Vertex 55X II. Linear axes (X, Y, Z) strokes are 550 mm (21.7") × 600 mm (23.6") × 500 mm (19.7").

"One of the key new features is an enhanced ultra-high accuracy package," said Tom Dolan, vice president of sales and marketing. "This option enhances Mitsui Seiki's existing, well-established construction techniques for accuracy and precision. As such, the Vertex line of machines are very well suited for tight-tolerance mold and die work, aerospace, energy, and other high precision component applications. Users can gain significant production improvements eliminating the traditional machine 'warm up' time for very demanding precision jobs."

Mitsui Seiki now offers a new 30,000 rpm spindle with the Vertex 55X II, in addition to the 15,000 and 25,000 rpm choices. Customers can now take advantage of the machine's acceleration and deceleration characteristics and high-speed machining functions. An HSK-80 taper spindle connection (for those requiring more heavy-duty machining) is available as an option to

up rolls used in tapered roller bearing manufacturing including Cincinnati #2 and #3, Koyo, Nissin, Seibu, and others up to 350 mm diameter and 750 mm of thread length. It is capable of producing crowns with radii from 1.9 m to 999 m with lead angles to 5° RH/LH.

For more information:
Drake Manufacturing Services Co., LLC
Phone: (330) 847-7291
www.drakemfg.com

complement the existing HSK-63 and 40-taper tool interfaces.

The Vertex 55X II line includes several configurations in the range, based on table sizes and types from 225 mm (9") to 400 mm (15.7") diameter. A choice of rotary axis drive systems — high-torque geared type or direct drive — allows for the optimum machine configuration to suit the customer needs.

Additionally, the new Vertex is available in the "B"-series version. This is a high-speed 5-axis VMC dedicated to turbine blade production. High-performance coolant and chip handling systems are available to suit customer needs. Automation devices and systems may also be integrated for on-machine inspection and work handling to further reduce setup time, and improve overall quality throughput.

The Vertex 55X II geometric accuracy is monitored in a temperature-controlled factory. The machine features a proprietary cast iron bed, which provides an ultra-rigid and thermally stable machine structure. As will all Mitsui Seiki machines, guide way mounting surfaces are hand-scraped, achieving high volumetric accuracies.

For more information:
Mistui Seiki USA, Inc.
Phone: (201) 337-1300
www.mitsuiseiki.com

Oelheld

CLAIMS DIAMILL HEF 100 IS 'IDEAL ALTERNATIVE TO WATER SOLUBLE COOLING LUBRICANTS'

DiaMill HEF 1100 is a high-performance product based on hydrocrack oils. It has nearly no odor, has high shearing stability, is resistant to aging and is physiologically safe (no aromatic content). DiaMill HEF 1100 does not contain chlorine or any heavy metals.

High-performance additives, in combination with interfacial active substances, allow for high cutting speeds and quality surface finish. Tool life is increased while the formation of a built-up cutting edge is prevented.

DiaMill's low tendency towards vaporization and misting results in a high level of safety during use and also results in high profitability. This product is not aggressive towards varnishes and elastomers. DiaMill HEF 1100 has a high flash point, greater than 302°F (150°C), even with its low viscosity.

DiaMill HEF 1100 is an ideal alternative to water soluble cooling lubricants for turning, milling, drilling, hobbing, and cutting operations in modern CNC-controlled machining centers. DiaMill HEF 1100 is especially designed for use with high alloyed steel, cast iron, or non-ferrous metals.

For more information:
Oelheld U.S., Inc.
Phone: (847) 531-8501 ext. 206
www.oelheld-us.com


HIGHEST QUALITY
LEADER IN GROUND TOOTH SPIRAL BEVEL GEARS
KLINGELNBERG
G 60
OUR BRAND-NEW, STATE-OF-THE-ART FACILITY IS AS9100 CERTIFIED, PRODUCING THE HIGHEST QUALITY SPIRAL BEVEL, HYPOID, SPUR, AND HELICAL GEARS.
OUR CLOSED-LOOP SYSTEM, COUPLED WITH OUR GRIND-FROM-SOLID TECHNOLOGY, ENSURE CONSISTENT QUALITY AND QUICK TURNAROUND.
FASTEST DELIVERY
SPIRAL BEVEL AND HYPOID GEARS FROM DESIGN TO DOORSTEP IN AS LITTLE AS FIVE WEEKS.
RAVE GEARS AND MACHINING
TALENT AND TECHNOLOGY DRIVEN
+1 855 RAV GEAR
sales@ravegears.com
WWW.RAVEGEARS.COM
425 STREMPEL ST., SEGUIN, TX 78155

German Machine Tools of America

RELEASES THE PRÄWEMA SYNCHROFINE 205 HS

Now available from German Machine Tools of America (GMTA), the Präwema SynchroFine 205 HS gear honing machine features direct-driven, digitally controlled spindles for the tool and the workpiece, enabling precise, rigid synchronization. The Präwema Honing gear finishing process produces quality comparable to grinding results for spur and helical gears, as well as shafts. The machine's software checks the stock allowance and workpiece runout and then optimizes the X-axis approach distance.

Measuring the workpiece does not affect the cycle time and the process can reduce cycle times by 3 to 5 seconds.

The machine features a pick-up design to enable automation. The workpieces and dressing tools are loaded and unloaded by the workpiece spindle. The large X-axis travel enables placement of additional stations adjacent to the loading/unloading station inside the machine, such as a two-flank roll-checking device. External robots and conveyor systems can also be integrated by GMTA engineering.

The honing machine is constructed on a natural granite bed to promote stability and control thermal fluctuations. The X and Z axes are equipped with linear motor drives. The cutting tool is clamped with a hydraulically operated system and the tool spindle can be swiveled into a vertical position, enabling easy access. Additional options are available for machining oversized drive shafts as long as 850 mm and the Präwema SynchroFine 205 HS-D model, equipped with two spindles, is offered for further reduction of cycle times.

For more information:
German Machine Tools of America
Phone: (734) 973-7800
www.gmtamerica.com

GWJ Technology

LAUNCHES NEW VERSION OF SYSTEM CALCULATION FOR GEARBOXES

GWJ Technology GmbH recently launched a new version of its system calculation for gearboxes. SystemManager enables the user to determine complete systems and is a system add-on to GWJ´s software applications eAssistant and TBK2014.

SystemManager supports axially parallel shaft systems for multistage cylindrical gears with or without power split transmission, manual gearboxes, planetary gear trains as well as perpendicular transmission systems.

The progress of the nominal tooth force along the facewidth has already been calculated and displayed graphically for single tooth meshes of gear pairs within the system. This load distribution along the facewidth will be considered in the calculation of the load capacity by means of the face coefficient Khß. It is possible now to consider flank line corrections such as lead crowning, end relief or helix angle corrections in the calculation of the load distribution along the facewidth. Different modifications for the respective gear mesh can be easily checked and graphically displayed. It makes it very easy to find an optimal correction. The new version includes bevel gear stages with shaft angle unequal 90°.

In addition, new force elements for worms and worm wheels were added and the new calculation module for worms was connected to SystemManager. A whole series of additional innovations are also featured in this new version.

For more information:

GWJ Technology GmbH
Phone: +49 (0) 531 · 129 399-0
www.gwj.de

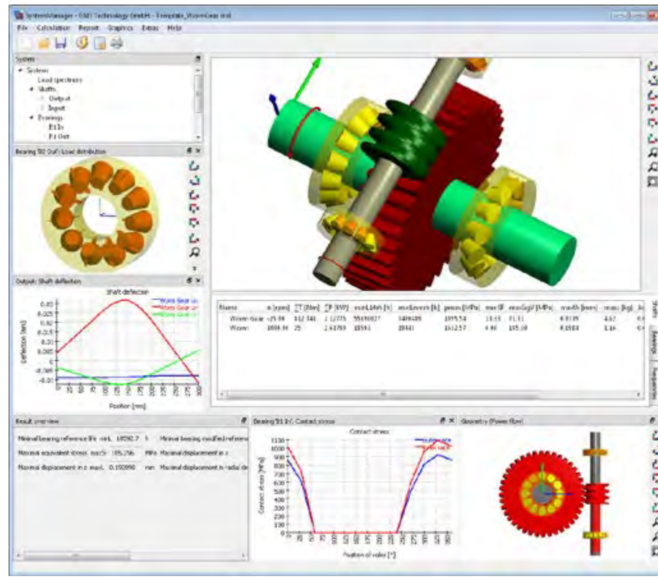

Mahr Federal

ADDS SELECTABLE RESOLUTION TO MARCATOR 1086 & 1087 DIGITAL INDICATORS

Mahr Federal recently added a selectable resolution option to MarCator 1086 and 1087 digital indicators. These digital indicators provide easier operation, a large display and a built-in wireless system for simple transmission of measurements.

The new resolution option offers five different resolutions, ranging from 0.00002" to 0.0005" (0.0005 - 0.01 mm). MarCator digital indicators with the selectable option include the 1086 R with large display, the 1086 WR large display/Wetproof IP 54, and the 1087 R and BR with analog/digital display and dynamics. These indicators are also available in the Ri integrated wireless version. Additionally, the MarCator 1086 and 1087 digital indicator line is available with 8 mm (3/8") mounting stems and a full range of backs for mounting into existing gages.

Using the selectable resolution option with Ri indicators provides a way of creating a wireless data collection package. With an i-stick USB receiver and MarCom software, users can record data from work pieces that have varying tolerances. Integrated wireless digital indicators are the most economical way to update an existing bench or hand gage for data collection. It involves no change in the operator's way of measuring parts, but allows those measurements to be documented and used for process and quality decisions.

To switch the indicator's resolution, enter the main menu of the indicator and scroll over to the "resolution display," which is typically defaulted to 0.0001" (0.002 mm). From there, users can use the up arrow option to choose the appropriate resolution to accommodate varying gaging applications.

For more information:
Mahr Federal Inc.
Phone: (401) 784-3100
www.mahr.com

Sunnen

INTRODUCES SSH-1680 HONING SYSTEM

Sunnen's new SSH-1680 honing system features zero shutoff for automatic cycle control and consistent bore size, finish and geometry with minimal operator attention. Rough-and-finish honing capability eliminates preliminary reaming, boring and grinding operations to help lower per-part costs.

The SSH-1680 makes quick work of parts with keyways, splines and blind bores. An adjustable spindle allows the operator to eliminate mandrel runout, making it easier to achieve precision bore geometry. Multiple land and tandem bores are bridged with Sunnen's long stones, maintaining alignment and consistent size without camber or washout.

"This machine is designed for small shops looking for a cost-effective way to streamline processes and increase the consistency of bore sizing operations," said Phil Hanna, product manager of machines/gages. "It is a 'hone-of-all-trades' and delivers a high ROI through increased productivity and part quality."

The SSH-1680 provides fast, clean cuts in a wide variety of materials, and handles part lengths up to 250 mm with bore diameters from 3-60 mm.

"Diameters 40 mm and smaller are a particular 'sweet spot' for this machine, when compared to ID grinders," Hanna said.

A rigid cast iron machine base provides strength for handling heavy parts and isolates moving components to eliminate vibration problems. The machine's design enables rapid stroking for shorter cycle times. Incrementally adjustable stroke rate (80-310 SPM) and spindle speed (250-2500 RPM) deliver fast stock removal rates. The spindle and stroker are both powered by variable frequency drives, eliminating drive belt changes and allowing dial-adjustment of speeds via the convenient swiveling control panel.

The SSH-1680 accepts all standard Sunnen tooling, including K, P20 and P28 mandrels. A universal honing fixture is standard, with a variety of workholding options available to securely fixture odd shapes and thin walled parts without distortion.

All electrical components are housed in an interlocked, side-mounted enclosure. Standard equipment includes a universal honing fixture, parts tray, spindle runout indicator, side splash guards, and detachable 25-gallon (96-litre) coolant cart, which is mounted on casters for easy filling and maintenance.

For more information:
Sunnen
Phone: (314) 781-2100
www.sunnen.com

Reishauer

NOW OFFERS IN-HOUSE PRODUCED CLAMPING FIXTURES

Reishauer recently introduced a new generation of grinding machines that produce at cycle times below 10 seconds for automotive planetary gears. Because of this, clamping times had to be reduced to match the machine capability. Additionally, change-over accuracies of less than 0.003 mm deviation have to be held over long-term production cycles. In order to maintain such low cycle times, Reishauer began to manufacture its own clamping fixtures in 2010.

Reishauer uses resistant steel that reduces the wear in the clamping area, increases the service life of the clamping fixture and, as a consequence, lowers the costs per workpiece.

Correct wall thickness, clamping pressure and piston diameter have a fundamental influence on the clamping process. These factors have to be analyzed and correctly matched to the specific gear part to be ground.

With the in-house fixture production, Reishauer now offers customers a single point of contact for all issues relating to the gear grinding process. Close cooperation between the different specialist departments ensures that the requirements of the machine tool, the tooling and clamping fixture are coordinated correctly.

Reishauer engineers establish the clamping clearance between the workpiece and the clamping tool diameter to suit the requirements of specific grinding tasks, be it for automatic loading in high volume production or for manual loading of smaller batch sizes. The choice of clamping system depends on manufacturing volume and desired flexibility.

The DH30 one-piece design, for example, is the most rigid option as it is fixed directly on the C-axis workpiece spindle. The modular system DH16 for medium-sized batches provides more flexibility combined with a robust design. This type of self-centering clamping fixture is mounted on a base unit, which in turn, is bolted directly on the workpiece spindle drive.

In the case of very small lot sizes, short set-up times are important. For this purpose, the quick-change system DH19 is best suited.

For more information:
Reishauer AG
Phone: +41 44 832 22 11
www.reishauer.com


GoldENgineering
Gear Up with Ingersoll!
Your most experienced source in the design & manufacture of ICI gear machining tools
Gear Shapers
• Roughing at three to four times faster than conventional methods
Gear Gashers
• Custom indexable roughing & finishing cutters
• Designed to your specific tooth profile
Hobbing Cutters
• Segmented designs with angled screw holes for simple, accurate indexing
• Single, double and even triple-start designs
Member IMC Group
Ingersoll
Cutting Tools
845 South Lyford Rd · Rockford, IL 61108-2749 · 866/690-1859 · Fax: 815/387-6968 · www.ingersoll-imc.com

Things are HEATING UP in 2015

In this special section, our editors have gathered recent news and information related to the heat treatment of gears. Here you'll find a comprehensive assortment of news and upcoming events that will help you understand the various heat treatment processes available for gears and choose the best option for your projects, whether you heat treat in-house or send your gears to a commercial heat treating provider.

HEAT TREATING EVENTS

Ipsen Offers Comprehensive Heat Treatment Course

Ipsen recently held its first Ipsen U class of 2015. The three-day course gives attendees a broad overview of furnace equipment, processes and maintenance. The course provides a hands-on approach to learning while receiving qualified tips and knowledge directly from the experts.

Participants in the February 2015 Ipsen U course came from across the country, including Colorado, Illinois, Michigan, Pennsylvania and Texas. Reflecting on the class, attendees found that it offered a "comprehensive overview of the general construction and mechanics of the furnace," as well as an in-depth look at "the furnace's hot zone and areas to focus on for preventive maintenance."

Throughout the course, attendees were able to:

- Learn about an extensive range of topics – from an introduction to vacuum furnaces and heat treating to furnace subsystems, maintenance and more
- View the different furnace components firsthand while learning how they affect other parts of the furnace and/or specific processes
- Take part in one-on-one discussions with Ipsen experts
- Participate in a leak detection demonstration
- Tour Ipsen's facility

Upcoming Ipsen U courses are scheduled for June 2-4, August 4-6 or October 6-8. Learn more at *IpsenUSA.com/IpsenU*.

ASM Introduction to Heat Treating

This course is designed as a basic introduction to the fundamentals of steel heat treatment and metallurgical processing. It is intended for technicians, sales professionals and managers who are new to heat treating or who need a state-of-the-art update.

Attendees will learn about time-temperature transformation diagrams and the relationships between phase transformations and microstructure. They will also learn to predict the mechanical properties and microstructures that result from heat treatment. The course covers general aspects of heat treatment, steel mechanical properties, microstructure, austenite and its transformation, the classification of steels, and various specific types of heat treatment processes, including annealing, normalizing, hardening, tempering and heat treatment of tool steels.

The course is taught by Jon L. Dossett, P.E., a process metallurgist and materials engineer with more than 42 years' experience in practical induction heat treating and who is an expert in thermal processing and other heat treatments.

The next course takes place June 15-17 at the ASM headquarters in Materials Park, OH. The cost is $1,391 for non-members and $1,228 for ASM members. For more information, visit *www.asminternational.org/learning/courses/classroom*.

HTS
Heat Treating Society
ASM INTERNATIONAL

Wall Colmonoy Modern Furnace Brazing School

This hands-on brazing seminar preserves the tradition originated by the late Robert Peaslee, a brazing pioneer who invented the first nickel-based brazing filler metal.

Engineers, technicians, quality managers, production managers, and others will participate in "hands-on" practical applications while learning about brazing technology from leading brazing engineers.

This three-day seminar offers knowledge and practical application on brazing design, metallurgical aspects of brazing operations, brazing equipment, brazing material selection and applications and quality control.

Unlike other *classroom-only* seminars, Brazing School attendees will tour the facility and see the actual brazing application on the shop floor. They will also have the opportunity to apply different forms of filler metal to supplied samples, have them vacuum brazed and discuss the outcomes.

The spring session of Wall Colmonoy's Modern Furnace Brazing School takes place May 5-7, 2015 at Wall Colmonoy Aerobraze in Cincinnati, Ohio. Cost is $1,950. For seminar details and registration information, contact Jim Nicoll, Marketing Associate, at *brazingschool@wallcolmonoy.com* or 248.585.6400, ext. 233.

The Bright World of Metals 2015

The Bright World of Metals, which takes place June 16-20 in Düsseldorf, Germany, consists of four related technology trade fairs. GIFA is the international trade fair for foundry machinery, castings and foundry technology. METEC is the international trade fair for metallurgy, steel casting and steel production. THERMPROCESS is the international trade fair for thermoprocess technology and heat engineering. And NEWCAST is the international trade fair for precision castings.

For more information, visit *www.thermprocess-online.com*

COMINGS AND GOINGS

Jason Ackerman Named COO of Seco/Warwick

Jason Ackerman has joined SECO/WARWICK Corp. as Chief Operating Officer at the Meadville, Pennsylvania engineering and manufacturing facility. As COO, Ackerman is responsible for the company's day-to-day operating activities, including project management, purchasing, quality, construction, and manufacturing operations for North America.

Ackerman previously spent 11 years with GE Transportation, serving in a variety of roles of progressing responsibility including Purchasing Manager, Master Black Belt of Lean Six Sigma, and Plant Manager. He graduated from Penn State University with a degree in Industrial Engineering and an MBA.

Ipsen Announces New VP of Sales, Patrick McKenna

Ipsen USA announced **Patrick McKenna** as Vice President of Sales. He has replaced Art Tsubaki, who is now Managing Director of Ipsen Japan. Reporting to Geoffrey Somary, CEO of Ipsen USA and COO of Ipsen Group, McKenna is responsible for all new equipment and aftermarket sales. He is also a member of the Ipsen USA Executive Team and the global Ipsen Group Management Committee.

McKenna earned his bachelor's degree in mechanical engineering (BSME) from the University of Illinois at Chicago and a master's degree in manufacturing engineering (MME) from Northwestern University. Previously, McKenna was Vice President of Nevada Heat Treating, Inc. (including California Brazing), which specializes in the heat treating and brazing of critical components found at the heart of complex machines. As an active member of the company's board of directors since 2002, McKenna was instrumental in their growth, helping the company increase revenues more than 15x.

McKenna has also served on the Metal Treating Institute (MTI) Board of Trustees since 2006 and has held the following positions: President Elect (2015), Treasurer (2014) and Membership Committee Chairperson (2008-2014). In addition, he was selected to serve on the MTI Furnaces North America Technical Program Committee in 2008 and 2010, during which he was chosen both years to be a moderator for their technical sessions. McKenna has received several awards from the MTI, including the President's Award (2014) and the Heat Treater of the Year/Master Craftsman award (2011).

Eric Buchanan Joins J.L. Becker as Sales Engineer

J.L. Becker Company has announced the hiring of Eric Buchanan for the position of Sales Engineer. Prior to joining J.L. Becker, Eric gained industry experience working with OEM automotive companies and its suppliers, in both account and quality management roles. He has managed large-scale projects from initial request through launch and serviced both international and domestic accounts.

Buchanan attended Schoolcraft College in Livonia, Michigan, earning multiple degrees along with concentrated coursework in the Applied Sciences of Metallurgy and Material Sciences. He has successfully completed Six Sigma Green Belt Training and Karrass Development Courses.

PRODUCTS

Grieve Introduces Ovens for Preheating Gears, Job Shop Operations

Grieve Corporation introduces No. 815, a 500°F electric rotary hearth oven, currently in use for preheating gears at a customer's facility.

Workspace dimensions inside this unit measure 76" wide × 76" deep × 24" high. A 72" diameter rotary hearth is constructed from angle rings with 90 1⅜" wide × 7⅜" long × 3⅝" high slots to hold the workpieces on edge while processing. The hearth is driven by a ¼ HP motor through a gear reducer with torque limiting device. The hearth indexes one position each time the loading door is opened and closed.

Two 2,000 CFM, 2 HP recirculating blowers provide a vertical downward airflow over the workload. Special safe-

ty equipment for handling flammable solvents is featured on this Grieve rotary hearth oven, including a manual reset excess temperature controller, separate heating element control contactors, a 325 CFM powered exhauster, and a purge timer.

No. 815 features an aluminized steel interior and exterior, plus 4" insulated oven walls. The unit was entirely designed, engineered, built and full tested by Grieve.

The No. 979 is a 850°F (454°C), electrically-heated, universal style oven from Grieve, currently used for various machine shop heat treating operations at the customer's facility. Workspace dimensions of this oven measure 36" W × 36" D × 36" H in each of the two compartments. 24 kW (12kW per zone) are installed in Incoloy-sheathed tubular elements to heat the dual oven chambers, while a 600 CFM, ½-HP recirculating blower provides front-to-back universal airflow to the workload in each compartment.

This Grieve universal oven features 6" insulated walls, aluminized steel exterior with enamel finish, Type 304 stainless steel interior, double doors, three roller shelves rated for 200 lb. loading, five nickel plated, 100 lb. capacity shelves in the top chamber, three nickel plated, 100 lb. capacity shelves in the bottom chamber and an integral leg stand.

No. 979 controls include a digital indicating temperature controller for each compartment, recirculating blower airflow safety switches, a 10" diameter circular chart recorder for each compartment to record part temperature and manual reset excess temperature controllers with separate contactors.

For more information:
The Grieve Corporation
500 Hart Road
Round Lake, IL 60073-2898
Phone: (847) 546-8225
Fax: (847) 546-9210
sales@grievecorp.com
www.grievecorp.com

OTHER NEWS

Solar Manufacturing to Provide Large Horizontal Vacuum Furnace to California Affiliate

In order to accommodate its increasing vacuum processing requirements, Solar Atmospheres of Fontana, California recently placed an order with affiliate Solar Manufacturing to supply a large capacity horizontal vacuum heat treating and brazing furnace. This Solar Manufacturing Model HFL-84144-2EQ has a work zone that measures 54" (1371 mm) high × 54" (1372 mm) wide × 144" (3658 mm) deep and is capable of pro-

cessing a work load of 30,000 pounds at 2200°F. It is expected that this furnace will increase plant processing capacity by more than 25%.

This furnace is being designed to not only satisfy the normal daily processing requirements, but to also handle larger loads at higher processing temperatures. The furnace will have an operating temperature of up to 2650°F and will be capable of achieving high vacuum. Temperature uniformity will be ±10°F (5°C) between 900°F (482°C) and 2200°F (1204°C).

For more information:
Solar Manufacturing
(267) 384-5040
pkr@solarmfg.com
www.solarmfg.com

Automotive Supplier Invests In New AFC-Holcroft Pusher Equipment

A leading global automotive supplier has placed an order with AFC-Holcroft for a rebuild/retrofit of an existing Pusher Furnace line, along with contract additions for companion ancillary equipment, as part of a multi-phase project.

The first phase rebuild/retrofit portion involves restoration of an existing 3-Row pusher furnace line including: pusher furnace with quench, post washer, temper furnace, and transfers/conveyors, electrical control panels, and flowmeter panels. As part of the order, the existing equipment will receive a number of modifications and upgrades to meet current industrial, safety and supplier standards.

The equipment for rebuild/retrofit is already in storage at AFC-Holcroft's build partner, MATTSA, in San Luis Potosi, Mexico. MATTSA will rebuild/retrofit the existing pusher furnace line and provide the new companion ancillary equipment. Once completed, each piece will be cold-tested and shipped to the supplier's plant for installation, start-up, commissioning and formal operator training by MATTSA and AFC-Holcroft. Completion of the first phase is expected in 2015.

For Related Articles Search
heat treating
at www.geartechnology.com

Solving the Forgings Paradox

Why forging technology is changing while also staying exactly the same

Erik Schmidt, Assistant Editor

The process of forging metal into shapes possesses a surprisingly long and storied history.

For example, the method of hot rolling can trace its protracted existence all the way back to an enigmatic Italian polymath named Leonardo da Vinci (you may have heard of him), who reportedly invented the rolling mill one lazy day in the 1400s.

And in the centuries that followed the glory days of the Renaissance — when the idea of a rolling mill sprung from da Vinci's head among other scattered works of genius like armored vehicles, flying machines and the *Mona Lisa* (you may have heard of it) — the method used to roll metal has…stayed almost exactly the same.

"The process has remained mostly unchanged for about 250 years," says Wil Kantus, vice president of operations at Ajax Rolled Rings (York, SC).

Well, then.

Apparently, there's nothing to see here. Move along. Run home to your history books, flip to Chapter One and read of the brawny early humans who would wallop an anvil with a hammer to force pieces of iron to bend against their will — that right there was the pinnacle of forging technology.

Period. Case closed. The end.

Or is it?

See, the inherent problem with finding innovations in the forging process lies in its simplicity.

Metalworking, in some rudimentary form or another, has been around almost as long as humans have stood upright. So here's a question for the anthropologists out there:

When was the last major breakthrough in bipedal movement? How about eating? Sleeping? Breathing?

That's the rub. Producing forgings is a vital procedure in the industrial word, no doubt — but it's also a fairly barebones operation.

Not a whole lot of room for growth, right?

Bud Kinney says not so fast.

"There have been recent innovations," says Kinney, vice president of sales of the IMT Forge Group. "We are actively pursuing new innovations which would include merging forging and heat treating that would produce material properties that cannot be achieved any other way. That's our goal. We are really trying to be on the cutting edge."

"I'm sure [Kantus] is right, and I'm also sure that I'm right. Both statements are true."

Now, if you feel like you just fell down a flight of steps built by M.C. Escher, it's just because what Kinney said is pure paradox. It's simply not possible for forging to be *progressing* while at the same time *not changing*.

Kinney says it is. Kantus says it's not. Who should you believe?

Both.

Photos on Pages 30-31 courtesy of Clifford-Jacobs Forging

A Heated Debate

To even begin to dissect this paradoxical problem, it would be of great use to first understand the basics.

Here's a quick crash course:

"[Most closed die] forgings are used for medium to high-volume production. The [forged] form is made as close as possible to the finish contour of the part to reduce machining time and to keep the amount of wasted material low. Forging tolerances are [commonly] held within ±0.030" (0.8 mm) and machining stock allowance is in the range of 0.080 to 0.120 per side. The surface finish of forged surfaces [for steel parts] is around 500 micro-inches.

"The advantages of forgings include: [shortened] machining times, as the raw material is shaped close to the final contour of the part and excess material can usually be removed in a single [operation], thus less machining and nonfunctional surfaces do not require machining."

That's per gear blanking expert Robert Endoy — it's accurate, informative and completely up-to-date.

And it was published in an issue of *Gear Technology* in 1992.

Seems impossible that almost 25 years have gone by and key data remains totally untouched, but here we are. Of course, none of this is to say staying the course is a *bad* thing. Some great things remain steadfast and constant through the years, stubbornly defiant in the face of Father Time himself.

There can be elegance in simplicity, after all. And, by most accounts, creating forgings is just that.

"The process looks very simple," Kantus said of Ajax's method of making rolled rings. "We start out with bar material and we cut it to a weight, and then we forge it into a pre-form so it looks like a donut. That then goes on a rolling mill where you can roll it out to the required dimensions. Then most of them go to heat treat and then machining.

Shawn O'Brien, vice president of sales and marketing at McInnes Rolled Rings (Erie, PA) also peppered the word "simple" into his explanation of McInnes' forging process.

"We keep our process simple by focusing exclusively on seamless rolled ring forgings with rectangular cross sections," O'Brien says. "We have three distinct ring manufacturing areas.

Each area has dedicated furnaces, blanking presses and material handling equipment located and optimally sized to provide the mills with hot metal in the most efficient manner possible."

Rolled rings, which both Ajax and McInnes specialize in, are a unique type of forging that offer a distinct set of pros and cons when compared to products made from die forging, the process that Clifford-Jacobs uses.

"The geometry of the gear or bearing typically dictates which forging method is best," O'Brien says. "Open die forging covers the broadest size range but typically requires most gross input weight and processing time. Impression die methods are best suited for high volume, near net shape orders that will likely repeat. However, the initial time and expense of creating dies make this a cost prohibitive method for low volume, short lived programs."

Clifford-Jacobs Forging (Champaign, IL), a company owned by IMT that produces steel forgings for the mining, gear, aerospace, energy, and defense industries, normally makes its forgings from special bar-quality steel. As steel bars are rolled, the grain structure within the steel is forced to flow along the centerline of the bar. When a standard or custom forging is produced from the bar, this inherent grain flow bends to follow the contour of the forged shape.

"In some cases, we actually use pre-forms," Kinney says. "We produce more near net products than, in most cases, a rolled ring could produce. We actually could use a rolled ring as a preform for what we do. That's really what, in a sense, differentiates us. [IMT] has a lot of companies, but Clifford-Jacobs is probably our premier company on the gear side."

O'Brien adds:

"For gears or bearings with a basic OD × ID × height geometry, seamless rolled rings provide the best of all forging options," he says. "There are a wide variety of ring mills in terms of size and control technology. The latest in ring rolling technology enables quick set-up times, minimal stock allowances and size consistency from ring to ring."

Photos on Pages 32-34 courtesy of McInnes Rolled Rings.

So, as O'Brien clearly states, the process for making forgings hasn't changed in — wait what?

The latest in ring rolling technology.

Somewhere at Château d'Amboise da Vinci is rolling over in his grave.

Forging Ahead

To truly understand the forgings paradox you must first realize that preservation and change aren't always mutually exclusive.

It is possible, for instance, to make alterations to a car without completely transforming the car into an entirely new entity (though detractors of the "Ship of Theseus" thought experiment would argue differently, but that's a paradox for a different day).

Such is the case with creating forgings — the process is fundamentally the same, there have just been a few recent upgrades.

"While forging as a process remains quite similar to what was done generations ago, the application of engineered innovations such as direct-from-forge-heat-treating makes it considerably more efficient and effective today," Kinney says.

Forgers and ring rollers aren't trying to reinvent the wheel, so to speak. They're simply trying to make the wheel easier to produce and easier to use.

"There have been a lot of innovations in the press and forging market to use modeling and simulation to give you better results," Kinney says. "We're really immersed in that process — giving you a better idea of the grain flow and what the final near net part is going to look like.

"Specific to Clifford-Jacobs, we are also involved in development work with SCRA (South Carolina Research Authority) to produce what we call direct forge intensively quenched parts that we believe will be a game-changing approach to the forging and heat treating process. It's a development project that's underway, but our goal is to better integrate forging and heat treating to produce superior parts. We're really excited about that."

For companies that specialize in rolled rings, like McInnes and Ajax, innovation has come in the form of newer machinery and more advanced, intuitive software.

"It's like comparing a car being manufactured a decade ago to now," O'Brien says. "You didn't have XM Radio but you had radio — is it really different if the music is still coming out?

"A lot of the difference is user interface and how much more you're able to rely on technology. That's not to say the operator's experience isn't valuable, but if you combine an experienced operator with the newest technology, then the horsepower behind it is that much greater.

"The hydraulics, the frame upon which they sit, the method of forging, that all remains the same. It's kind of the 'sheet music' that's different—the software, the computerized rolling methods, et cetera. The newer the machine the latest you have in terms of that.

"Newer is better in terms of control, user interface and maintenance diagnostics."

For gear manufacturers, the main cause for concern isn't necessarily how easy it is to make the forgings—nor should it be—but in the quality of the forgings once they're made.

And the good news for buyers of forgings and rolled rings is that besides being more quickly and efficiently made than ever before from a supplier's perspective, they're also produced at a higher quality, and more consistently so.

"The percentage of rings that are within your nominal size range are going to be better over time," O'Brien says. "If it's a manual controlled mill, you're going to have inconsistencies from piece to piece. Within a single job, a computer controlled mill is going to be putting out the same piece consistently.

"I think [the difference is] repeatability, consistency, and you're going have tighter tolerances and less allowance."

And with that, the paradox that began tangentially with da Vinci hundreds of years ago becomes less of a riddle and more of minor problem solved by good old fashioned persistence and ingenuity.

Now if we can just get da Vinci to tell us where that darn Holy Grail is.

For more information:

Ajax Rolled Rings
Phone: (803) 684-3133
www.ajaxring.com

McInnes Rolled Rings
Phone: (814) 459-4495
www.mcinnesrolledrings.com

Clifford-Jacobs Forging
Phone: (217) 352-5172
www.clifford-jacobs.com

For Related Articles Search forging at www.geartechnology.com

3-D Printing: We Ain't Seen Nothing Yet

Jack McGuinn, Senior Editor

A long time ago, in a galaxy far, far away—otherwise known as The '50s—3-D was shorthand for a new motion picture technology designed to get the public back in the movie theaters and away from their TVs.

Especially in the Westerns genre (extremely popular then), moviegoers were presented scene upon scene filled with spears, arrows, fists, chairs—or whatever was handy—seemingly flying off the screen and headed straight for them and their seatmates. But the public was underwhelmed by the new "technology" and 3-D-filmed movies were soon merely considered a quaint, less-than-awe-inspiring exercise in ho-hum.

Today, aside from a much improved 3-D technology that we can experience on our home flat screens and at the local IMAX, we now have 3-D *printing*—AKA additive manufacturing. But what's even more awesome—NASA is now 3-D-printing spare parts up at the ISS (International Space Station). And in *zero-gravity* environments. And some of these parts are small gears and actuators, *for starters*. Every indication is that the list of power transmission-type parts to be converted will soon grow.

"We have technically already printed a gear. The ratcheting wrench part, which is still the last thing we printed, contained a gear mechanism within its body," said Brad Kohlenberg, Made In Space business development engineer, adding, "We can also print mechanical actuators." Made In Space is a California start-up that has also partnered with NASA on a "recycler" project that will turn trash aboard the orbiting lab into 3-D-printed objects. That reportedly will happen by next year, if not sooner. Made In Space supplies 3-D printers and technical support.

But unknowns remain. The parts printed in the zero-gravity space environment will be brought back for comparison testing—especially materials—with parts printed when the printer was earthbound. These findings should shed some further light on other potential gear, bearing, actuator, pump—who knows?—applications that are candidates for in-space environments.

ISS commander Butch Wilmore displays a working socket wrench—with ratchet action capability—that was printed using digital plans emailed to the station by NASA Mission Control (Photo courtesy of NASA).

What remains unknown, according to Made In Space, is the why behind the observed "minor differences" between made-in-space parts and parts printed on the same printer on Earth. To sort that out, "all of the parts printed as part of this initial technology demonstration will be brought back to Earth for tests conducted by the NASA Marshall Space Flight Center. These tests include the use of high-power microscopes and destructively flexing, pulling, twisting, and compressing some of the objects in controlled ways to determine standard material properties. The data that NASA generates from these tests will likely aid in the design of future materials and future commercial devices going to space."

OK—they're not printing complex bevel gear sets at the ISS yet. But does anyone doubt where this is going? Does anyone yet know how far this technology can take us? Or NASA?

Using the glass-half-full/half-empty analogy, Kohlenberg says that "If you mean half-full or half-empty in an optimism vs. pessimism way, we are just scratching the surface here. This technology will completely change how we plan space missions forever. The glass is very much half-full in that regard. If you mean how full is the glass in terms of progress, I think that depends on what your end-point is, or what your optimal 'full-glass' is filled with. Our goal is to create the technologies that will enable our species to become multi-planetary. To that end, off-world manufacturing is a crucial technology for us and we are still very much in the nascent stages of its development."

Indeed, it was just last year, as reported at *NASA.gov*, "A 3-D printer, designed and built by (Made In Space), created an extruder plate—a piece of itself—on Nov. 24, 2014—an hour-long process. The milestone marks a key step toward a future in which voyaging spaceships print out their own spare parts on the go and colonists on other worlds make what

they need from the dirt beneath their boots."

The extruder plate — measuring approx. 3 inches long by 1.5 inches wide by 0.25 inches thick (7.6 by 3.8 by 0.6 centimeters) — displays the logos of both Made In Space and NASA. Said Made In Space CEO Aaron Kemmer, "This is the first object truly manufactured off of planet Earth. It's a huge milestone, not only for Made In Space and NASA, but for humanity as a whole." Choosing the plate, which holds in the printer's electronic board and wiring, for the first part has symbolic significance for Kemmer. "It represents the idea that if something goes wrong on the space station, or future space stations, the crew and NASA now have the ability to build a solution."

For the uninitiated, 3-D print technology enables the design and production of parts (gears, bearings, couplings), modules, etc., from a "blank page" by pancaking thin layers of extruded materials on top of each other — as specified by blueprints via computer display. Acknowledged advantages thus far for this nascent yet already somewhat ubiquitous technology include faster production, increased flexibility, i.e. — the ability to create components in shapes impossible to accomplish through standard methods — and, one of 3-D printing's most attractive capabilities for any cost-sensitive process — rapid prototyping of complex, expensive parts (tools, gears, etc.) — in *minutes*, not days or weeks.

But 3-D printers in space stations, spitting out replacement parts — *that* gets the mind racing. The technology is already being heralded by NASA as a means to further develop space exploration in that no longer will astronauts manning space installations need to wait (months) for, say, a new actuator or bearing replacement part before continuing their work.

Made In Space CEO Aaron Kemmer stares through the windows of the Microgravity Science Glovebox with the Zero-G 3D Printer enclosed (Photo: Made In Space).

Made In Space's NASA-contracted, first 3D printer, was sent to the ISS on September 21st, 2014. The ivory objects on top are duplicates of what will soon be some of the first objects ever printed off-Earth. In the background is the Microgravity Science Glovebox that will contain the printer during the 3D Printing in Zero-Gravity Experimentation (Photo: NASA/Emmett Given).

Indeed, a recent study by the space agency found that about 30% of parts aboard the orbiting lab could be manufactured with a 3-D printer.

And manufactured, apparently, with little difficulty; training, for example, seems to be a value-added non-issue.

"The printer was designed to be calibrated and operated remotely and thus be as easy and efficient for the astronauts as possible," said Made In Space's Kohlenberg. "The complexity of parts is not a factor in training as 3-D printing drastically reduces the complexity of manufacturing parts which would otherwise be difficult or impossible to produce. Another way of saying this is that complexity is essentially free with 3-D printing."

For now, all 3-D printed parts have by necessity been designed by Made In Space engineers. But that will change soon — especially with the arrival of commercial-type 3-D printers, as mentioned here by Kohlenberg.

"Our in-house engineers have designed everything from the printer itself to the parts that the printer has printed. This is mostly due to the fact that we are still wrapping up the very first technology demonstration and are just now finding customers. As soon as we launch the commercially available printer later this year, we expect the lion share of the designs to primarily come from our customers while our engineers will provide design support as it relates to printing on our printers in the zero-gravity environment."

Said Jason Crusan, director of NASA's Advanced Exploration Systems Division, "Additive manufacturing with 3-D printers will allow space crews to be less reliant on supply missions from Earth and lead to sustainable, self-reliant exploration missions where resupply is difficult and costly." And the technology will become even more important for manned missions to deep-space destinations such as Mars, according to NASA officials.

What's more, 3-D parts printing will have a much-needed, salutary effect on NASA's deep-space budget. Doing more with less is definitely an advantage — whether on the ISS or factory floor.

"We really want to see these things (3-D printers) become the building blocks for the future of exploration," Made in Space lead engineer Mike Snyder told *Space.com*. "They really can lead into sustainability in space, and actually make these missions that cost a lot of money be reduced just because you don't have to launch as much mass."

Adds Kemmer, "It starts with tools and spare parts, things like that, and eventually leads to habitats, structures and really everything that you need to live off-world."

'Live off-world'—the man says it as if it were already a reality—perhaps a sign that for NASA as well as space age entrepreneurs like Elon Musk—populating Mars is no longer a question of if—but when.

Not wishing to be left behind, the European Space Agency (ESA) plans to launch its own 3-D printer to the International Space Station in the first half of this year. In fact the agency also recently teamed with industrial partners to investigate using 3-D printing technology to build a moon base using lunar materials.

"3-D printing offers a potential means of facilitating lunar settlement with reduced logistics from Earth," Scott Hovland, of ESA's human spaceflight team, said in a statement last year. "The new possibilities this work opens up can then be considered by international space agencies as part of the current development of a common exploration strategy."

The NASA site explains the 3-D printer's presence on the space station as being part of the 3-D Print Project—a collaboration between NASA and Made In Space. The unit sent up last September aboard SpaceX's unmanned Dragon cargo capsule was then on Nov. 17 installed in the orbiting lab's Microgravity Science Glovebox by Expedition 42 commander Barry Wilmore.

Taking things one step beyond, Made In Space plans to launch another printer to the space station, on a production rather than a demonstration mission. This printer will be used for the aforementioned "recycler" project.

The second phase of the project will focus on actual use of production/replacement parts printed on the ISS, according to 3-D print program manager Niki Werkheiser, of NASA's Marshall Space Flight Center in Huntsville, Alabama. As with her counterparts, Werkheiser is thrilled with developments thus far. After all, not everyone gets a chance to be in on the ground floor of a new technology that by all indications definitely has legs.

"I think we're making history by, for the first time ever, being able to make what we need, when we need it, in space," Werkheiser said on *NASA TV* when the printer was installed. "Even though it may sound a little like science fiction, we're actually able to email our hardware to space instead of launching it." (Sources: *NASA.GOV*, NASATV.GOV and *SPACE.COM*.)

For Related Articles Search
3-D printing
at www.geartechnology.com

NASA Embraces 3-D Printing

The ability to "print" everything from human body parts to works of art to rocket engines is rapidly changing the world of manufacturing. NASA has been involved in additive manufacturing, or 3-D printing, since the 1990s when it was still an emerging technology. In the early days, it was often called rapid prototyping. Designers used printers to make plastic models to explore possibilities before they built a more costly part with metal. Printers were too small and could not make the quality parts needed for NASA flight hardware.

Now, making a part with additive manufacturing is not only more cost-effective, but also the printers can make larger parts of higher quality and with different materials — or even combinations of materials. NASA is exploring the use of many types of additive manufacturing that can benefit every phase of NASA missions — from launch to science payload development to robotic exploration to deep space missions. Across the agency, engineers and designers are trying out many types of 3-D printers that work with a variety of plastics and metals, including titanium, aluminum, Inconel and other nickel alloys widely used in aerospace manufacturing. Often a computer sends a design to a 3-D printer, and the machine makes the part in fewer pieces than would be required with traditional welding and assembly. Some additive manufacturing processes melt plastic or metal wire to form a part. For example, electron beams can be used to melt metal wire. Others use lasers to melt metal powders layer by layer until a part is formed.

To put this new type of manufacturing to the test, NASA is printing and testing rocket parts, telescope optics, and even parts of experiment equipment. When it makes sense, NASA plans to take advantage of 3-D printing in almost every type of mission from launch vehicles to robotic landers to parts needed in a space habitat. The International Space Station has become a test bed for this new technology to explore additive manufacturing in space — the first step toward in-situ resource utilization on orbit or at exploration destinations. Indeed, the technology could prove critical to space explorers on future long- and deep-space missions. (*NASA.GOV*)

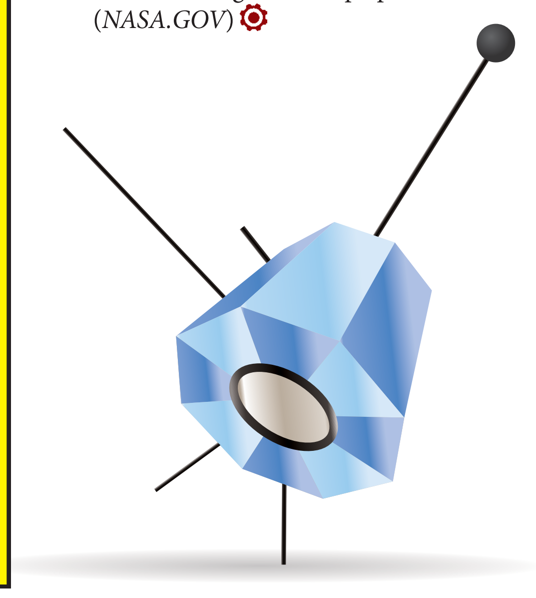

Gleason

WORKPIECE CHANGEOVER – IN THE TIME IT TAKES TO READ THIS AD

SOLUTIONS FOR CYLINDRICAL AND BEVEL GEARS OF ALL TYPES AND

- ✓ Bevel Gear Solutions, Up to 2,500 mm
- ✓ Cylindrical Gear Solutions, Up to 10,000 mm
- ✓ Metrology Solutions, All Types of Gears, Gear Tools
- ✓ Cutting Tools and Workholding Solutions, All Processes

For worldwide sales locations and additional information, visit:

Calculating KHβ

Email your question — along with your name, job title and company name (if you wish to remain anonymous, no problem) to: *jmcguinn@geartechnology.com*; or submit your question by visiting *geartechnology.com*.

QUESTION #1

How should we consider random helix angle errors fHβ and housing machining errors when calculating KHβ? What is a reasonable approach?

For Related Articles Search
load distribution
at www.geartechnology.com

Expert response provided by Hans-Peter Dinner:

Let us look at a mesh between a pinion and a gear. Both shafts are supported in a housing. Then, we should consider the following three errors:

1. Helix slope deviation of pinion, *fH*β1
2. Helix slope deviation of gear, *fH*β2

These errors describe how much the flank of each gear is misaligned to the gear axis.

3. Shaft parallelism error, *fpar*

This error describes how the two gear axes are misaligned with respect to each other. This is often simpli¬fied to the gear shaft misalignment with respect to the shaft of the pinion (or vice versa).

The errors are with respect to the plane of action, for a definition of the error see, e.g. — ISO1328 or AGMA2015.

The errors *fH*β1 and *fH*β2 can either be measured and averaged values from production or they can be determined from the gear quality number Q; e.g. — Q = 6 (gear quality 6 as per ISO1328). The error *fpar* is more difficult to determine, as it not only considers the misalignment of one shaft to the other due to the misalignment of the housing bores, but it should also consider variations in bearing operating clearances and the misalignment between the gear pitch cylinder with respect to the corresponding shaft axis. For the sake of simplicity, let us assume the housing bore arrangement is tolerated in such a way that we know the permissible shaft or gear axes parallelism error from the manufacturing drawing.

All errors are considered as random and the mean is zero (e.g. — tolerances given in drawing are symmetrical). The errors are hence described as a tolerance around zero, i.e. — *fH*β1 = ±a, *fH*β2 = ±b and *fpar* = ±c where *a*, *b*, *c* are values in micron.

Now the question is how the tolerances or permissible errors — *a*, *b*, and *c* — are to be combined for the calculation of *KH*β. For the resulting misalignment we define the tolerance by the character *d* and find in general terms:

$$fma = \pm d \tag{1}$$

In a worst-case scenario, the values would be added up giving a resulting misalignment:

$$fma = \pm(a + b + c) \tag{2}$$

However, as the errors *a*, *b*, *c* are random values, this approach is clearly conservative and not realistic. It is unlikely that if we combine two gears and a housing that, for all three components, we happen to select the worst-case of each. The resulting error will be overly high and will result in too high a crowning value, resulting in an unnecessary stress concentration on the flank in operation.

Let us assume that the manufacturing errors *fH*β1, *fH*β2 and *fpar* follow a normal distribution. As mentioned above their mean and average value is zero. Let us further assume that 99.73% of all gears are within specification and that 99.73% of housings are within specification — or that the 3-Sigma rule applies. The 3-Sigma rule means that "nearly all" values are within plus/minus three standard deviations from the mean value. We may translate the 3-Sigma rule to the following image: if we produce a gear every day, it takes one year until one gear is out of specification.

If 99.73% of all gears and housings are within specification (3-Sigma rule applies), we know that three times the standard deviation of the manufacturing error is equal to the tolerance value *a*, *b* and *c*. Thus assuming that 99.73% of all gears and housings are within specified tolerances, we may define the manufacturing errors as normal distribution *N*, with mean value μ, standard deviation σ, valid over the range of the tolerance fields defined above:

$$\begin{aligned} fH\beta1 &= N(\mu_1, \sigma_1^2, x) = \frac{1}{\sigma_1\sqrt{2\pi}} e^{-\frac{1}{2}\left(\frac{x-\mu_1}{\sigma_1}\right)^2} \quad with -a < x < +a, \mu_1 = 0, \sigma_1 = \frac{a}{3} \\ fH\beta2 &= N(\mu_2, \sigma_2^2, x) = \frac{1}{\sigma_2\sqrt{2\pi}} e^{-\frac{1}{2}\left(\frac{x-\mu_2}{\sigma_2}\right)^2} \quad with -b < x < +b, \mu_2 = 0, \sigma_2 = \frac{b}{3} \\ fpar &= N(\mu_3, \sigma_3^2, x) = \frac{1}{\sigma_3\sqrt{2\pi}} e^{-\frac{1}{2}\left(\frac{x-\mu_3}{\sigma_3}\right)^2} \quad with -c < x < +c, \mu_3 = 0, \sigma_3 = \frac{c}{3} \end{aligned} \tag{3}$$

Also, we may express the resulting error, *fma*, as a probability density function as follows:

$$fma = N(\mu_3, \sigma_4^2, x) = \frac{1}{\sigma_4\sqrt{2\pi}} e^{-\frac{1}{2}\left(\frac{x-\mu_4}{\sigma_4}\right)^2} \quad with -d < x < +d, \mu_4 = 0, \sigma_4 = \frac{d}{3} \tag{4}$$

Because *fH*β1, *fH*β2 and *fpar* are independent of each other, we find the standard deviation σ_4 as follows:

$$\sigma_4 = \sqrt{\sigma_1^2 + \sigma_2^2 + \sigma_3^2} \tag{5}$$

Again assuming that 3-Sigma rule applies for *fma* (i.e. — d = 3*σ_4) we find:

$$d = 3 * \sqrt{\left(\frac{a}{3}\right)^2 + \left(\frac{b}{3}\right)^2 + \left(\frac{c}{3}\right)^2} \tag{6}$$

And

$$fma = \pm 3 * \sqrt{\left(\frac{a}{3}\right)^2 + \left(\frac{b}{3}\right)^2 + \left(\frac{c}{3}\right)^2} \tag{7}$$

Which means that after assembly, 99.73% of all gearboxes have a total misalignment of the flanks with respect to each

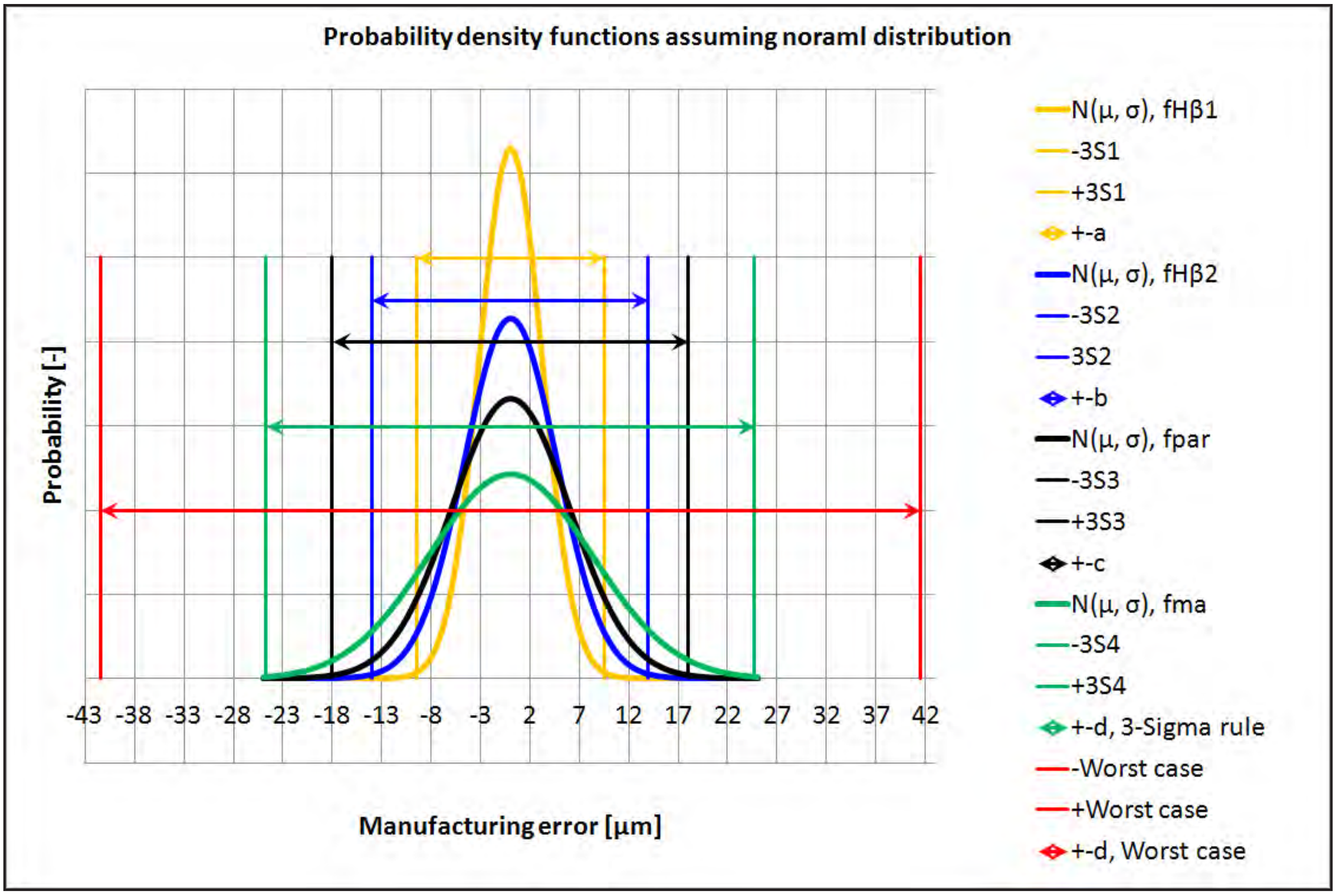

Figure 1 Normal distribution of manufacturing errors, resulting error, and worst-case scenario.

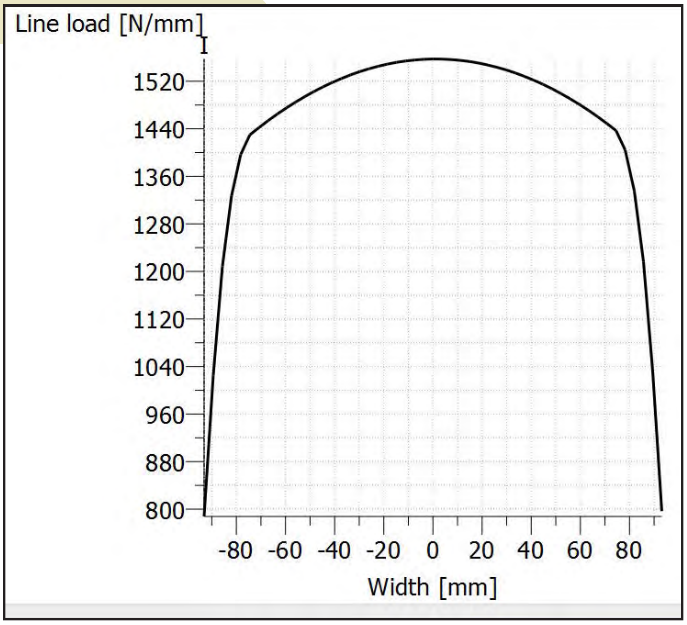

Figure 2 **Line load distribution in the mesh for the example — not considering any random manufacturing errors; *KHβ* = 1.08.**

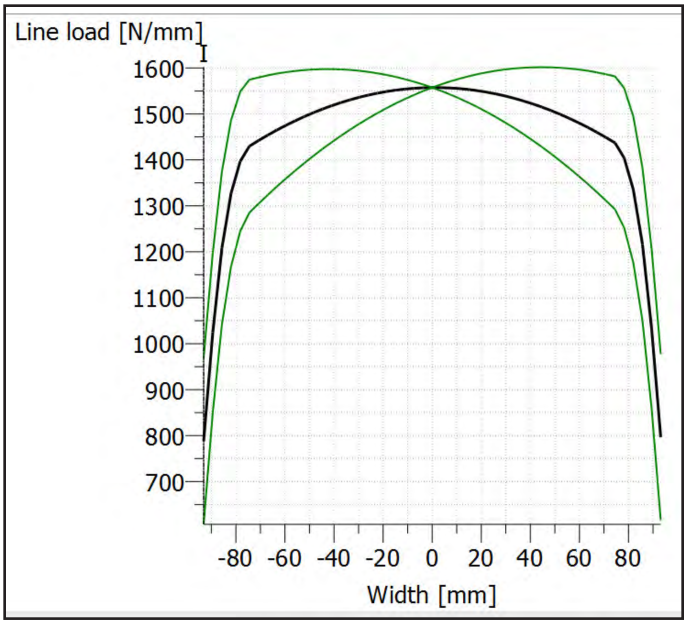

Figure 3 **Line load distribution considering random manufacturing errors *fma* = ±24.7μm (green lines); *KHβ* = 1.11; highest line load occurs well within the crowned area of the face width; design considered suitable.**

other of *fma* = ±*d* — where *d* is calculated using the above formula.

The above relationships are shown in Figure 1.

The probability density functions (assumed to be normal distributions) of the three basic errors — *fH*β1, *fH*β2 and *fpar* — are shown in orange, blue and black. Also shown are the tolerances ±*a*, ±*b*, ±*d* corresponding to $\pm 3*\sigma_1$, $\pm 3*\sigma$, $\pm 3*\sigma_3$ (where σ is the standard deviation).

Combining these three random errors, we find the probability density function (again assumed to be a normal distribution) of the resulting error *fma* in green. Also shown is the tolerance ±d corresponding to $\pm 3*\sigma_4$.

For comparison, the worst-case scenario where $d = a + b + c$ is shown in red.

We can clearly see that if we use the worst-case scenario, the value for *d* is much higher than the value for *d,* were we to use a statistical approach.

Applying the above formulas we find that the resulting tolerance range ±d if we apply 3-Sigma Rule as:

$$fma = \pm d \pm 3 * \sqrt{\left(\frac{9.50\mu m}{3}\right)^2 + \left(\frac{14.0\mu m}{3}\right)^2 + \left(\frac{18.0\mu m}{3}\right)^2} = \pm 24\mu m \quad (8)$$

And if we apply a worst-case scenario, we find:

$$fma = \pm d \pm (a + b + c) = \pm 41.5\mu m \quad (9)$$

Considering the above statement that the worst-case approach is considered as overly conservative, then, for the above gear pair, we would consider a random manufacturing error in the mesh of *fma* = ±d = ±24.7μm, when calculating *KHβ* along ISO6336-1, Annex E.

KHβ ***calculation using statistical or worst-case scenario for*** fma**.** Let us consider again the above gear example. We apply helix angle modifications on the pinion such that we compensate the shaft bending, shaft torsion and bearing deformation.

Table 1 Gear data used in example calculation

Property	Symbol	Unit, Referenc	Value Pinion	Value Gear
Number of teeth	*z*	-	24	99
Normal module	*mn*	mm	8.00	8.00
Quality grade	*Q*	ISO1328	5	6
Helix slope deviation	*fHβ*	μm	9.5	14.0
Shaft parallelism error	*fpar*	μm	18.0	

The result is a symmetrical line load distribution, calculated along ISO6336-1, Annex E. If we ignore the random manufacturing error (assuming *fHβ*1 = *fHβ*2 = *fpar* = 0.0μm), the load distribution is then symmetrical and highest value lies in the middle of the gear face width due to an applied crowning of *Cβ* = 20μm. Let us also apply a curved end relief over 10% of the gear face width per side; the amount is *CβI* = *CβII* = 45.0μm (notations as per ISO21771 apply).

The resulting line load distribution is shown below, the resulting face load distribution factor is *KHβ* = 1.08.

If we now consider the random manufacturing error *fma* = ±24.7μm (from the 3 Sigma-Rule), we find three line load distributions (one without manufacturing error, one using *fma* = +24.7μm, and *fma* = −24.7μm), as shown below. The face load distribution factor has now increased to *KHβ* = 1.11. And yet, the highest line load remains within the crowned part of the face width; thus the design would be deemed quite acceptable.

But if we consider the worst-case manufacturing error — *fma* = ±41.5μm — we find the below line load distributions. The face load factor is now *KHβ* = 1.16 and we find that the highest line load is just where the end relief is about to start, thus rendering the design unacceptable in this case.

Conclusion

An easy-to-use approach has been presented showing how random gear helix slope deviations and shaft parallelism errors due to housing errors can be considered in the calculation of

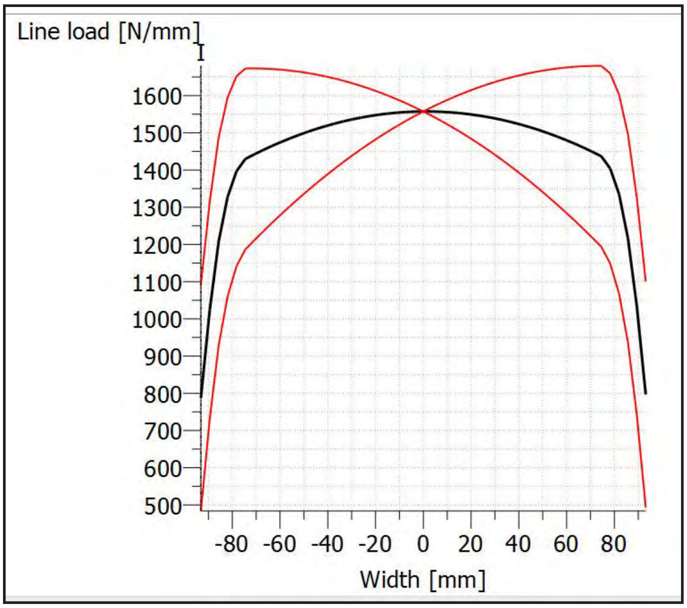

Figure 4 Line load distribution considering random manufacturing errors *fma* = ±41.5μm (red lines); *KHβ* = 1.16; highest load occurs in the transition area between crowning and end relief; design considered as not suitable.

KHβ. It is shown that adding up all random errors in a worst-case scenario is overly conservative. Applying the 3-Sigma Rule, errors may be combined in a different way such that the resulting error covers 99.73% of all cases. The difference in the resulting *KHβ* values when using this worst-case approach (in the above example, *KHβ* = 1.16) vs. the more realistic statistical approach (*KHβ* = 1.11) is significant when optimizing a design.

The use of the above statistical approach in consideration of manufacturing errors in the calculation of *KHβ* along ISO6336-1, Annex E or AGMA927 is recommended.

A word of caution: experience shows that when designing gear lead modifications, or when calculating gear load distributions, much attention should also be paid to the bearing deformation and variation in bearing operating clearance. These effects are not elaborated above, but are summarized in the error *fpar*.

Hans-Peter Dinner studied mechanical engineering at the Swiss Federal Institute of Technology (ETH), where during his studies he spent time with Mercedes Benz working on FEM of car bodies; with Buhler in South Africa for training; and with the National University of Singapore for writing his thesis on FEM analysis of medical devices. He began as an FEM engineer, working with the leading consultant in Switzerland on welded structures, pressure vessels and satellite structures. Dinner later joined a leading roller coaster design company, being responsible for all strength verifications. He then moved on to KISSsoft AG, supporting customers in the use of their gear software, working on gear optimization projects, and ultimately transitioning to sales of KISSsoft products, with a focus on the Asian market. In 2008 he started his own consultancy firm, EES KISSsoft GmbH, sharing his time between KISSsoft support and sales in Asia and project work. Key projects included design and testing of SCD3MW and SCD6MW wind gearboxes, and large-bearing calculations for cranes and wind turbines as well as gear optimizations for sugar mills, vertical roller mills and tractors. Dinner's main interests are planetary gearboxes, tooth contact analysis and testing.

Measuring Residual Stress in Gears

Email your question — along with your name, job title and company name (if you wish to remain anonymous, no problem) to: *jmcguinn@geartechnology.com*; or submit your question by visiting *geartechnology.com*.

QUESTION #2

I have heard that X-ray diffraction does not tell the whole story and that I should really run a fatigue test. I understand this may be the best way, but is there another method that gives a high degree of confidence in the residual stress measurement?

Expert response provided by Robert Errichello:

X-ray diffraction (XRD) analysis is the accepted quantitative method for determining residual stresses. Other methods such as dissection, hole drilling, ultrasonic, and Barkhausen noise analysis are either not quantitative or do not have sufficient spatial or volumeric resolution to adequately characterize residual stress distributions.

XRD measures the lattice spacing (d-spacing) between atoms; you can think of XRD as a strain gage. Tensile stress increases d-spacing and compressive stress decreases d-spacing. Hence, XRD actually measures strain and the residual stresses producing the strain are calculated assuming a linear, elastic deformation of the crystal lattice. The elastic constants (modulus of elasticity, E, and Poisson's ratio, ν) must be known or determined empirically (Ref. 1) to calculate residual stresses from measured strains.

Additionally, XRD analysis has the capability to detect the FCC phase of austenite, the BCC phase of ferrite, and the BCT phase of martensite, because each phase has different d-spacing. Therefore XRD is a quantitative method that is considered to be the most accurate method to determine the amount of retained austenite. Fatigue life, fracture toughness, and machinability are all strongly influenced by the percent-retained austenite. So if you are concerned with these properties, you need to know the amount of retained austenite.

Generally, tensile residual stresses are detrimental, and compressive residual stresses are beneficial to fatigue strength. Classic bending fatigue cracks originate at the surface of the root fillet in gear teeth. XRD analysis can measure the surface residual stresses non-destructively at the surface of the root fillet and allow you to determine whether the residual stresses are sufficiently compressive. If not, shot peening can be used to increase the compressive residual stresses.

If Hertzian fatigue life is important, you need to know the subsurface residual stress profile — in addition to the surface residual stresses — because the controlling stresses are subsurface. Unfortunately, XRD analysis can only measure subsurface residual stresses destructively by successively removing layers of the surface by electrolytic polishing, which tends to be slow and costly. Nevertheless, the subsurface profile of residual stresses strongly influences the Hertzian fatigue strength and you need to assess their values if you wish to determine the resistance to Hertzian fatigue. Furthermore, if you are interested in the crack propagation phase of bending fatigue, the subsurface residual stresses are important.

XRD is an indispensible tool for failure analysis. For example, it is used to investigate changes in residual stress profiles in Hertzian contacts in gears and rolling element bearings that are caused by Hertzian stresses that exceed the yield strength in local areas beneath the surface. Generally, residual compressive stresses increase with rising Hertzian stress, and are displaced to greater depths. By comparing the residual stresses in failed components to those of unused components, one can draw conclusions about the actual Hertzian stress that acted on the failed component.

XRD is also very helpful in understanding why different materials and heat treatments lead to different fatigue strengths. For example, Reference 2 showed that carburized bearings are more durable than through-hardened bearings in wind turbine gearboxes because carburized bearings have higher compressive, residual stresses and greater amounts of retained austenite.

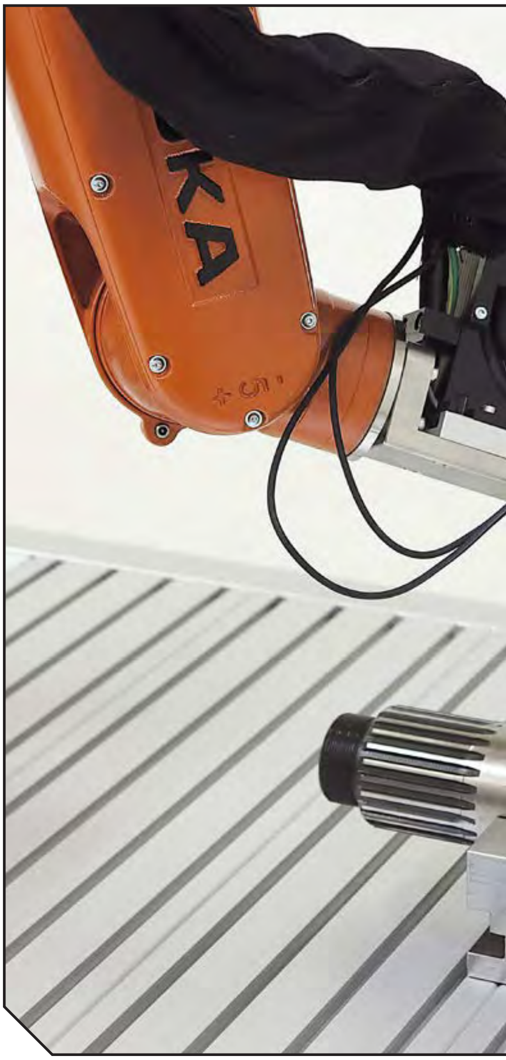

For Related Articles Search

x-ray diffraction

at www.geartechnology.com

Applications for XRD analysis include:

- ***Materials research.*** For example, characterizing surface and subsurface residual stresses and retained austenite profiles in through hardened, surface hardened, and case hardened gear teeth and rolling element bearing raceways.

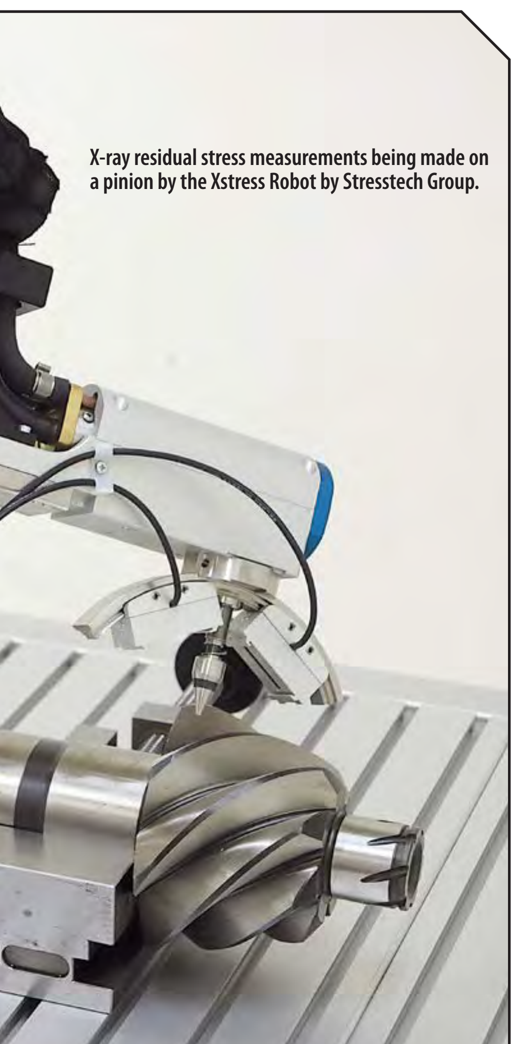

X-ray residual stress measurements being made on a pinion by the Xstress Robot by Stresstech Group.

- ***Process quality control.*** For example, determining surface compressive stresses produced by shot peening, tensile residual stresses produced by abusive grinding, or alterations of residual stresses caused by stress-relieving heat treatment. In general, surface and subsurface residual stress profiles are required to fully characterize effects of heat treatment, machining, grinding, shot peening, and other manufacturing processes.
- ***Failure analysis***. For example, investigating whether residual stresses and retained austenite meet quality specifications and whether residual stresses were altered due to loading, plastic deformation, or thermal stressing.
- ***Fracture mechanics damage tolerance***. Near surface and subsurface residual stresses control the growth of fatigue cracks and need to be considered when estimating damage tolerance.

Limitations of XRD analysis include:

- Line of sight is required for the X-ray beam.
- Only a shallow layer (< 10 µm deep) is measured.
- Subsurface surveys are destructive (require electrolytic polishing).
- The sample must have reasonably fine grains that are not severely textured.
- The elastic constants of the material must be known.

References

1. ASTM E1426. “Standard Test Method for Determining the X-Ray Elastic Constants for Use in the Measurement of Residual Stress Using X-Ray Diffraction Techniques.”
2. Errichello, R., R. Budny and R. Eckert. “Investigations of Bearing Failures Associated with White Etching Areas (WEAs) in Wind Turbine Gearboxes,” *Tribology Transactions,* Vol. 56, No.6, 2013, pp. 1069-1076; (also published in *Power Transmission Engineering,* March 2014, pp. 38-44).

Robert Errichello heads his own gear consulting firm, GEARTECH, and is founder of GEARTECH Software, Inc. He has over 50 years of industrial experience. He has been a consultant to the gear industry for the past 37 years and to over 50 wind turbine manufacturers, purchasers, operators, and researchers. He has taught courses in material science, fracture mechanics, vibration, and machine design at San Francisco State University and the University of California at Berkeley. He has presented numerous seminars on design, analysis, lubrication, and failure analysis of gears and bearings to professional societies, technical schools, and the gear, bearing, and lubrication industries. A graduate of the University of California at Berkeley, Errichello holds BS and MS degrees in mechanical engineering and a Master of Engineering degree in structural dynamics. He is a member of several AGMA Committees, including the AGMA Gear Rating Committee, AGMA/AWEA Wind Turbine Committee, ASM International, ASME Power Transmission and Gearing Committee, STLE, NREL GRC, and the Montana Society of Engineers. Bob has published over 80 articles on design, analysis, and application of gears, and is the author of three widely used computer programs for design and analysis of gears. He is technical editor for GEAR TECHNOLOGY and STLE Tribology Transactions. Errichello is recipient of the AGMA TDEC Award, the AGMA E.P. Connell Award, the AGMA Lifetime Achievement Award, the STLE Wilbur Deutch Memorial Award, the 2015 STLE Edmond E. Bisson Award, and the AWEA Technical Achievement Award.

Prediction of Surface Zone Changes in Generating Gear Grinding

Matthias Ophey and Dr. Jan Reimann

One process for hard finishing gears is generating gear grinding. Due to its high process efficiency, generating gear grinding has replaced other grinding processes such as profile grinding in batch production of small- and middle-sized gears. Yet despite the wide industrial application of generating gear grinding, the process design is based on experience along with time- and cost-intensive trials. The science-based analysis of generating gear grinding demands a high amount of time and effort, and only a few published scientific analyses exist. In this report a thermo-mechanical process model that describes influences on the surface zone in generating gear grinding is introduced.

Introduction and Motivation

In order to improve load carrying capacity and noise behavior case hardened gears usually are hard finished (Ref. 1). One possible process for hard finishing of gears is generating gear grinding. Generating gear grinding has replaced other grinding processes in batch production of small and middle sized gears due to the high process efficiency.

Despite the wide industrial application of this process, only a few scientific analysis exist (Refs. 2–5), because the science-based analysis of generating gear grinding needs a high amount of time and effort and the continuously changing contact conditions complicate the investigation.

The lack of knowledge of cause-effect relationships results in an empirical process design in industrial practice. Therefore in most cases several trials must be performed to find a stable process design. By stock fluctuation or by an unfavorable process design an undesirable process result up to a process-related thermal damage of the external zone can occur. Therefore it is necessary to get a better understanding of the cause-effect relationships between process parameters, tool specifications and process in generating gear grinding.

State of the Art

Hard finishing technology is used to remove deviations from hardening, to machine tooth flank modifications and to meet quality requirements. The case hardening process is necessary to enable the gear to transmit high torque with smaller gears in high power applications. In industrial applications generating gear grinding, profile gear grinding and gear honing are most commonly used as hard finishing processes for gears. Each of these high-performance processes is using geometrically undefined cutting edges. Continuous generating gear grinding has evolved to the dominant process in batch production for small and middle sized gears due to the high productivity.

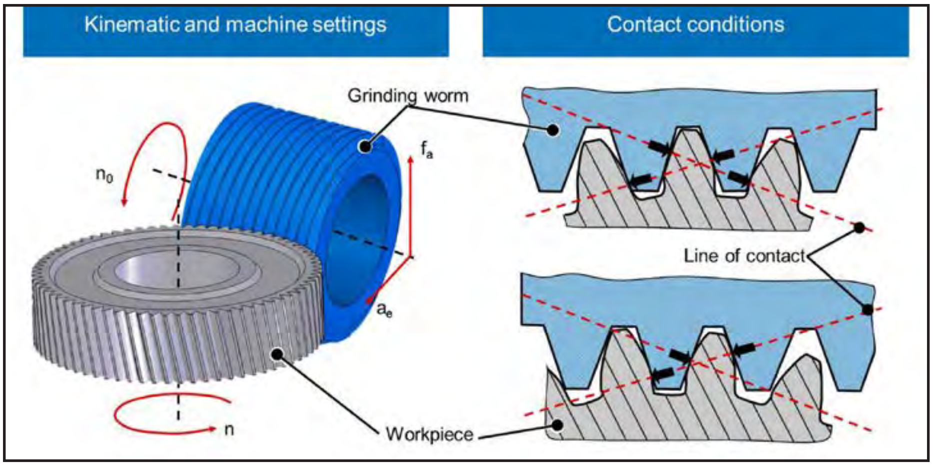

Figure 1 **Generating gear grinding: principle, machine settings, and contact conditions (Ref. 9).**

Generating gear grinding. One of the most efficient processes for hard finishing of gears in batch production of external gears and gear shafts is generating gear grinding. Generating gear grinding is used for hard finishing of gears with a module of $m_n = 0.5$ mm to $m_n = 10$ mm (Refs. 6, 4). By the application of new machine tools the process can be used for grinding large module gears with an outside diameter up to $d_a = 1{,}000$ mm (Ref. 7).

The cylindrical grinding worm, whose profile equates a rack profile in a transverse section, meshes with an external gear (Fig. 1, left). The involute is generated by continuous rolling motion of grinding worm and workpiece by the profile cuts method (Refs. 8, 4). Profile cuts method in generating processes means that the profile form is generated by a finite number of profiling cuts. Due to the closed grinding worm no generating cut deviations, as in gear hobbing process, occur during generating gear grinding.

In generating gear grinding multiple points of the grinding worm are in contact simultaneously. The number of contact points changes continuously during tool rotation (Fig. 1, right). In the upper right part of Figure 1 the contacts on the right and left flanks are balanced, with an even number of contact points. This leads to a consistent distribution of forces. With an uneven number of contact points, as shown in the lower right part of Figure 1, the distribution of forces will be unbalanced. This leads to an inconsistent distribution of the cutting forces. In the example with an uneven number of contact points, the force on the line of contact of the left tool flanks is split into two contact points. On the right tool flank the cutting force is not split, because only one contact point exists. This situation can lead to higher stock removal at the single contact point potentially resulting in higher excitation. The consequence can be the appearance of profile form deviations which reduce the achievable gear quality. Scientific publications of Meijboom (Ref. 2) and Türich (Ref. 3) describe this relation theoretically.

In comparison to other gear grinding processes the stock removal rate in generating gear grinding is very high. In most cases the stock removal rate is limited by the demanded gear quality (Ref. 4). Furthermore, the appearance of a detrimental process-related surface zone inducement (grinding burn) can be the limiting factor.

Publications (Refs. 10–12), and the doctoral thesis of Meijboom (Ref. 2), Türich (Ref. 3) and Stimpel (Ref. 5) show the influence of several parameters on the process results. But several technological correlations have not been analyzed or verified in experimental trials yet.

Current challenges. Due to limited scientific studies the technology users, grinding tool suppliers and machine tool manufactures face two main challenges.

On the one hand the process design and optimization is based on know-how of the process user. In cases, where no sufficient experience (e.g., new gear geometry, new grinding tools) exists, cost-intensive trials have to be performed to find a favored and robust process design. In this case, several trial iterations are usually necessary to obtain high process stability. In order to reduce the number of needed iteration loops the technological cause-effect relationships must be analyzed in detail.

On the other hand, the demand for increasing productivity leads to an increase of axial feed and cutting speed. With an increase of productivity the cutting force and thus the heat flow towards the workpiece are rising. This in turn leads to an increased risk of grinding burn during the grinding process. The challenge is to increase the productivity without causing grinding burn.

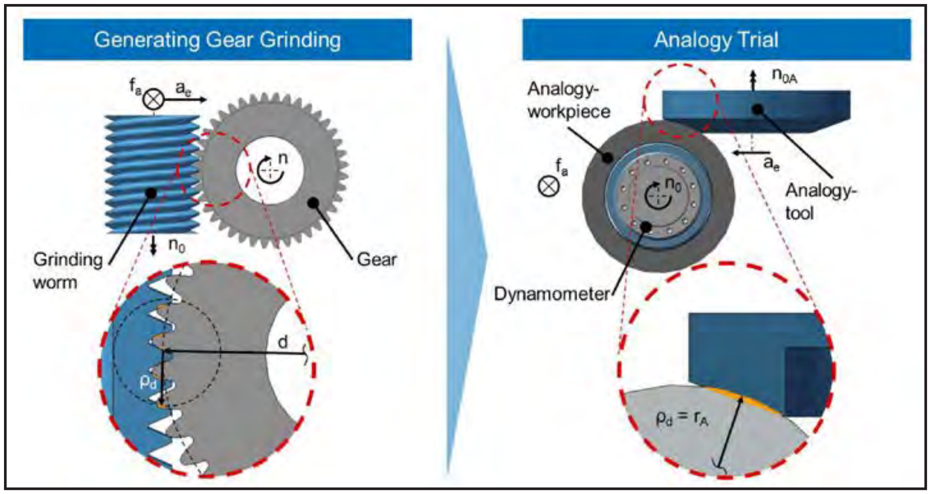

Figure 2 Analogy trial for generating gear grinding: principle and deduction of analogy workpiece geometry (Ref. 9).

Research Objective and Approach

The research objective for generating gear grinding at WZL is the increase of process efficiency and process reliability in generating gear grinding by description of the technological cause-effect relationships for cutting forces as well as for occurrence of grinding burn in a model. For the analysis of the cause-effect relationships an analogy trail has been developed and will be introduced in this report.

The aim of this report is to present a model to predict grinding burn for generating gear grinding. Therefore cutting forces in analogy trails are measured and the interactions between process parameters and occurred grinding burn are taken into account. The measured cutting forces will be combined in an empirical cutting force model. With the ability to calculate the cutting force the heat flow density towards the workpiece can be estimated. With a comparison of the heat flow density and the grinding burn occurrence a critical heat flow density that leads to grinding burn can be determined. Thereby a model to predict grinding burn can be derived. In conclusion the prediction model will be transferred onto generating gear grinding and will be validated by generating gear grinding trials.

Analogy trail for Generating Gear Grinding

The complexity of the contact conditions between tool and workpiece during generating gear grinding complicates the analysis of generating gear grinding. On the one hand, the penetration volumes change over the tooth profile height during grinding. On the other hand, the number of engaged tool flanks and workpiece flanks is variable. To investigate generating gear grinding on a single fixed point on the tooth profile, a geometric-kinematic model, the analogy trail, has been developed (Refs. 12, 9). The principle of the analogy trail for generating gear grinding is shown (Fig. 2).

For each point of the involute the local radius of curvature ρ_y can be calculated (Ref. 13). For the analogy trail the contact conditions at different positions of the involute can be approximated. The radius of the workpiece in the analogy trail r_A equals the radius of curvature at the investigated point of the involute profile. Thus the diameter of the analogy workpiece depends on the number of teeth z, the module m_n, the helix angle β and the pressure angle α_n of the mapped sample gear. The rack profile of the grinding worm can be approximated in the investigated contact point by a face wheel with a conic working surface (Ref. 9).

Besides the workpiece and the tool geometry the chip geometry in the analogy trail has to be comparable to the chip geometry in generating gear grinding.

Therefore the cutting length l_{cuA} and the chip thickness h_{cuA} have to be comparable between analogy trail and generating gear grinding.

Furthermore the kinematics of chip formation and the velocities must be fitted to generating gear grinding. During chip formation the lateral sliding speed v_{tA}, the axial feed speed v_{aA} and the cutting speed v_c interfere with each other. The cutting speeds in generating gear grinding and analogy trail are the same. The lateral sliding speed v_{tA} can be calculated by the rotational speed n_A of the workpiece and the requirement to be synchronous. The axial feed speed v_{aA} can be adjusted according to the generating gear grinding process as the product of rotational speed n_A and axial feed f_a. Rotational speed as well as axial feed in analogy trail and generating gear grinding is identical. The tool is a grinding wheel with an angled surface. The angle corresponds to the pressure angle α_{n0} of the grinding worm.

The mapped grinding process and the machine tool used are shown (Fig. 3). The mapped grinding process is carried out with a spur gear with a number of teeth of $z = 31$ and a normal module of $m_n = 4.5$ mm. The material is 20MnCr5. The gears are case-hardened with a surface hardness of 60 HRC and a case-hardening-depth of CHD550HV = 1.4 mm. The material and heat treatment of the analogy workpieces match the spur gears. All generating gear grinding and analogy trails were performed on a model LCS380 grinding machine from Liebherr-Verzahntechnik GmbH that can perform both generating and profile gear grinding. For both analogy and generating gear grinding trials, corundum tools with a grain size F120 (average grain diameter 109 µm) from Winterthur Technology AG are used.

Figure 3 Workpiece data and machine tool.

The experimental set-up of the analogy trails is shown (Fig. 4); the cutting force can be determined with a dynamometer which is integrated in the flow of forces. For further information, a full description of the analogy trail design can be found in (Ref. 12).

With this experimental set-up, 129 analogy trails were performed. In these analogy trails the following process parameters were taken into account. The axial feed f_a, the number of starts z_0, the cutting speed v_c, the stock Δ_s, the pressure angle of the analogy tool α_{n0A} and the cooling lubricant volume flow V_{CL}. In addition, the diameter of the analogy workpiece was varied to investigate different points on the involute profile.

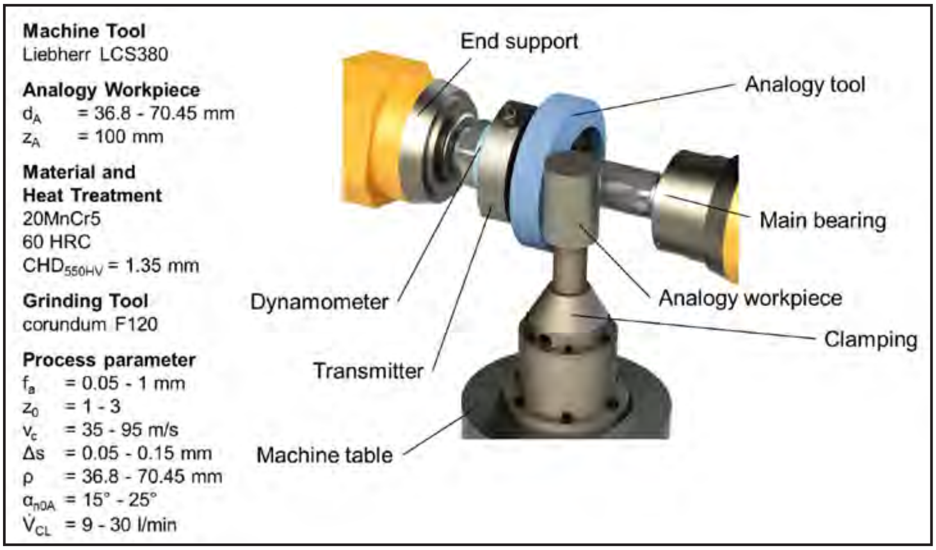

Figure 4 Experimental set-up analogy trial generating gear grinding.

Prediction Model for Surface Zone Inducements

Based on the empirical data of the analogy trails an empirical-physical model is built up in the following. Using the model, the occurrence of a process-related damage of the surface zone can be predicted. For this purpose, an approach to describe the surface zone inducement is presented. Subsequently the required parameters are determined and the prediction model is derived.

Analytical model approach. To predict the surface zone inducement the heat flow density, which describes the energy flow in the contact zone between tool and workpiece, must be determined. To prevent grinding burn the heat flow density towards the workpiece q_w must always be lower than a critical heat flow density $q_{w,crit}$ that leads to a detrimental influence on the surface zone.

The heat flow density towards the workpiece q_w corresponds to the current energy flow through the contact area between tool and workpiece A_c. In general for grinding the majority of the cutting energy is thermal energy, which is produced by intense friction, shear and separation processes as well as by friction of the abrasive grain and bond (Ref.14). Assuming that also for generating gear grinding almost all cutting power is converted into thermal energy, the total energy flow in the contact area can be calculated by the product of cutting force F_c and cutting speed v_c. In order to estimate the heat flow density towards the workpiece q_w correction factors must take the distribution of the heat flow from the contact zone into account. These corrections factors are K_{CLF} which takes into account the cooling lubricant flow and K_W which considers the heat flow towards the workpiece. With these factors the heat flow density towards the workpiece q_w can be estimated with Equation 1(Ref. 15) as:

$$q_w \approx K_{CLF} K_W \frac{F_c v_c}{A_c} \leq q_{w}, crit \tag{1}$$

Determination of model parameters. In the following, the correction factors K_{CLF} and K_W, the cutting force F_c and the contact area between workpiece and tool A_c must be determined to calculate the heat flow density. With correlation of the known heat flow density and the occurrence of grinding burn for every trial the critical heat flow density can be determined.

Cutting Force

The cutting force was measured during the analogy trails with a dynamometer. During the analogy trails various process parameters were investigated to get a statement about the influence on the cutting force. In order that the cutting force does not have to be determined empirically for each combination of process parameters, a cutting force model is derived in the following.

The cutting force model is set up based on the obtained data from the analogy trails using a regression analysis. For regression analysis, the influence of the process parameters axial feed f_a, number of starts z_0, cutting speed v_c, stock Δ_s, cooling lubricant flow V_{CL} and tool pressure angle α_{n0A} are considered. The regression analysis of the cutting force is carried out with a cubic approach considering the interactions. For regression analysis, the significance level was set to $\alpha = 0.05$. The comparison of the calculated forces using the force model and the measured forces is shown (Fig. 5). Good correlation between calculated and measured forces is evident; this is confirmed by a coefficient of determination of $R_2 = 0.950$.

In summary it can be stated that the cutting force model maps the measured cutting forces very well and offers a high stability due to a widely varying database. Thus, the cutting force model is suitable as a basis for calculating the heat flow density and to derive a prediction model for surface zone changes for generating gear grinding.

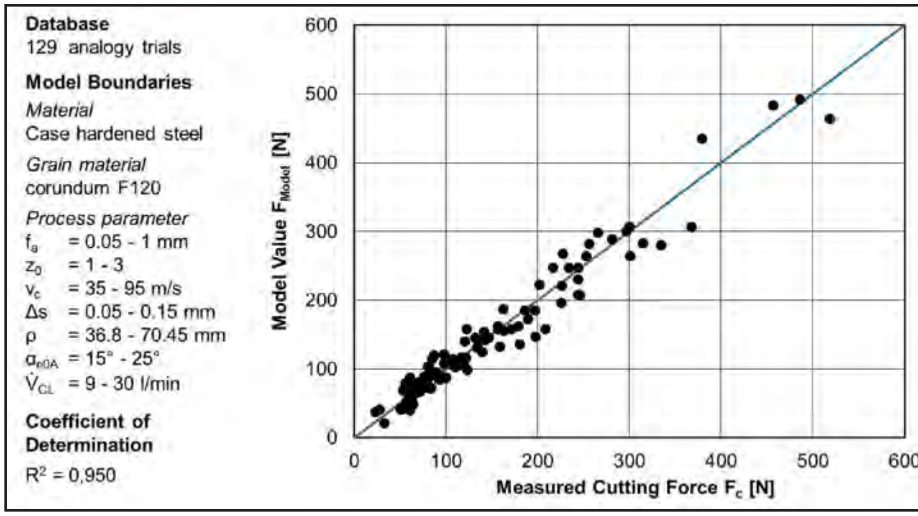

Figure 5 Model results and observations of the cutting force.

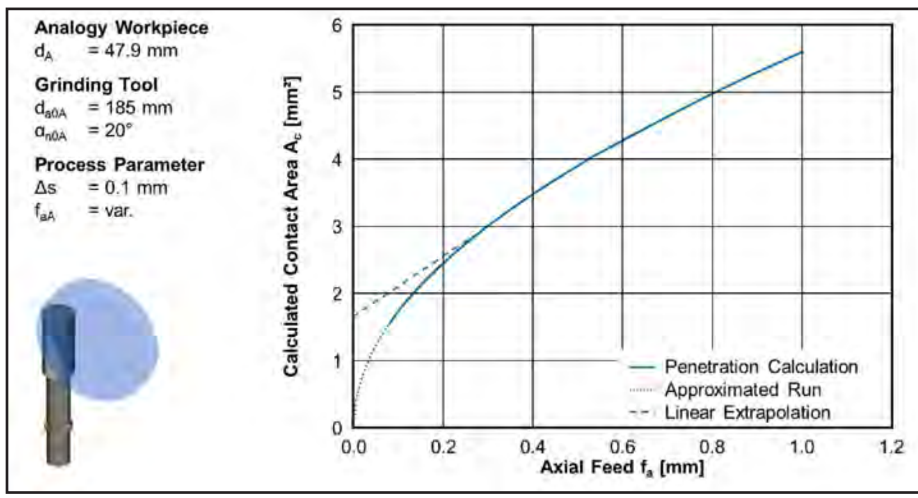

Figure 6 Determination of contact area.

Contact Area

To define the heat flow density the contact area between tool and workpiece must be calculated. The contact area A_c between tool and workpiece is corresponding to the zone of heat transfer between tool and workpiece. The contact area for the analogy trails can be calculated with a penetration calculation considering various stocks and axial feeds. Figure 6 shows the contact area for a constant pairing of tool and workpiece over axial feed. For an axial feed of $f_a < 0.2$ mm, the contact area drops sharply. For an axial feed of $f_a < 0.08$ mm no penetration volume between workpiece and tool could be calculated with the penetration calculation.

Due to numerical inaccuracies, the calculated contact area for small axial feeds is not exact. From kinematics it can be derived that in the absence of axial feeding a contact between tool and workpiece must exist for the first rotation of tool and workpiece. The contact area for low axial feeds of $f_a < 0.25$ mm is calculated from an axial feed by linear extrapolation. The extrapolated contact area is indicated by the dotted line in the diagram. Using this functional relationship, the contact area A_c can be determined for the prediction model.

Correction Factors

Finally, the two correction factors to calculate the heat flow density must be determined. The heat distribution for each combination of tool, workpiece and cooling lubricant is different and variable over the contact zone (Ref. 16). Due to the different thermal material parameters such as specific heat capacity c_p and thermal conductivity λ, as well as the inability to determine the temperatures in the contact zone, the heat distribution factor K_W cannot be calculated for generating gear grinding. In several studies heat distribution factors have been estimated for different grinding processes (Refs. 17–22). The evaluation of these papers shows that up to 80% of the thermal energy can flow into the workpiece. For surface grinding of unhardened steel a heat distribution factor $K_W = 0.65$ was determined (Ref. 19). A heat distribution factor for grinding of hardened 20MnCr5 cannot be found in the literature. Because of the poor accessibility of the contact area during generating grinding a heat distribution factor $K_W = 0.8$ is assumed in this work. This corresponds to the standard assumptions in literature and provides an assessment on the safe side (Refs. 23–24).

In addition to the constant heat distribution factor K_W, a variable factor K_{CLF} to determine the influence of the cooling lubricant flow is necessary. For this purpose, the heat flow densities of the analogy trails were normalized to the maximum heat flow density and analyzed in relation to the cooling lubricant flow. Using a regression analysis the influence of the cooling lubricant flow on the heat flow density was determined.

The normalized heat flow density q_{norm} at constant process parameters decreases with increasing cooling lubricant flow (Fig. 7). This effect is based on the better supply of the contact area with cooling lubricant. With increasing cutting speed, the influence of the cooling lubricant flow decreases. The rotation of the tool produces a flow of air, which deflects the coolant. The higher the cutting speed the greater the cooling lubricant is dispersed and the worse the contact area is supplied with cooling lubricant (Ref. 6). Therefore, the correction factor for the cooling lubricant, which represents the influence of the cooling lubricant flow on the heat flow, is dependent on the cutting speed v_c as well.

For constant cutting speeds, the heat flow towards the cooling lubricant can be approximated by an exponential function depending on the cooling lubricant flow V_{CL}. The correction factor K_{CLF} can be described by Equation 2. The factors a and b were determined as a function of cutting speed using regression analysis. The coefficient of determination for the equation of the correction factor K_{CLF} is:

$$K_{CLF} = \frac{2.6919 v_c^{-0.173}}{a} V_{CL}^{\frac{0.0864\ln(v_c)-0.4733}{b}} \qquad (2)$$

The energy flow towards the workpiece can be estimated by the product of the two correction factors K_W, K_{CLF} and the cutting power. Depending on the cutting speed and cooling lubricant flow, the percentage of the energy flow towards the workpiece is between 60% and 80% of the total cutting power.

Empiric analytical prediction model. Based on the empirical knowledge of cutting force and the analytical considerations of an analytical heat flow density an empirical-analytical prediction model is derived in the following. The model is used to predict the process-related influences on the surface zone taking into account the heat flow density towards the workpiece.

Using the presented empirical force model and the mathematical description of the model parameters, the heat flow density can be calculated for every trial. In addition to the magnitude, the residence time of the heat flow density also has a major impact on the influence on the surface zone. The residence time of the heat flow density for one point on the surface equals the contact time t_c between tool and workpiece for the same point. The contact time for generating gear grinding can be calculated with Equation 3, (Ref. 25).

$$t_C \approx \frac{\Delta\varphi_C z}{2\pi n_0 z_0} \qquad (3)$$

As with tool and process variables, the contact time is also dependent on the workpiece geometry. The contact time is calculated by the rotational speed of the tool n_0, the number of starts z_0, the number of teeth of the workpiece z and the

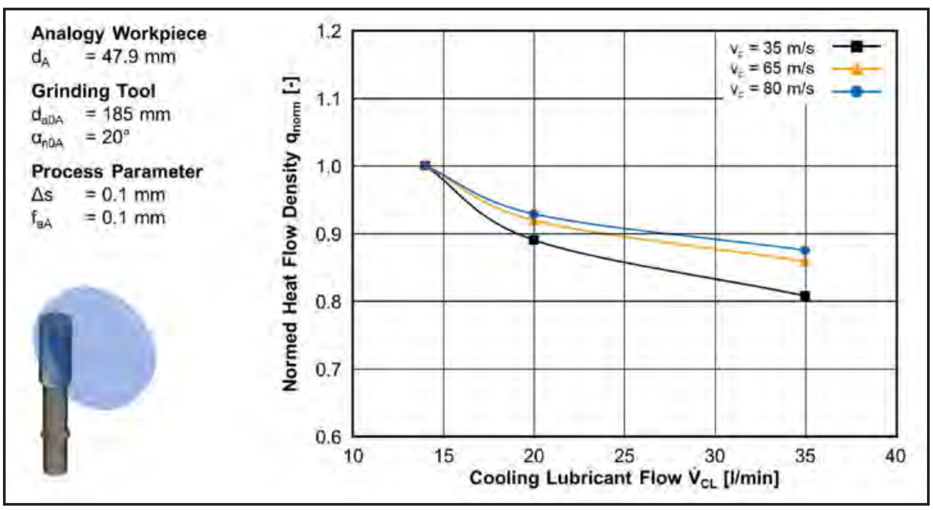

Figure 7 Determination of correction factor for consideration of cooling lubricant.

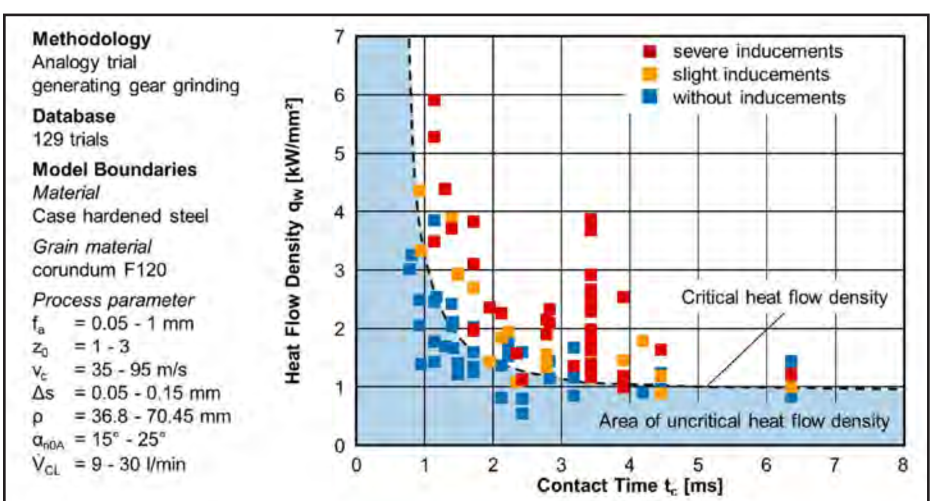

Figure 8 Surface zone inducements depending on heat flow density.

rolling angle of the cutting width $\Delta\varphi_c$. The rolling angle describes the required arc segment, which must be passed in order to achieve the width of contact between tool and workpiece at the respective profile point.

For the analogy trails, the heat flow density is plotted against the contact time (Fig. 8). For this purpose, the heat flow density was calculated for each point of the analogy trails. The workpieces from the analogy trails are marked in different colors according to the type of influence on the surface zone. Points that have been highlighted in yellow and red show a slight to strong influence on the surface zone of the analogy workpiece. Points marked in blue represent non influenced surface zones. As a detection method nital etching was used. For disposition of detrimental surface zone inducements an additional quantitative damage classification was performed using the measurement of Barkhausen noise.

The analysis shows that for a short contact time a high heat flow density can flow into the workpiece without causing damage. In contrast, at long contact times only a low heat flow density is necessary to harm the surface zone. With increasing contact time, the critical limit asymptotically approaches a constant level. From this distribution, the contact time depending limit of the critical heat flow density can be determined from the graph and described mathematically.

The calculated critical heat flow density is shown as a black dashed line in the graph. Considering the simplified assumptions for the calculation of the correction factors as well as the contact time and the dispersion of results, a very well approximation for determining the critical heat flow density can be found.

In summary it can be stated that the empirical-analytical model is suitable to determine the critical limit, which leads to grinding burn. However, it must be determined whether the model, which is based on analogy trail results, can be applied to actual generating gear grinding. For this purpose, the prediction model must first be validated with the sample gear that is mapped in the analogy trail.

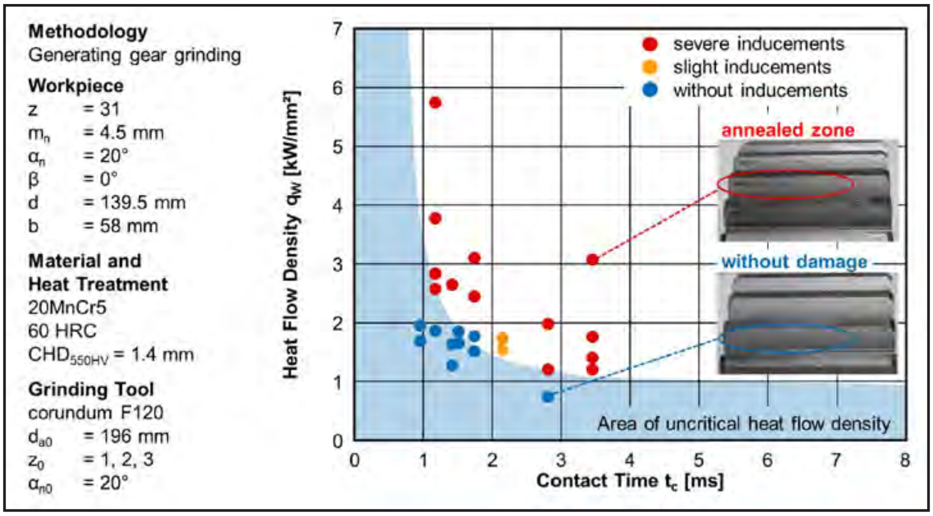

Figure 9 Model validation for sample gear.

Validation of the Prediction Model

The prediction model constructed on basis of analogy trails is compared and validated in the following with results from generating gear grinding trials. First, the transferability of the model to generating gear grinding is validated. For this purpose grinding tests are carried out with the sample gear that is mapped in the analogy trail. Subsequently, the model is validated on an additional gear.

Transfer to generating gear grinding. For the validation of the prediction model a deductive approach is chosen in the following. The general model was applied to a particular case to validate the findings. For the gear that is mapped in the analogy trail, the heat flow densities have been calculated for each set of process parameters. The classification of heat flow densities and surface zone inducements in the analytical empirical prediction model is shown in Figure 9.

The results of generating gear grinding trials were arranged in the characteristic field of the heat flow density of the prediction model. The heat flow densities shown are calculated for the pitch circle diameter of the sample gear. The degree of influence on the surface zone has been marked in analogy to the previous illustrations. The range of non-critical heat flow density is identical due to the geometric relationship between analogy trail and sample gear.

All points for which no detrimental surface zone inducement was observed after generating gear grinding are with one exception within the non-critical area. The heat flow densities of the components with slight and severe detrimental inducements are larger than the calculated critical heat flow density of the prediction model.

The evaluation shows that the prediction model is able to predict the occurrence of grinding burn in good accuracy for the sample gear. The results of the generating gear grinding trials reflect the determined findings and identified relationships from the analogy trail. Thus, the prediction model has been validated for the sample gear. Whether the prediction model can be applied to additional gears must be examined in the following.

Validation with additional gears. In order to test the transferability of the empirical-analytical prediction model, the model is applied to another spur gear. Therefore further generating gear grinding trials were performed.

The design of experiments was defined by using the prediction model. For this, the process parameters were predicted for both clearly damaged and not affected tooth flanks. The gears have been inspected after grinding by means of nital etching to evaluate and document surface zone inducements.

As a second application a planetary gear of a construction machine is selected. In contrast to the previous gear, the present gear has a higher module and a higher face width. The gear geometry and further details of material and heat treatment can be found in Figure 10.

The results of the second gear geometry are shown (Fig. 11); for these trials tools with different number of starts were used.

The calculated critical heat flow density for the pitch circle diameter limits the damaged and non-damaged gears with a good accuracy. Different forms of surface zone inducements are shown in the lower part of Figure 11. All workpieces with a detrimental inducement show a damaged zone near the tip area.

Severely damaged components show a dark coloration over a large part of the profile. In addition to the qualitative statement about whether surface zone damage is to be expected, the heat flow density can be calculated on the basis of the local approach for any point of the gear flank.

To explain the process-related detrimental inducement in the tooth tip area, the distribution of the heat flow density has been calculated for a process design for the entire tooth profile. The results are compared with results of nital etching in Figure 12.

The occurrence probability of a surface zone inducement is marked in color on the tooth height. In the black and blue areas no surface zone inducement is to be expected. In the transition between the light blue and the yellow area there may be a slight damage. In the tooth tip area, the critical heat flow density is exceeded and therefore a damaged surface zone is expected. This area is marked in red.

The distribution over the tooth height can be explained by the cause-effect relationships, determined in the analogy trails. With an increase in the radius of curvature the cutting forces increase as well. This results in a varying heat input over the tooth profile. The highest cutting force and therefore the largest heat flow density on the tooth flank is present at the tooth tip. This result is well-correlated with the results of nital etching.

In feed direction the affected zone is growing in contrast to calculation results. The main reason for the expansion of the damaged zone is wear of the grinding worm. With increasing machining time also the friction and therefore the cutting force as well as the heat flow density increases. In the prediction model the wear of the grinding wheel is not taken into account. For this reason, predicted and actual damage differ.

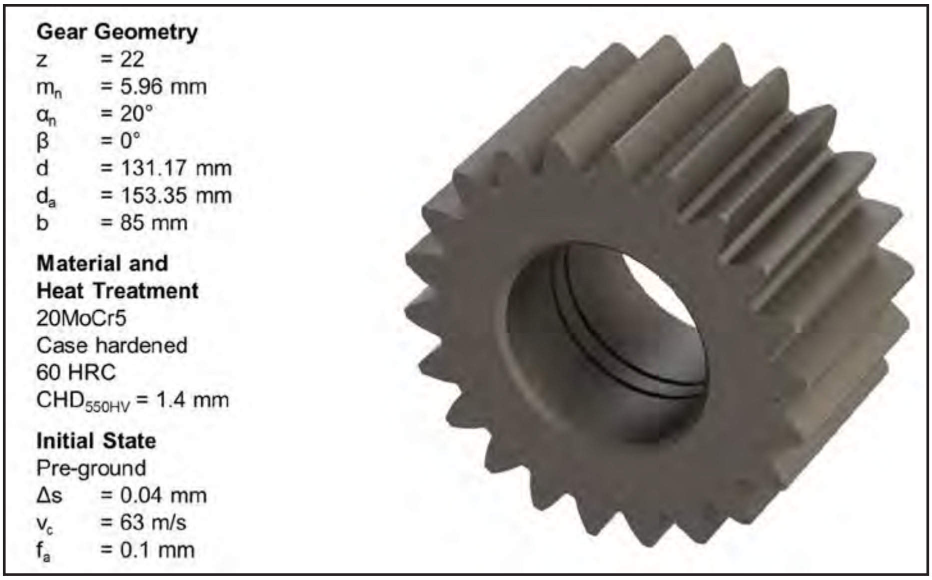

Figure 10 Gear geometry of planetary gear.

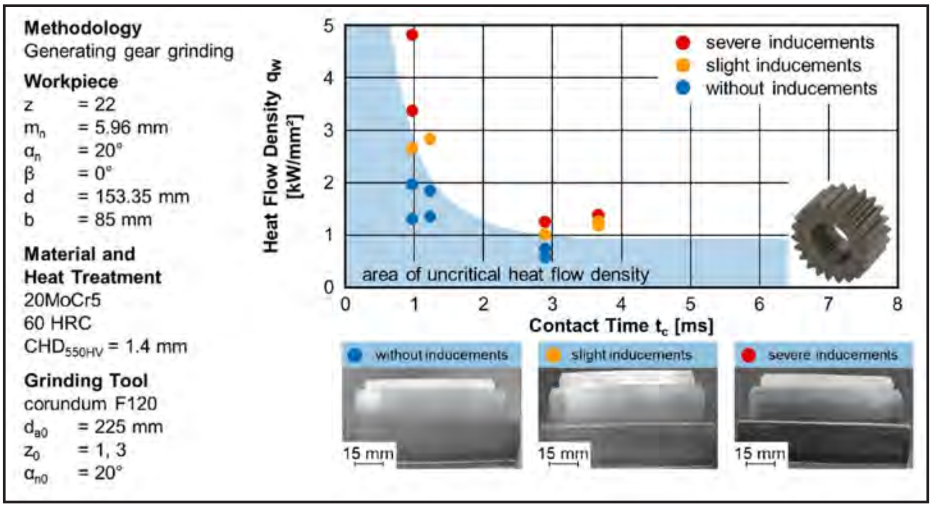

Figure 11 Application of prediction model for planetary gear.

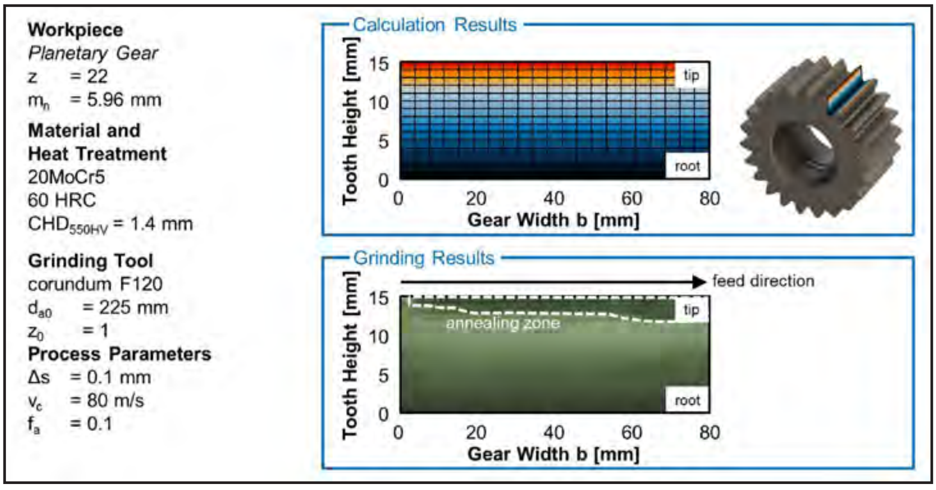

Figure 12 Comparison of local heat flow density and process results.

By applying the predictive model to an additional gear, the applicability was tested for other geometries. It turns out that the prediction model derived from the analogy trail can also be used to predict a detrimental inducement of the surface for additional geometries.

Summary and Outlook

The thermo-mechanical surface zone inducement is an important quality criterion for functionality of gears. Also for generating gear grinding it is necessary to determine thermal and mechanical loads and their influencing factors to avoid damage of the surface zone.

The research objective of this report was to derive a model to describe and predict detrimental surface zone inducements for generating gear grinding. Therefore, the necessary model parameters and correction factors were determined. Subsequently, the model was validated using two gear geometries.

The objective of this report was met through validation of the predictive model. The model for predicting detrimental surface zone inducements will help increase the efficiency and process reliability of continuous generating gear grinding and improve the description and understanding of the technological cause and effect relations.

In the next step the derived empirical analytical prediction model should be linked with a manufacturing simulation. The combination of a local determination of chip geometries and the automated calculation of the existing model parameters will allow widespread use of the model in industrial applications. Furthermore, it will significantly improve the process design and optimization in continuous generating gear grinding. In addition, the cutting force model can be extended with a link to a manufacturing simulation. With the help of calculated chip geometries it is likely possible to find a correlation between chip geometries and the measured cutting forces.

Besides the optimization of the model a further development of the analogy trail is possible. With the analogy trail, an evaluation of the performance of grinding worms for generating gear grinding can be performed. So on the one hand, a pre-selection of grinding worm specifications is possible and on the other hand the wear behavior could be analyzed better due to the simple geometry of the grinding tool.

References

1. Schlattmeier, H. Diskontinuierliches Zahnflankenprofilschleifen mit Korund, Dissertation, RWTH Aachen, 2003.
2. Meijboom, L. Erhöhung der Wirtschaftlichkeit beim Wälzschleifen durch Verbesserung des
3. Zerspannvorgangs, Dissertation, RWTH Aachen, 1979. 3. Türich, A. *Werkzeugprofilerzeugung für das Verzahnungsschleife*, Dissertation, Universität Hannover, 2002.
4. Bausch, T., *Moderne Zahnradfertigung. Verfahren und Maschinen zur kostengünstigen Herstellung von Stirn- und Kegelrädern mit hoher Qualität,* 3. Auflage, Expert Verlag, Renningen-Malmsheim, 2006.
5. Stimpel, F.*Technologische Kenngrößen für das kontinuierliche Wälzschleifen von Evolventenverzahnungen,* Dissertation, Universität Hannover, 2009.
6. Klocke, F. and König, W., *Fertigungsverfahren Band 2: Schleifen, Honen, Läppen.* 4. Auflage, VDIVerlag, Düsseldorf, 2005.
7. Reichel, F. *Verfahrensauswahl beim Schleifen von Großverzahnungen,* Seminar: Feinbearbeitung von Zahnrädern, WZL der RWTH Aachen, November 2007.
8. Sulzer, G. *Werkzeugmaschinen zum Feinbearbeiten der Zahnradflanken von vorverzahnten Zahnrädern,* Europäische Patentschrift EP0282046, Liebherr Verzahntechnik, Kempten, 1993
9. Klocke, F., C. Gorgels, and J. Reimann. *Generating Gear Grinding – New Possibilities in Process Design and Analysis,* AGMA Fall Technical Meeting 2011, 11FTM02, ISBN 978-1-61481-001-8.
10. Klocke, F., C. Gorgels and J. Reimann. *Analyse des kontinuierlichen Wälzschleifens mithilfe der Durchdringungsrechnung,* In: 50. Arbeitstagung „Zahnrad und Getriebetechnik", Hrsg.: Klocke, F.; Brecher, C., Eigendruck Getriebekreis Aachen, S.14-1 - 14-40, 2009.
11. Klocke, F., C. Gorgels and J. Reimann. *Kontinuierliches Wälzschleifen von Verzahnungen – Softwareunterstützte Prozessoptimierung,* In: WB Werkstatt und Betrieb, Jg. 142, Heft 5, S.62-63, 2009.
12. Klocke, F., C. Gorgels and J. Reimann. *Ansatz für ein Prozesskraftmodell für das kontinuierliche Wälzschleifen von Verzahnungen,* In: 51. Arbeitstagung „Zahnrad und Getriebetechnik", Hrsg.: Klocke, F.; Brecher, C., Eigendruck Getriebekreis Aachen, S.8-1 - 8-40, 2010.
13. DIN 3960. *Begriffe und Bestimmungsgrößen für Stirnräder (Zylinderräder) und Stirnradpaare (Zylinderradpaare) mit Evolventenverzahnung,* Hrsg. Deutscher Normenausschuss, März 1987.
14. Vits, R. *Technologische Aspekte der Kühlschmierung beim Schleifen,* Dissertation, RWTH Aachen, 1985.
15. Takazawa K. *Effects of Grinding Variables on Surface Structure of Hardened Steel,* In: Bulletin of the Japan Society of Grinding Engineers, Volume 2, S. 14-21, 1966.
16. Hoffmeister, H.-W and B. Denkena. *Jahrbuch Schleifen, Honen, Läppen, Polieren: Verfahren und Maschinen*, Vulkan-Verlag, Essen, 63. Ausgabe, ISBN 3-802-72941-2, Oktober 2007.
17. Gorgels, C. *Entstehung und Vermeidung von Schleifbrand beim diskontinuierlichen Zahnflankenprofilschleifen*, Dissertation, RWTH Aachen, 2011.
18. Grof, H.E. *Beitrag zur Klärung des Trennvorgangs beim Schleifen von Metallen,* Dissertation, TU München, 1977, 15 14FTM02.
19. Hoffmeister, H.-W. and H.K. Tönshoff. *Jahrbuch Schleifen, Honen, Läppen, Polieren: Verfahren und Maschinen,* Vulkan-Verlag, Essen, 61. Ausgabe, 2004.
20. Lowin, R. *Schleiftemperaturen und ihre Auswirkungen im Werkstück,* Dissertation, RWTH Aachen, 1980.
21. Rowe, W.B., S.C.E. Black, B. Mills, H.S. Qi and M.N. Morgan. *Experimental Investigation of Heat Transfer in Grinding*, In: Annals of the CIRP, Volume 44/1/1995, S. 329-332.
22. Steffens, K. *Thermomechanik des Schleifens,* Dissertation, RWTH Aachen, 1983.
23. Heinzel, C. *Schleifprozesse verstehen: Zum Stand der Modellbildung und Simulation sowie unterstützender experimenteller Methoden,* Habilitation, Universität Bremen, 2008.
24. Tönshoff, H.K., J. Peters, I. Inasaki and T. Paul. *Modelling and Simulation of Grinding Processes,* In: CIRP Annals 41(2):677–688, 1992.
25. Schriefer, H., W. Thyssen, W., Wirz, G. Scacchi and M. Gretler. *Kontinuierliches Wälzschleifen von Verzahnungen*, 1. Auflage, Eigenverlag Reishauer AG, Wallisellen, 2008.

Dipl.-Ing. Matthias Ophey studied mechanical engineering at RWTH Aachen University with a focus on production engineering. Upon graduation in 2013 he became a scientific research assistant in the gear department of the Laboratory of Machine Tools and Production Engineering (WZL). Ophey's research is dedicated to focusing on hard finishing of gears — especially generating gear grinding, and manufacturing-related properties.

Dr. Jan Reimann is a 2008 graduate of RWTH Aachen University, having studied mechanical engineering with a focus on production engineering. He began working in 2008 — first as scientific research assistant and later as team leader — in the gear department of the Laboratory of Machine Tools and Production Engineering (WZL). While there he has published his doctoral thesis on generating gear grinding. Today Reimann is a production engineer at Siemens Mechanical Drives in Bocholt, focusing on manufacturing technology development.

Fundamental Study of Detection of Plastic Gear Failure Signs (Synchronization of a Non-Linear Oscillator with Mesh Frequency)

Daisuke Iba, J. Hongu, Hidetaka Hiramatsu, M. Nakamura, T. Iizuka, A. Masuda, I. Moriwaki and A. Sone

This paper proposes a new method — using neural oscillators — for filtering out background vibration noise in meshing plastic gear pairs in the detection of signs of gear failure. In this paper these unnecessary frequency components are eliminated with a feed-forward control system in which the neural oscillator's synchronization property works. Each neural oscillator is designed to tune the natural frequency to a particular one of the components.

Introduction

The trend towards an increase in plastic gear usage has continued because it is cost-effective; low-density; capable of absorbing vibration; its ability to operate with no lubrication, and so on. If the limitation of plastic gears relative to metal gears were to be improved as a result of new developments in both materials and processing, plastic gears could be used under more severe conditions, such as high load and/or high rotation speed. But even before that, if, say, an emergency shutdown system could be provided to respond in a safe manner, applications for plastic gears would be more widespread. And yet, there are not many studies concerning a failure detection system for plastic gears compared with metal gears.

Iba et al (Ref. 1) carried out rotation fatigue tests of POM (polyoxymethylene) gears using their developed power-absorb-type gear test rig, and analyzed effects of gear tooth cracks at their root on measured acceleration responses. The acceleration responses were measured with a pick-up set at the top of a housing of the driven-side gear shaft bearing during the operation tests; frequency analyses were carried out to identify dominant frequency components in the tests. As a result of the frequency analyses the responses included not only the DC, shaft frequency, its harmonics, fundamental meshing frequency, some mesh harmonics and its modulating sidebands, but also rolling elements noise of bearings, motor vibration and its harmonics, and so on. The particularly conspicuous frequency components in the responses were the shaft rotation frequency; fundamental meshing frequency; and some meshing harmonics and its modulating sidebands — whose frequency is the same as the shaft frequency. The responses were strongly affected by amplitude and frequency modulations. These modulation phenomena may be due to the fact that plastic gears are so flexible in that their tooth stiffness is lower than that of metal gears, and are thus subject to greater dimensional instabilities due to their larger coefficient of thermal expansion. These modulating components complicate the procedure of analysis of the acceleration responses and hide plastic-gear-failure signs. In the frequency analyses of the response data, the peak of the meshing frequency results in a slight change in complete tooth fracture. The response data include amplitude modulation; frequency modulation; rolling elements noise of bearings and motor; driving torque variation; and so on. Such complex data make detection of gear failure signs difficult, because the detection requires distinguishing slight changes in complex data.

On the other hand, non-linear oscillators — which were models for rhythm generators consisting of neurons — have been studied in biological study (Ref. 2) and are known as "neural oscillators." Neural oscillators have a specific property to synchronize with periodic, external inputs in a certain frequency range. Mathematical models of the neural oscillators were also proposed and examined (Refs. 3–4), and their applications to walking robots were reported (Refs. 5–6). Iba and Hongu studied a new control system for active, mass dampers using the mathematical model of the neural oscillators that can track the vibration behavior of high-rise buildings due to this synchronization characteristic (Refs. 7–8). These studies provide the knowledge that the neural oscillator can be used as an adaptive notch filter that filters out the background noise of vibration and follows a variation of a designated frequency — autonomously.

In this study a new signal processing method has been developed using neural oscillators to filter out the background noise of vibration in meshing plastic gear pairs for detection of failure signs. As mentioned above, the acceleration responses — which are measured at the top of the bearing housing during operating tests — include multiple frequencies. If these unnecessary frequency components were eliminated from the responses, it would be easy to detect gear failure signs. But the normal notch filter cannot follow the change in the designated, unnecessary frequencies by driving torque variation, and the adaptive notch filter needs a periodic reference signal to follow the change. Therefore a new filter system (or feed-forward-type noise-cancelling system) — using neural oscillators that can autonomously follow the change due to their synchronization properties — is developed in this study. Each neural oscillator is designed to tune the natural frequency to a particular frequency of the components. This tuning process is called on for the removal. Moreover, the output phase of the oscillators is set at a difference of 180° from the input phase, and is combined with

This paper was originally presented at the 2014 International Gear Conference, Lyon Villeurbanne, France and is republished here with the authors' permission.

the original, measured response to eliminate unnecessary components. The ultimate goal is to detect the failure signs of gears from the output of the proposed filter system, but while development of the filter system is discussed in this paper, there is no direct mention of its failure detection method. The basic concept of the proposed system is introduced, after which the neural oscillator that constructs the proposed filter system and the configuration of the feed forward control system are explained. Next, a simulated acceleration response of a meshing gear pair is constructed and the proposed noise cancellation system is applied to the simulated response to confirm the validity of the proposed system.

Neural Oscillator

In this section the mathematical model of a neural oscillator is introduced, and the synchronization property of the oscillator — a key capability of nonlinear oscillators — is explained.

Mathematical model. Here Matsuoka's neural oscillator is used as the neural oscillator (Refs. 3–4). The mathematical model of Matsuoka's neural oscillator is expressed as follows:

$$\dot{X}_{M,i}(t) = A_M X_{M,i}(t) + B_M \max(0, X_{M,i}(t)) + C_M = F_M(X_{M,i}(t)) \cdots i = 1,2 \tag{1}$$

Where, t is a time, and

$$X_{M,i}(t) = [x_{e,i}(t) \;\; x_{f,i}(t) \;\; x'_{e,i}(t) \;\; x'_{f,i}(t)]^{tr} \tag{2}$$

$$A_M = \begin{bmatrix} -1/\tau & 0 & -b/\tau & 0 \\ 0 & -1/\tau & 0 & -b/\tau \\ 0 & 0 & -1/T & 0 \\ 0 & 0 & 0 & -1/T \end{bmatrix}, B_M = \begin{bmatrix} 0 & -a/\tau & 0 & 0 \\ -a/\tau & 0 & 0 & 0 \\ 1/T & 0 & 0 & 0 \\ 0 & 1/T & 0 & 0 \end{bmatrix}, C_M = \begin{bmatrix} s/\tau \\ s/\tau \\ 0 \\ 0 \end{bmatrix} \tag{3}$$

This model contains two first-order lag elements to express excitation and inhibition, and can generate sustained oscillation. Generally, the five coefficients — s, τ, T, b, a — have been decided by identification of a biological neuron, but the specified animate being is not considered in this study. These parameters are chosen by our design method to generate the oscillation with a desired natural frequency (Ref. 8).

Further, in order to narrow the synchronization region to the rhythm generator, a mutual inhibition connection consisting of two neural oscillators is considered as follows:

$$\begin{cases} X_{M,1} = F_M(X_{M,1}) + G\max(0, X_{M,2}) \\ X_{M,2} = F_M(X_{M,2}) + G\max(0, X_{M,2}) \end{cases} \tag{4}$$

Where, considering the connection weight w, the matrix to connect the two oscillators is obtained as follows:

$$G = \begin{bmatrix} w & -w & 0 & 0 \\ -w & w & 0 & 0 \\ 0 & 0 & 0 & 0 \\ 0 & 0 & 0 & 0 \end{bmatrix} \tag{5}$$

Moreover, if $X_D = [X_{M,1} \;\; X_{M,2}]^{tr}$, the equation, which expresses the dynamics of the neural oscillator, is given as follows:

$$X_D = F_D(X_D) \tag{6}$$

Synchronization property. When the oscillator is subjected to an external periodic signal $p(\Omega t)$, the mathematical model of Matsuoka's neural oscillator becomes:

$$\dot{X}_D(t) = F_D(X_D) + E_D p(\Omega t) \tag{7}$$

Where, E_D is an input matrix as follows:

$$E_D = [\varepsilon \;\; -\varepsilon \;\; 0 \;\; 0 \;\; 0 \;\; 0 \;\; 0 \;\; 0]^{tr} \tag{8}$$

Here, ε is an input gain, and $p(\Omega t)$ is a normalized sinusoidal signal whose frequency is Ω. If the frequency Ω is partially close to the Eigen frequency ω_D of the neural oscillator, the oscillator is thus synchronized with the external sinusoidal wave.

This synchronization phenomenon can be seen when the detuning Ω-ω_D between the oscillator's frequency ω_D and the external periodic force's frequency Ω is a finite value. According to an analysis by the phase reduction method (Refs. 9–10), the synchronization region $\varepsilon\Gamma_{min} < \Omega\text{-}\omega_D < \varepsilon\Gamma_{max}$ is decided. Here, $\Gamma_{min, max}$ is the phase coupling function of the oscillator.

Figure 1 shows a synchronization region of the neural oscillator (Table 1). The colored area is the region also known as Arnold's tongue. In this figure the horizontal axis is the frequency Ω of input, and the vertical axis is the amplitude ε of input. It is clear that the synchronization region has spread from the oscillator's frequency $\omega_D = 1$ — when the amplitude of the external forcing is increased. The synchronization region depends on the amplitude of the forcing. Increased the coefficient for the external forcing in the neural oscillator, the region can be freely adjusted. The color in this figure shows the phase difference (phase locking points) between input/output of the neural oscillator.

Table 1 Parameters of neural oscillator

Parameters	Value
s	1.634
τ	0.212
T	2.54
b	2.52
a	2.52
w	-7.046

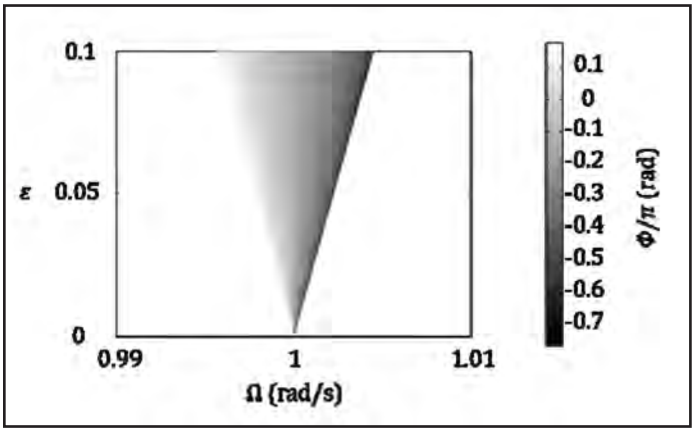

Figure 1 Synchronizing region of neural oscillator.

While the neural oscillator has a sensitive reaction to the sinusoidal input within the synchronization region, it does not have the same sensitivity to the input outside of the region. Thus the neural oscillator can be used as an adaptive, single-frequency generator, and as an adaptive notch filter to cancel the unnecessary frequency component in the vibration response of the meshing gears.

Gear Meshing

In this section a model of gear meshing vibration in a circumferential direction — used for verification of a proposed noise-cancellation system by simulation — is explained. Later, amplitude and frequency modulation caused by the eccentricities of gears are considered.

Dynamic loads on gear teeth. A simple vibration model in meshing gear pairs is used for simulation (Fig. 2). Each gear has a mass and is connected to the other by a spring and damper (Ref. 11). This vibration model — in a circumferential direction — is considered to be a single-degree-of-freedom vibration system as follows:

$$\ddot{x}_{th,\ meshing}(t) + 2\zeta_g \omega_g \dot{x}_{th,\ meshing}(t) + \omega_g^2 x_{th,\ meshing}(t) = \omega_g^2 e(t) \tag{9}$$

Where, $\ddot{x}_{th,\ meshing}(t)$ is spring deflection of the vibration system; ω_g is the natural frequency of the system; ζ_g is the damping ratio depending on the gear material; $e(t)$ is tooth profile

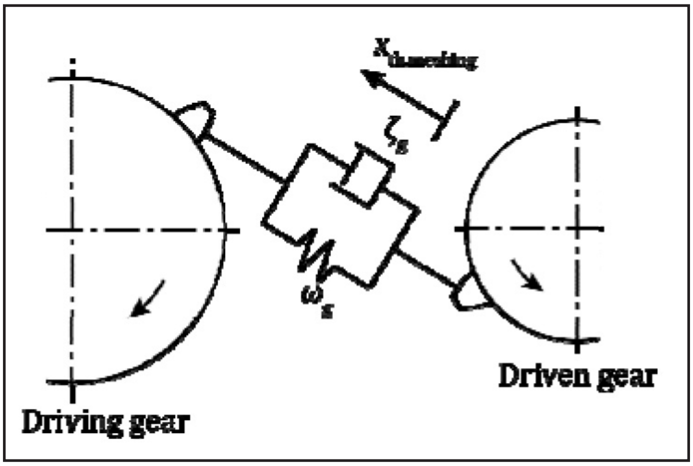

Figure 2 Vibration model in meshing gear pairs.

error — and this error is the input displacement to the system. Here it was assumed that the driving torque variation of the rotating shaft was small and the effect of the shaft stiffness on the line of action of force was small as well.

A meshing condition of a spur gear pair varies with time t. Considering the meshing period T_z, periodic change of total tooth stiffness during $0 \leq t < z_2 T_z$ is expressed as follows:

$$T_{smooth}\dot{\omega}_g(t) + \omega_g(t) = \begin{cases} \sqrt{\omega_{g,j-1}{}^2(t' + T_{1-2}) + \omega_{g,j}{}^2(t')} & if\, 0 \leq t' < T_{1-2} \\ \omega_{g,j}(t') & else \end{cases} \tag{10}$$

In this study, the tooth profile error $e(t)$ is also expressed as follows:

$$e(t) = \begin{cases} E_0 \sin\left(\dfrac{\pi}{\varepsilon_{th} T_z}(t' + T_{2-1})\right) + E_0 \sin\left(\dfrac{\pi}{\varepsilon_{th} T_z} t'\right) \\ E_0 \sin\left(\dfrac{\pi}{\varepsilon_{th} T_z} t'\right) \end{cases} \tag{11}$$

Where, ε_{th} is contact ratio of the spur gear pair, and is obtained as follows:

$$t' = t - (j-1) \times T_z - r \times z_2 T_z \tag{12}$$

$\omega_{g,j}$ is the time-varying, natural frequency of the meshing gear system during meshing period that is derived from Ishikawa's tooth stiffness variation and the equivalent inertia mass on the pitch circle (Ref. 12). In addition, subscript j indicates the number of meshing tooth pairs, obtained as follows:

$$\begin{cases} j = fix\left(\dfrac{t - r z_2 T_z}{T_z}\right) + 1 \\ r = fix\left(\dfrac{t}{z_2 T_z}\right) \end{cases} \tag{13}$$

By using contact ratio ε_{th}, the transition time $T_{2\text{-}1}$ from two pair teeth in mesh to a single pair is obtained as follows:

$$T_{2-1} = (\varepsilon_{th} - 1) \times T_z \tag{14}$$

And T_{smooth} is a time constant of a first-order lag system to vary the natural frequency smoothly, here as $T_{smooth} = \sigma_{smooth} T_z$.

$X_{th,meshing}$ changes periodically, the timeframe dependent upon the rotation of the driven gear as follows:

$$x_{th,\ meshing}(t) = x_{th,\ meshing}(t + z_2 T_z) \tag{15}$$

Amplitude and frequency modulation by an eccentric error of a driven gear. Generally the vibration caused by the tooth-to-tooth meshing of a rotating gear pair contains various frequency components that are due not only to amplitude and frequency modulation caused by eccentricity of gears, but also to the rolling-elements noise of bearings, motor vibration and its harmonics, and so on. The effects of these unnecessary components on the measured vibration make detection of gear faults — such as gear tooth cracks — difficult.

In this subsection a model that includes the amplitude and frequency modulation caused by an eccentric error of a driven gear is considered. Considering the meshing frequency $\omega_z = 2\pi/T_z$, the periodic variable is expressed as follows:

$$x_{th,\ meshing}(\omega_z t) = x_{th,\ meshing}(\omega_z t + 2\pi) \tag{16}$$

The effect of amplitude and frequency modulation on the variable can be expressed as follows
(Ref. 13):

$$x_{th,\ meshing,\ AM,\ FM}(t) = \{1 + k_a \cos(\omega_m t)\} \times x_{th,\ meshing}\{\omega_z t + m_f \sin(\omega_m t)\} \tag{17}$$

Where,

$$\begin{cases} \omega_m = \omega_z / z_2 \\ m_f = e_2 \times \dfrac{z_2}{(1 + z_2/z_1)\sin\alpha} \end{cases} \tag{18}$$

and e_2 is the ratio of the radius of pitch circle of the driven gear to the eccentric error of the gear; k_a is the amplitude modulation factor; m_f is the frequency modulation factor; α is the pressure angle; and z the tooth number.

Numerical simulation of meshing gear vibration. According to the abovementioned gear model, numerical simulations of

Table 2 Parameters of gears

	Driving gear	Driven gear
Module (mm)	1.0	
Pres. angle (deg)	20.0	
Number of teeth	67	48
Face width (mm)	10	8
Equivalent inertia weight (kg)	1.8195	0.0085
Damping ratio	0.2	
Stiffness (GPa)	230	2.6
k_a	-	0.5
e_2	-	0.003
E_0 (mm)	0.001	
Revolution per second	-	50

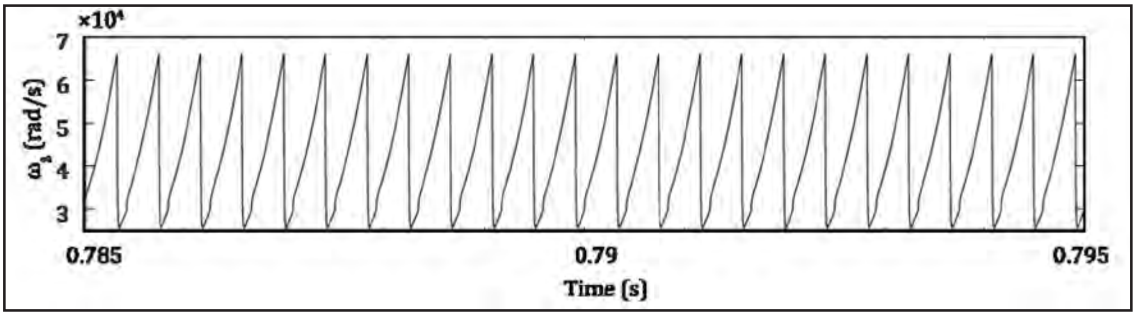

Figure 3 Natural frequency of gear meshing.

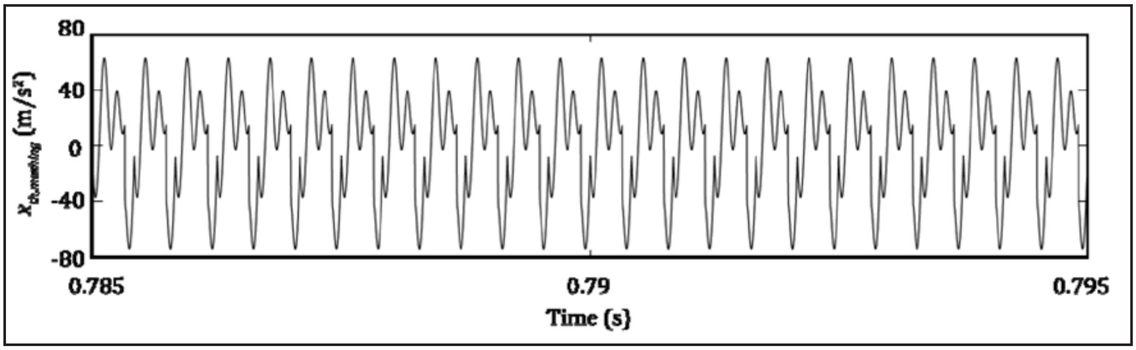

Figure 4 Acceleration response of gear meshing.

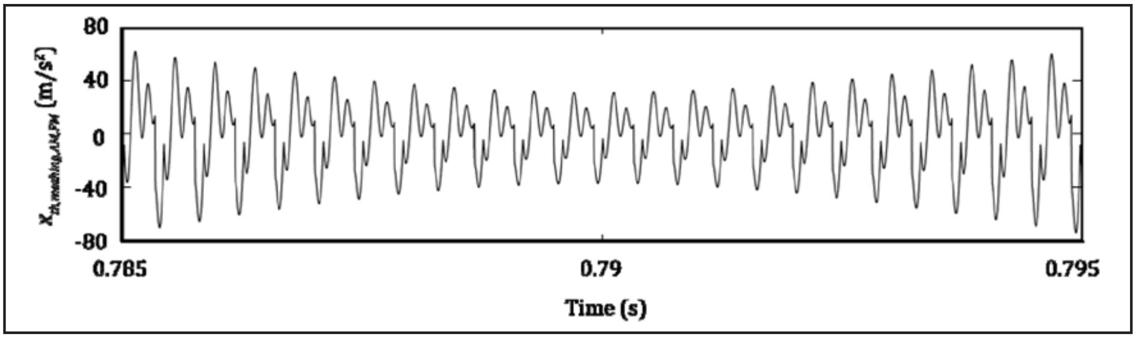

Figure 5 Acceleration response of gear meshing with AM and FM.

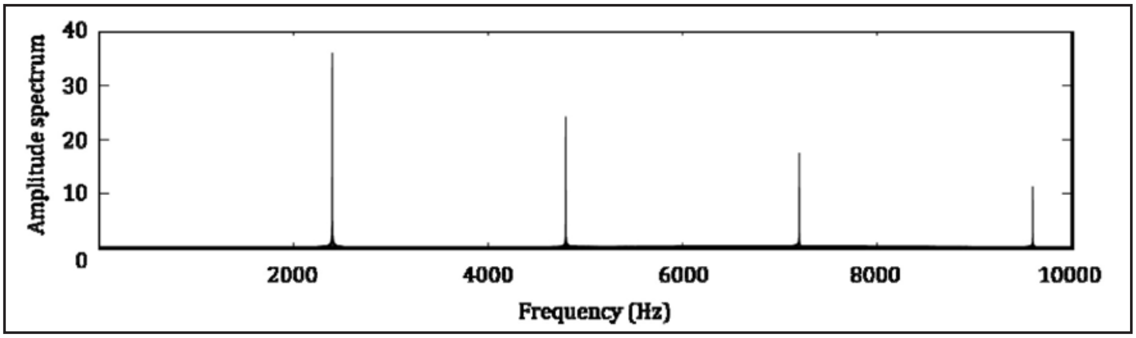

Figure 6 FFT of gear meshing.

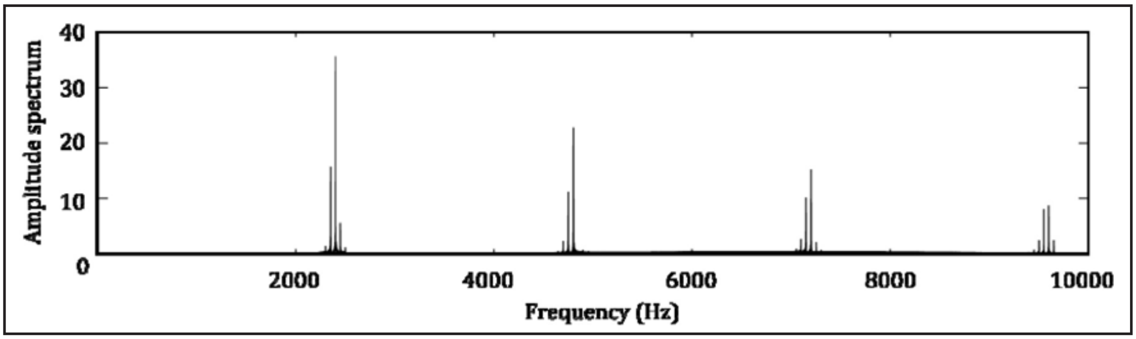

Figure 7 FFT of gear meshing with AM and FM.

meshing gears are carried out using the Runge-Kutta Fourth Order Method (Table 2). The step time of the simulations is $10^{-6}\,s$, and $\sigma_{smooth} = 10^{-2}$.

The results of numerical simulations are shown in following figures. Figure 3 shows the change of the natural frequency of the system. In this figure the natural frequency changed periodically because the meshing condition of a spur gear pair varied with time t. In considering the change of the natural frequency, the acceleration response of the system is obtained (Fig. 4). As for the eccentric error of the gear, the acceleration response of the system is subject to influence by both amplitude and frequency modulation (Fig. 5). Figures 6 and 7 show the frequency responses, with and without modulation, respectively. As a result of the modulation some sideband peaks can be seen (Fig. 7) when compared with Figure 6.

Noise-Canceling System

Here a noise cancellation system using neural oscillators to filter out the background noise of vibration in meshing plastic gear pairs for detection of failure signs of the gears is explained. The acceleration response, which is measured on the top of the housing at the gear shaft bearing, includes not only the DC; shaft frequency; its harmonics; fundamental meshing frequency; some mesh harmonics; and its modulating sidebands; but also rolling-elements noise of bearings, motor vibration and its harmonics, and so on. Detecting gear faults is much more difficult in the complex response; therefore these unnecessary frequency components should be eliminated from the response.

However, the frequency of the unnecessary components attracts a great amount of influence from the driving torque variation. The proposed new filter system using the neural oscillators can autonomously follow the frequency change of the unnecessary component due to the synchronization property (Fig. 8).

The proposed system has a measured signal and consists of some neural oscillators. The number of oscillators is the same as the number of unnecessary components. Each neural oscillator is designed to tune the natural frequency in to a particular frequency of the component. Moreover, the output of the oscillators is set to be out-of-phase with the input by 180° and is combined with the original, measured response to reduce the amplitude of the unnecessary components. The system is expressed as follows:

$$\begin{cases} X_{D,k} = F_{D,k}(X_{D,k}) + E_{D,k}\, s_g(t) \\ y(t) = s_g(t) - \sum_{k=1}^{n} \beta_{D,k}\, y_{D,k}(t - L_k) \end{cases} \tag{19}$$

where β_{Dk} is an arbitrary output gain of the oscillator, and L_k is a delay time of the system. Moreover, the output of the each oscillator is obtained as follows:

$$y_{D,k}(t) = [1\ \ -1\ \ 0\ \ 0\ \ 0\ \ 0\ \ 0\ \ 0] \cdot \max(0, X_{D,k}) \tag{20}$$

Results of Numerical Simulation

In this section the proposed noise-cancellation system is applied to the simulated response to confirm validity of the system. In this simulation the analyzed signal consists of the abovementioned acceleration response and an unnecessary component 20sin (2π *7,250*t), which is the same frequency of the modulated, third-order, high-frequency content.

Figure 9 shows the abovementioned acceleration response without the noise, and Figure 10 the signal with the noise; in both figures the time is multiplied by 2π *7,250.

As can be seen, the modulated noise complicates the acceleration response of gear meshing, even if the noise consists of the single component.

Next are shown the results of the noise cancellation system. The frequency of the neural oscillator was set to the frequency of the unnecessary component (Table 1). Figure 11 shows the output of the designed neural oscillator and the noise component; as can be seen, the output of the neural oscillator has the same frequency of the noise, and is out-of-phase by 180°.

Figure 12 shows the result of noise cancellation using the original output of the neural oscillator. In this simulation, ε =0.0002 $\beta_D = 20/7$, $L = 5.5s$. In the figure the unnecessary component was reduced by the effect of the proposed filter, but discontinuous changes can be seen due to the non-linear property of the neural oscillator. This non-linear oscillator — having a sinusoidal input — has a limit cycle. If "phase" is pre-defined on the limit cycle, the phase and amplitude of the neural oscillator as a sinusoidal wave can be constructed by the defined "phase." To realize this construction, a phase map was used (Ref. 14). Figure 13 shows the result of noise cancellation using the constructed sinusoidal wave by the neural oscillator and the phase map. As can be seen, the original vibration of gear meshing is reconstructed.

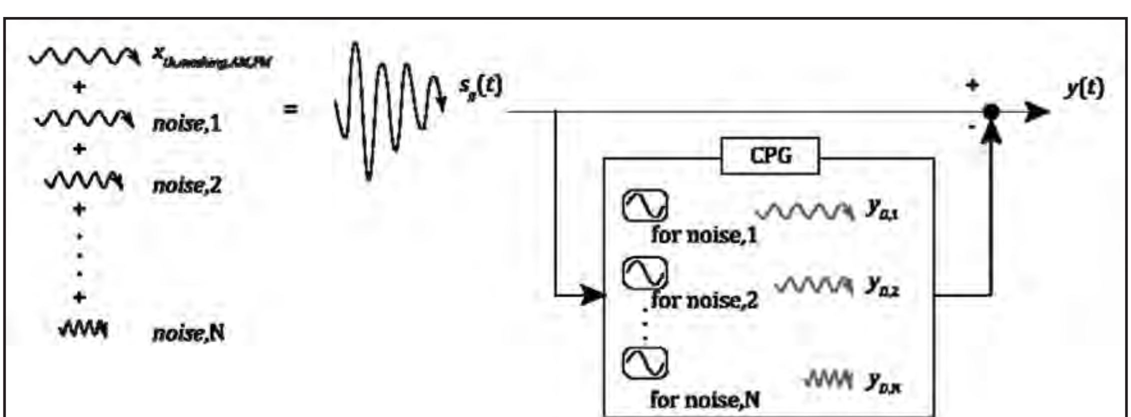

Figure 8 Concept of feed-forward noise cancelling system using neural oscillators.

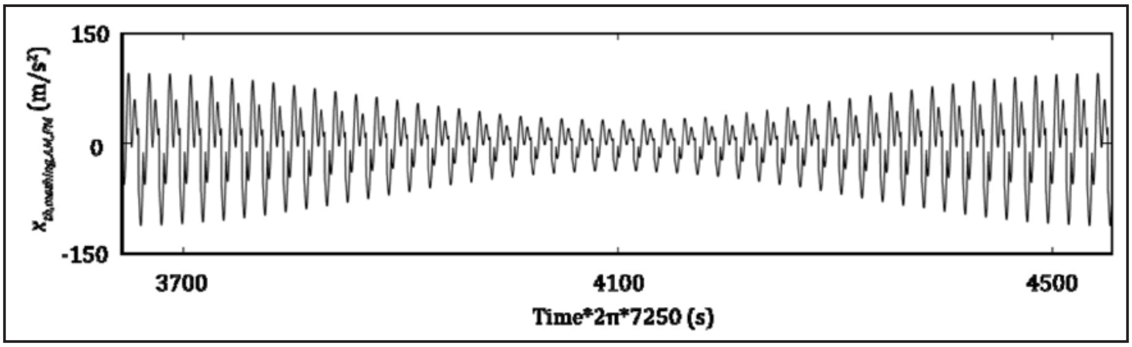

Figure 9 Acceleration response of gear meshing with AM and FM.

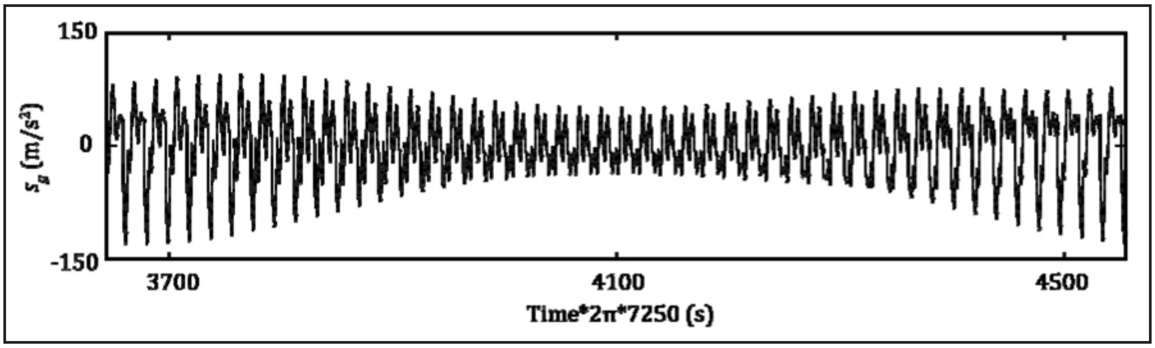

Figure 10 Acceleration response of gear meshing with AM, FM and external noise.

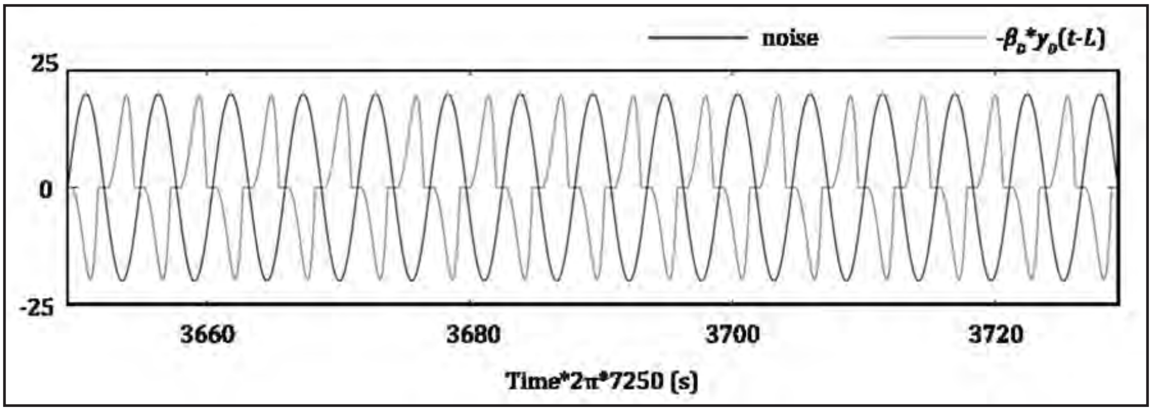

Figure 11 Output of the designed neural oscillator and noise component.

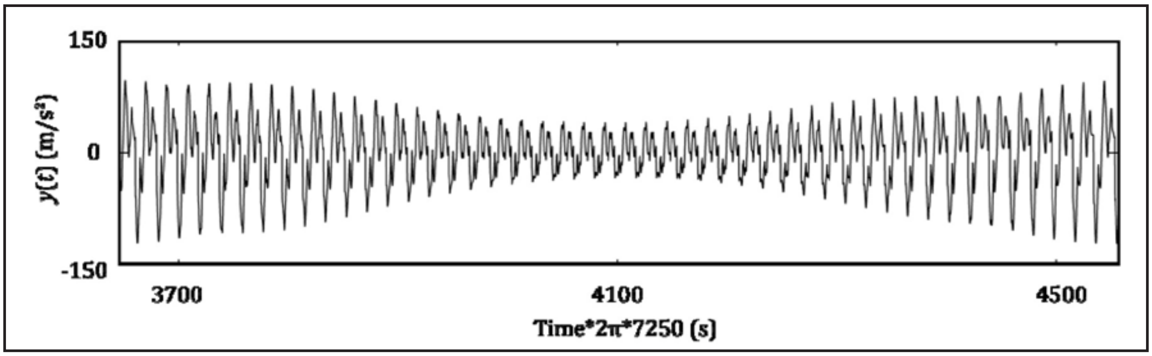

Figure 12 Result of noise cancellation using output of the neural oscillator.

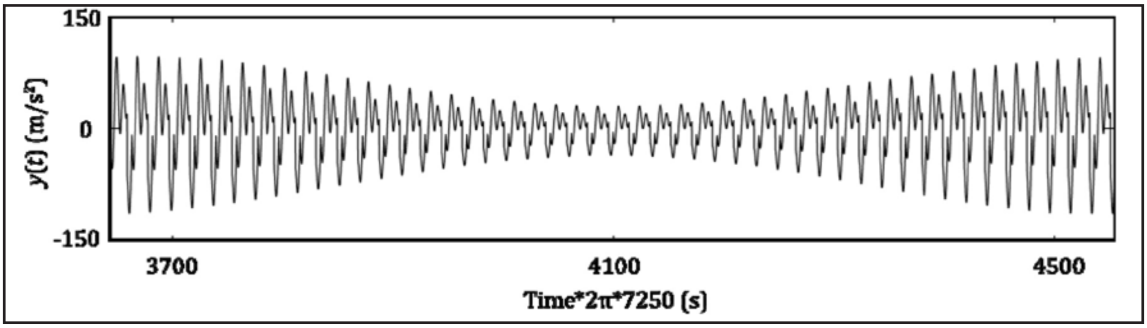

Figure 13 **Result of noise cancellation using the constructed sinusoidal wave by the oscillator and phase map.**

Conclusions

This paper proposed a new method using neural oscillators to filter out the background noise of vibration in meshing plastic gear pairs for detection of gear failure signs. It was shown how to eliminate unnecessary frequency components, with a feed-forward control system providing a neural oscillator's synchronization property. Each neural oscillator is designed to tune the natural frequency to a particular frequency of unnecessary components. The designed neural oscillators can follow the change in the driving torque variation autonomously, using their synchronization property. Moreover, the output of the oscillators is set to have a difference in the phase of 180 degrees from the input, and is included in the original measured response to reduce the amplitude of unnecessary components. The proposed noise cancellation method applied to the simulated response, and it was concluded that the proposed system could sufficiently eliminate unnecessary vibration content.

In future works we will design the suitable input and output gain for these oscillators, which could be determined through trial and error, and will confirm the oscillators' tracking properties. Furthermore, we will validate the multiple-elimination of unnecessary components and will apply the advanced system to the acceleration response measured by operating tests of gears, and assessing the efficacy of the system.

Acknowledgements. *The authors gratefully acknowledge the support of the department of mechanical and system engineering at the Kyoto Institute of Technology and Mitutoyo Association for Science and Technology, R1301.*

References

1. Iba, D., S. Ohmori, J. Hongu, M. Nakamura and I. Moriwaki. "Failure Detection of Plastic Gears Based on a Comparison of Fourier Coefficients of a Gear Mesh Vibration Model by Rectangle Pulse Train and Frequency Analysis of Acceleration Response," *2013 Trans. of the Japan Society of Mechanical Engineers Series C.* 79-808, 5138-5148, *http://dx.doi.org/10.1299/kikaic.79.5138.*
2. Shik, M. L. and G.N. Orlovsky. *Neurophysiology of Locomotor Automatism, Physiol.* Rev., 1976, 56, 465-501.
3. Matsuoka, K. "Sustained Oscillations Generated by Mutually Inhibiting Neurons with Adaptation," *Biological Cybernetics,* 1985, 52, 367-376.
4. Matsuoka, K. "Mechanisms of Frequency and Pattern Control in Neural Rhythm Generators," *Biological Cybernetics,* 1987, 56, 345-353.
5. Taga, G., Y. Yamaguchi and H. Shimizu. "Self-Organized Control of Bi-Pedal Locomotion by Neural Oscillators in Unpredictable Environment," *Biological Cybernetics*. 1991, 65, 147-159.
6. Fukuoka, Y. and H. Kimura. "Adaptive Dynamic Walking of a Quadruped Robot on Irregular Terrain based on Biological Concepts," 2003, *International Journal of Robotics Research,* 22-3-4, 187-202.
7. Iba, D. and J. Hongu. "Structural Vibration Control by Tuned Mass Damper Using Central Pattern Generator," 2011 *Proc. SPIE* 7981, *Sensors and Smart Structures Technologies for Civil, Mechanical, and Aerospace Systems,* 79814Q. DOI:10.1117/12.880406.
8. Hongu, J. and D. Iba. "Mutual Synchronization Between Structure and Central Pattern Generator," 2012 *Proc. SPIE 8345, Sensors and Smart Structures Technologies for Civil, Mechanical, and Aerospace Systems,* 83451E. DOI:10.1117/12.915045.
9. Kuramoto, Y. *Chemical Oscillations, Waves, and Turbulence*, 2003, Dover Press.
10. Pikovsky, A., M. Rosenblum and J. Kurths. *Synchronization: A Universal Concept in Non-Linear Sciences*, 2001, Cambridge University Press.
11. Umezawa, K., T. Sato and S. Ishikawa. "Simulation on Rotational Vibration of Spur Gears," *1983 Transactions of the Japan Society of Mechanical Engineers, Series C.* 49-441, 794-802 Series C.
12. Ishikawa, J. "On the Deflection of Gear Teeth," *1951 Transactions of the Japan Society of Mechanical Engineers,* 17-59, 103-106. http://dx.doi.org/10.1299/kikai1938.17.59_103.
13. Nishida, N. and Y. Maruki. "The Characteristic of Noise Spectrum of Gears with Eccentric Errors," *1981 Transaction of Japan Society of Precision Engineering,* 51 (3), 547-552.
14. Hongu, J., D. Iba, M. Nakamura and I. Moriwaki. "Vibration Control of Structures by a Dynamic Absorber Using a Neural Oscillator (Specification Method of Dynamic Absorber's Stroke Width Using an Amplitude Map), *The 56th Japan Joint Automatic Control Conference*, 2013, CD-ROM, No.129.

Hidetaka Hiramatsu is a student in Mechanical and System Engineering at Kyoto Institute of Technology, received his bachelor degree in mechanical engineering from Kyoto Institute of Technology in 2014. His research interest is gear failure detection by vibration analysis.

A PhD candidate student in design engineering at Kyoto Institute of Technology (KIT), **Junichi Hongu** began research in 2010 on application of neural oscillators for vibration control at KIT's Precision Manufacturing Laboratory. He subsequently in 2013 became a member of the project team researching gear failure by vibration analysis.

Daisuke Iba, associate professor of mechanical and system engineering at Kyoto Institute of Technology, received his Ph.D. degree in mechanical engineering from the institute in 2005, and his bachelor and master degrees in mechanical engineering from Hosei University in 1995 and 1997, respectively. Iba's research interests are structural response control and health monitoring, gear system condition monitoring and smart gear sensor development.

Arata Masuda, professor of mechanical engineering at Kyoto Institute of Technology, received his Ph.D degree in mechanical engineering there in 1999, and his BS from Kyoto University in 1990. His research has been in the area of smart structural systems and structural intelligence, including structural health monitoring, machine condition monitoring, vibration energy harvesting, vibration control and human motion monitoring and assistance.

Prof. Dr.Eng. Ichiro Moriwaki is a professor of mechanical and system engineering at Kyoto Institute of Technology and the director of the KIT Liaison Center. He received a doctorate degree of engineering from Kyoto University in 1989. He was the chairman of gearing committee in JSME in 2011-2013, and still a member of the committee. Moriwaki is also chairman of ISO / JIS standards committee in JGMA, a Japanese delegate for ISO TC 60.

Morimasa Nakamura has a Ph. D in engineering and is an assistant professor at the Kyoto Institute of Techonology. His primary research field is tribology, surface treatment technology and gearing.

Prof. Akira Sone earned his bachelor's, master's and Ph.D. degrees in mechanical engineering at Tokyo Metropolitan University in 1981, 1983 and 1987, respectively, working there as a research associate from 1987 to 1989. He has been on the faculty of the mechanical and system engineering department at Kyoto Institute of Technology since 1989. He has been an associate professor and a professor there since 1991 and 1999, respectively. Sone's research focus is seismic engineering and structural response control.

A Practical Approach for Modeling a Bevel Gear

Brendan Bijonowski

The geometry of the bevel gear is quite complicated to describe mathematically, and much of the overall surface topology of the tooth flank is dependent on the machine settings and cutting method employed. AGMA 929-A06 — Calculation of Bevel Gear Top Land and Guidance on Cutter Edge Radius — lays out a practical approach for predicting the approximate top-land thicknesses at certain points of interest — regardless of the exact machine settings that will generate the tooth form. The points of interest that AGMA 929-A06 address consist of toe, mean, heel, and point of involute lengthwise curvature. The following method expands upon the concepts described in AGMA 929-A06 to allow the user to calculate not only the top-land thickness, but the more general case as well, i.e. — normal tooth thickness anywhere along the face and profile of the bevel gear tooth. This method does not rely on any additional machine settings; only basic geometry of the cutter, blank, and teeth are required to calculate fairly accurate tooth thicknesses. The tooth thicknesses are then transformed into a point cloud describing both the convex and concave flanks in a global, Cartesian coordinate system. These points can be utilized in any modern computer-aided design software package to assist in the generation of a 3D solid model; all pertinent tooth macrogeometry can be closely simulated using this technique. A case study will be presented evaluating the accuracy of the point cloud data compared to a physical part.

Introduction

The first question that comes to mind from any engineer presented by this paper is why would anyone be interested in a close approximation to the tooth flanks of a straight or spiral bevel gear? It is a valid question. A bevel gear designer is typically interested in the minute details of the tooth flank's surface topology to gain the optimized contact conditions under loads that the bevel gears will operate. The method presented in this paper does not address any of these needs.

Purpose

One of the main purposes of this method is to create a working 3D model for visual interrogation? of fits and proportions. The bevel designer is typically concerned with the proportions of a myriad of geometric values describing the basic layout of the tooth form. Many of the values like top land balance, slot width tapers, spiral angle adjustments, etc., are hard to visualize for the engineer, and their impact on the tooth form can be drastic.

Thus the gear engineer's toolkit should include a method for generating a 3D model of a bevel gear, as dependency upon CAD for the general engineer is rapidly increasing. Many application engineers are demanded to provide 3D models to their customers. These customers then utilize their CAD system to validate fits and clearances between components in their systems. Gears should not be left out of this analysis. Advancements in 5- and 6-axis machining of gears are rapidly approaching the precision and capability of dedicated gear generating machines; most of these machining centers require a 3D model for programming. If the application engineer provides a fully developed gear model to the customer, the 5- or 6-axis machining techniques may become very attractive. For this case alone, many gear companies opt out of providing models of their designs.

Background

The method outlined in AGMA 929-A06 — *Calculation of Bevel Gear Top Land and Guidance on Cutter Edge Radius* — describes how to calculate the top land thickness for a bevel tooth at specific points of interest; these points of interest are at the toe, mean, heel, and the point-of- involute lengthwise curvature.

Reasons regarding the purpose for these calculation points are beyond the scope of this document. The formulas inside AGMA 929 can be generalized so that a set of equations can be devised to calculate the normal circular tooth thickness anywhere along the profile and length of the tooth.

Why this method is approximate. Given, as stated, that the geometry of a spiral bevel gear is mathematically complicated, the machine settings used to create a spiral bevel gear — whether using face milling or face hobbing — adjust the final flank form of the teeth. A thorough understanding of the machine settings and motions is necessary to achieve an accurate tooth model. AGMA 929-A06 uses the technique of a virtual spur gear to approximate the profile of a bevel tooth in the normal plane, without knowing the motions of the machine generating the final form. In doing so, the tooth thicknesses can be calculated quite simply using traditional methods for spur gears.

The virtual spur gear technique assumes that the tooth form will follow an involute in the profile direction in the normal plane. This is only a close approximation to the true form of a spiral bevel tooth. Most spiral bevels follow the octoid tooth form, which is similar — but not identical — to the involute tooth form found on most cylindrical gears.

What is missing in AGMA 929-A06 to complete a model. A generalized set of equations can be produced from the content of AGMA 929-A06 to calculate the normal tooth thicknesses of a bevel tooth anywhere in the profile or lengthwise direction. The purpose of this document is to fill in the gaps of AGMA 929-A06 so that a model can be generated. The majority of the content of this document pertains to how the normal tooth thicknesses are oriented in three dimensions and resolves these thicknesses into an array of Cartesian coordinates. (See Figure 1 for a visual depiction of the calculation method described within this document.) Additional information regarding the terminology described within the figure is in the subsequent sections.

This method's shortcomings. Enough has been presented to illuminate the reader as to why this method creates only an approximate method, but there are additional shortcomings worth mentioning. This method does not currently address the root fillet. The coordinates calculated in this method are strictly points following the involute curve that describes the approximate flank form. Coordinates for the root fillet are beyond the scope of this document.

The other major shortcoming is that all subsequent formulas are for spiral bevel gears — without a hypoid offset. Additional provisions would need to be made to generalize the formulas to account for hypoids.

Coordinate System Definition

All bevel gears are designed using a reference right cone called the "pitch cone." The pitch cone is used as a basis for describing all other geometric entities of the bevel gear. Since describing the motions of the generating process in three dimensions would be hard to visualize or comprehend, the general practice is to un-wrap the surface of the pitch cone into a tangent plane — or "pitch plane."

The point at the top of the pitch cone is called the "pitch apex." The pitch apex is significant because the axes of both gear and pinion intersect at this point. Figure 2 displays the pitch cone, the pitch plane unwrapped, and also describes the global Cartesian coordinate system, C_G. Figure 2 also shows the pitch cone sectioned through the YZ plane. This describes the definition of the pitch angle, Γ, and the face width, F — of a part. The global coordinate system follows the right-hand rule and its origin is located at the pitch apex of the member being modeled.

Basic Generation

The majority of all generated spiral bevel gears are manufactured in one of two processes, i.e. — face milling or face hobbing; both manufacturing methods have advantages and disadvantages. For the purposes of this method, a brief understanding of the generating method utilized during these processes is necessary to realize the 3D model.

Face milling. The face milling manufacturing method employs a circular, cup-shaped cutting tool moving in a timed relationship with the workpiece to roll through the gear blank and generate an individual slot. The cutter is then withdrawn,

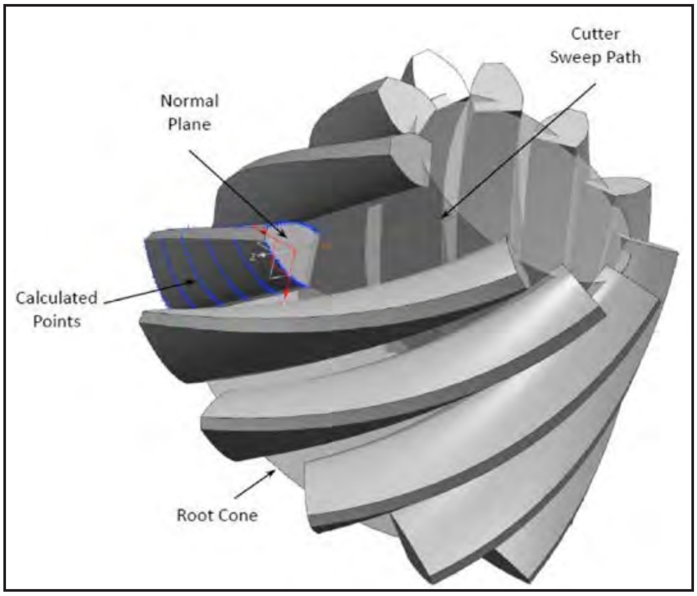

Figure 1 Visual depiction of calculation method.

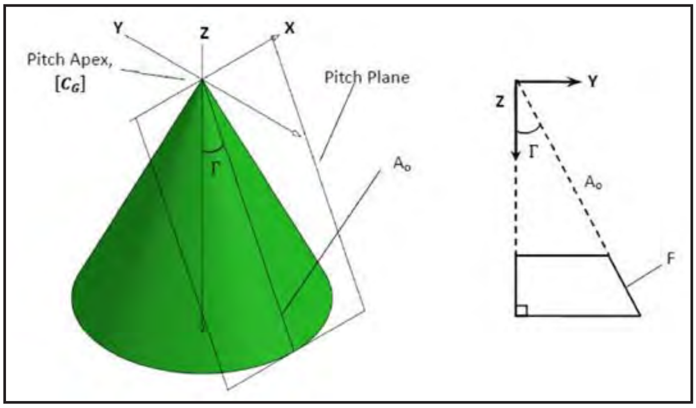

Figure 2 Pitch cone.

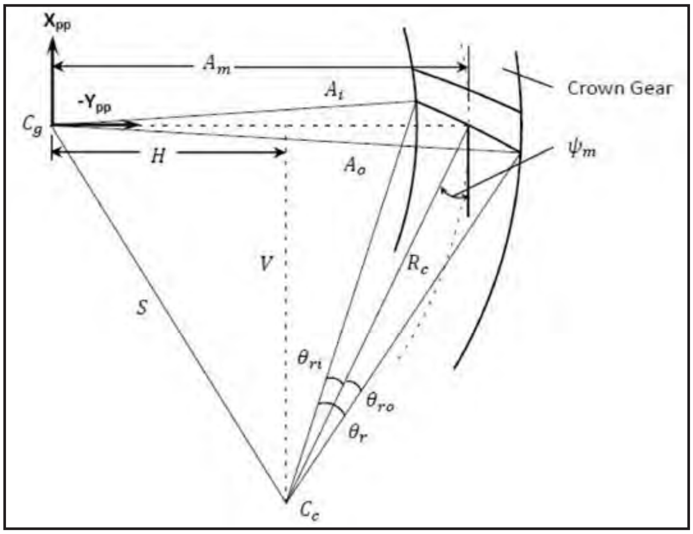

Figure 3 Generating triangle in pitch plane for face milling.

the work is indexed to the location of the next slot, and the process repeated. See Figure 3.

Figure 3 displays three instances of the cutter as it passes through the workpiece; these points are at the toe, mean, and heel of the crown gear. The path of the cutter sweeps a circular arc in the lengthwise direction, with the same radius as the radius of the cutter, R_c. The axis of the crown gear, C_g, is known as the machine center. The local coordinate system for the pitch plane is located at the machine center. *Xpp* correlates to *X* and *Ypp* lies along the line describing A_o in Figure 2.

The cutter axis, C_c. This location can be found by:

$$V = R_c \cos\psi_m \tag{1}$$

$$H = A_m - R_c \sin\psi_m \tag{2}$$

$$C_c = (V, H) \tag{3}$$

The sign of the vertical term, *V*, may either be positive or negative, depending on the hand of spiral to be modeled. Figure 3 shows a right-hand member (use negative value for *V* when calculating left-hand members). The cutter sweep angle, θ_r, is necessary to determine how much rotation is used during the cutting process. When calculating points to model the gear tooth, these will be the endpoints of the working portion of the cutter path.

$$S = \sqrt{V^2 + H^2} \tag{4}$$

$$\theta_r = \cos^{-1}\left[\frac{S^2 + R_c^2 - A_o^2}{2S\,R_c}\right] - \cos^{-1}\left[\frac{S^2 + R_c^2 - A_i^2}{2S\,R_c}\right] \tag{5}$$

$$\theta_{ro} = \cos^{-1}\left[\frac{S^2 + R_c^2 - A_o^2}{2S\,R_c}\right] - \cos^{-1}\left[\frac{S^2 + R_c^2 - A_m^2}{2S\,R_c}\right] \tag{6}$$

$$\theta_{ri} = \theta_r - \theta_{ro} \tag{7}$$

Discrete points can be calculated along the cutter sweep on the pitch plane. Using the general parametric formulas for a circle, the solution for a point, *p*, along the cutter path is:

$$p_x(t) = V + R_c \cos t \tag{8}$$

$$p_y(t) = V + R_c \sin t \tag{9}$$

Where *t* is a parameter that has the following ranges:

For left-hand members,

$$\pi + \psi_m - \theta_{ri} \le t \le \pi + \psi_m - \theta_{ro} \tag{10}$$

For right-hand members,

$$2\pi + \psi_m - \theta_{ri} \le t \le 2\pi + \psi_m - \theta_{ro} \tag{11}$$

This cutter path can be broken into as many discrete sections as desired.

Face hobbing. The face hobbing manufacturing method is a continuously indexing process. The cutting tool has groups of staggered blades; the workpiece moves in a timed relationship with the cutter so that a group of blades in the cutter passes through a slot of the workpiece. The face hobbing method generates an extended epicycloidal shape in the lengthwise direction. See Figure 4. for a detailed layout of the face hobbing generating triangle.

Since the lengthwise shape of a face hobbed part creates an extended, epicycloidal shape, a little trigonometry is necessary to calculate the discrete points along the path created by the cutter.

The crown gear tooth count,

$$N_c = \frac{N}{\sin\Gamma} \tag{12}$$

The lead angle of the cutter,

$$\nu = \sin^{-1}\left[\frac{A_m N_s}{R_c N_c}\cos\psi_m\right] \tag{13}$$

The first auxiliary angle,

$$\lambda = \frac{\pi}{2} \tag{14}$$

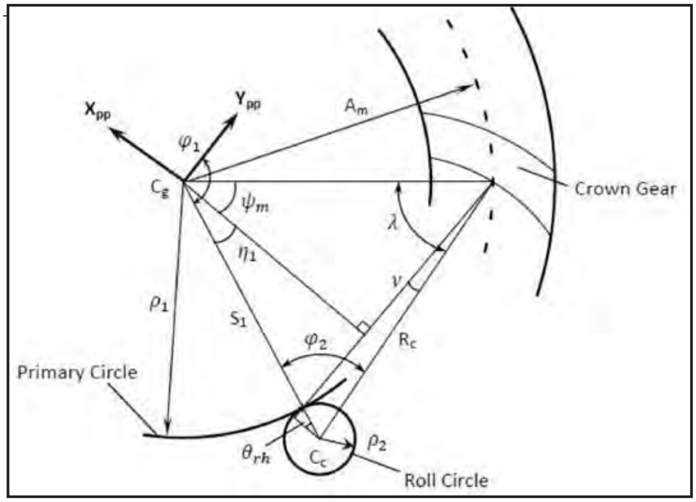

Figure 4 Generating triangle in pitch plane for face hobbing.

The center distance from crown gear center to cutter (Radial),

$$S_1 = \sqrt{A_m^2 + R_c^2 - 2A_m R_c \cos\lambda} \tag{15}$$

The second auxiliary angle,

$$\eta = \cos^{-1}\left[\frac{A_m \cos\psi_m}{S_1 N_c}(N_c + N_s)\right] \tag{16}$$

The second roll angle,

$$\varphi_2 = \pi - \eta_1 - \psi_m - \lambda \tag{17}$$

The auxiliary roll angle,

$$\theta_{rh} = \frac{\pi}{2} - \nu + \varphi_2 \tag{18}$$

The radius of the roll circle,

$$\rho_2 = \frac{R_c \cos\nu}{\cos\theta_{rh}} \tag{19}$$

The radius of the primary circle,

$$\rho_2 = S_1 - \rho_2 \tag{20}$$

The first roll angle (assuming rolling without sliding),

$$\varphi_1 = \varphi_2 \frac{\rho_2}{\rho_1} \tag{21}$$

Now that the dimensions of the cutting cycle's epicycloid, the cutter path, can be calculated, it would be very difficult to determine the angle of sweep that the cutter makes during the generating process because the cutter axis does not remain stationary during the cutting cycle. The face width of the bevel gear being modeled will be subdivided into discrete portions; the roll angles need to be recalculated for each discrete location individually.

The second roll angle as a function of cone distance,

$$\varphi_{p2}(A_\mu) = \cos^{-1}\left[\frac{S_1^2 + R_c^2 - A_\mu^2}{2S_1R_c}\right] \tag{22}$$

Where,

$$A_i \leq A_\mu \leq A_o \tag{23}$$

The first roll angle as a function of cone distance,

$$\varphi_{p1}(A_\mu) = \varphi_{p2}(A_\mu)\frac{\rho_2}{\rho_1} \tag{24}$$

The local Cartesian coordinates describing a point, p, along the cutter sweep path can be calculated.

$$p_x = -R_c\sin(\varphi_{p1}+\varphi_{p2}) + (\rho_1+\rho_2)\sin\varphi_{p1} \tag{25}$$

$$p_y = -R_c\cos(\varphi_{p1}+\varphi_{p2}) + (\rho_1+\rho_2)\cos\varphi_{p1} \tag{26}$$

Wrapping the Pitch Plane

The pitch plane is a tangent plane to the lateral surface of a right cone. This cone, as described earlier, is the "pitch cone." The diagrams take into account the set-up of the machine, the cutter size, and the motion of the cutter. Rotation of the workpiece also needs to be accounted for; this is accomplished by wrapping the pitch plane around the pitch cone. This transforms the local coordinates calculated for the cutter sweep path into global coordinates. These points in the global coordinates will define the center of a tooth slot. The following formulas will transform a point, p, from the local *XppYpp* plane to the global Cartesian coordinate system, C_G.

The first step is to determine the location of the point in the global Z axis direction,

$$z_p = \sqrt{p_x^2 + p_y^2}\cos\Gamma \tag{27}$$

Calculate the rotation angle that the point will wrap around the cone,

$$\theta_p = \frac{1}{\sin\Gamma}\tan^{-1}\frac{p_x}{p_y} \tag{28}$$

Calculate the radius of the cone at location, z_p,

$$R_p = z_p\tan\Gamma \tag{29}$$

Convert the cylindrical coordinates for the wrap point into global Cartesian coordinates.

$$x_p = R_p\cos\theta_p \tag{30}$$

$$y_p = R_p\sin\theta_p \tag{31}$$

Therefore, all the local cutter positions can be wrapped and transformed into the global Cartesian coordinate system.

Calculating Local Cutter Coordinate System

Since AGMA 929 effectively calculates the normal circular tooth thicknesses at a specific spot along the cutter path, the next step is to determine the correct orientation of the normal plane. A complete coordinate system will be oriented to have the x_ny_n plane normal to the cutter path, with the origin at each global coordinate of the cutter path calculated previously; this coordinate system will be called C_n.

Tangent axis, z_n. The tangent axis is defined by a vector that is tangent to the cutter sweep path at the location of the wrapped point. There are a couple of options for calculating this tangent vector. One could calculate the first derivative of the cutter sweep path formulas for both face milling and face hobbing so that the slope anywhere along that path can be predicted. Once that is accomplished a vector can be constructed in three dimensions to describe this tangent axis.

Since many assumptions are made throughout this method, the simplest method for calculating an approximate tangent vector is using finite difference; the finite difference method is described in the following equation:

$$f'(x) = \lim\Delta_{x\to 0}\left(\frac{f(x+\Delta x) - f(x)}{\Delta x}\right) \tag{32}$$

It is difficult to determine the correct size of Δx that will approximate the tangent close enough for this method. Since the cutter sweep path is smooth and continuous for all locations

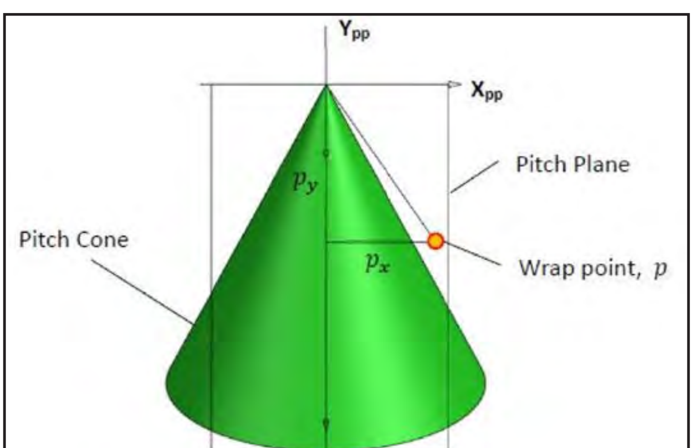

Figure 5 Normal view to pitch plane displaying wrap point.

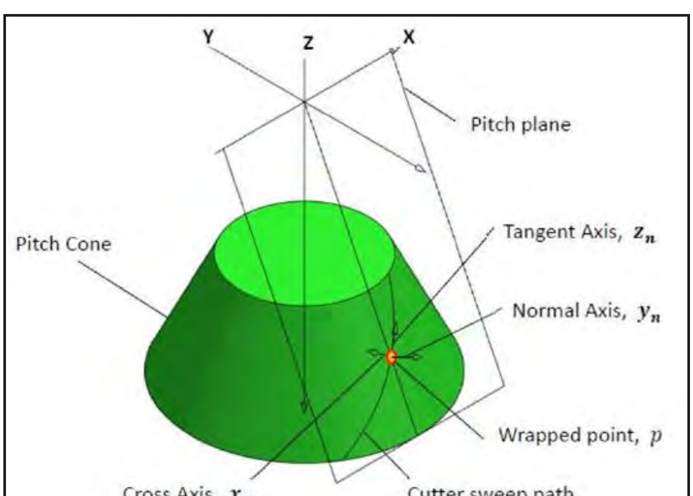

Figure 6 Definition of a wrapped point's local coordinate system.

along the arc, it is possible to quantify the error of our approximation using a Taylor expansion. This is beyond the scope of this document, but is mentioned here for further exploration.

The practical approach to applying the finite difference method is to calculate a neighboring wrapped point along the cutter sweep path for each wrapped calculation point. A vector can then be defined by passing through both sweep path points. As the points become closer and closer the vector connecting the two points approaches a tangent line.

Normal axis — y_n. The normal vector is defined as a vector radiating perpendicularly from the surface of the right cone at the wrapped point location (Fig. 6). The normal vector at wrap point $p = (p_x, p_y, p_z)$ can be calculated by the following equation:

$$y_n = (2p_x \cos^2\Gamma, 2p_y \cos^2\Gamma, -2p_z \sin^2\Gamma) \tag{33}$$

A brief derivation will follow to explain the calculation of the normal axis. The general function of a right cone,

$$C(x, y, z) = (x^2 + y^2)\cos^2\Gamma - z^2 \sin^2\Gamma \tag{34}$$

A gradient, ∇u, is always normal to a function when,

$$\nabla_u = u_x e_x + u_y e_y + u_z e_z \tag{35}$$

Where,

$$e_x = \langle 1, 0. 0 \rangle \tag{36}$$

$$e_y = \langle 1, 0. 0 \rangle \tag{37}$$

$$e_z = \langle 1, 0. 0 \rangle \tag{38}$$

Let,

$$u(x, y, z) = x^2 \cos^2\Gamma + y^2 \cos^2\Gamma - z^2 \sin^2\Gamma \tag{39}$$

Therefore,

$$\nabla_u = \langle 2x\cos^2\Gamma,\ 2y\cos^2\Gamma - 2z\sin^2\Gamma \rangle \tag{40}$$

The cross vector will complete the definition of the local Cartesian coordinate system. This vector is calculated by taking the cross product of the tangent vector and the normal vector.

$$x_n = z_n y_n \tag{41}$$

After calculating all the vector directions for the local coordinate system, all three of the vectors should be normalized.

Normal Circular Tooth Thickness Calculations

Generalizing AGMA 929-A06. As previously discussed AGMA 929-A06 utilizes the technique of converting the spiral bevel gear tooth to a virtual spur gear tooth to calculate the top lands at the toe, mean, and heel; the equations presented in AGMA 929-A06 are unique for each of these points of interest. General equations can be derived from AGMA 929-A06 so that the tooth thickness can be calculated anywhere along the profile and lengthwise direction. The generalized formulas for the conversion to a virtual spur gear are presented here (Fig. 7). Also, a handful of helpful formulas for calculating some spiral gear tooth geometry with respect to cone distance, A_μ, are developed. The cone distance range variable must correlate to the cone distances first chosen in the cutter path sections.

The notation in this section utilizes the terminology as if the member being modeled is the gear. Unless specifically specified the gear terminology should be replaced with pinion terminology in the formulas if the pinion is the part being modeled.

Spiral angle for face milling with respect to cone distance,

$$\psi(A_\mu) = \sin^{-1}\frac{2A_m R_c \sin\psi_m - A_m^2 + A_\mu^2}{2A_\mu R_c} \tag{42}$$

Generating angle for face hobbing with respect to cone distance,

$$q(A_\mu) = \cos^{-1}\frac{A_\mu^2 + S_1^2 - R_c^2}{2A_\mu S_1} \tag{43}$$

Spiral angle for face hobbing with respect to cone distance,

$$\psi(A_\mu) = \tan^{-1}\frac{A_\mu - Q\cos q(A_\mu)}{Q\sin q(A_\mu)} \tag{44}$$

Slot width with respect to cone distance for the gear member,

$$W_G(A_\mu) = W_e'\left[1 - \frac{A_\mu \cos\psi(A_\mu)}{A_m \cos\psi_m}\right] + \frac{A_\mu}{A_m}[t_{mP}\cos\psi(A_\mu)] - \left[\frac{A_\mu\cos\psi(A_\mu)}{A_m\cos\psi_m} b_G(\tan\Phi_1 - \tan\Phi_2)\right] + \frac{A_\mu\cos\psi(A_\mu)}{A_o\cos\psi(A_o)}\frac{B}{\cos\frac{\Sigma\Phi}{2}} + (A_m - A_\mu)(\tan\Phi_1 - \tan\Phi_2)\tan\xi \tag{45}$$

Slot width with respect to cone distance for the pinion member,

$$W_P(A_\mu) = \frac{A_\mu\cos\psi(A_\mu)}{A_m\cos\psi_m} p_n - \Sigma b_\mu(\tan\Phi_1 - \tan\Phi_2) - W_G(A_\mu) + \frac{A_\mu\cos\psi(A_\mu)}{A_o\cos\psi(A_o)}\frac{B}{\cos\frac{\Sigma\Phi}{2}} \tag{46}$$

Normal pitch radius with respect to cone distance (substitute proper pitch diameter and pitch angle for member to model),

$$r_N(A_\mu) = \frac{D A_\mu}{2\cos\Gamma\cos^2\psi_m A_o} \tag{47}$$

Normal base radius with respect to cone distance, concave,

$$r_{bN1}(A_\mu) = r_N(A_\mu)\cos\Phi_1 \tag{48}$$

Normal base radius with respect to cone distance, convex,

$$r_{bN2}(A_\mu) = r_N(A_\mu)\cos\Phi_2 \tag{49}$$

Figure 7 displays the base radii graphically. The value of r_{bN1} and r_{bN2} are shown as the same value because the pressure angle of the concave and convex flanks are the same. This is typical but not mandatory for bevel gears without a hypoid offset.

Normal pinion circular tooth thickness at pitch line with respect to cone distance,

$$t_{NP}(A_\mu) = b_G(A_\mu)(\tan\Phi_1 - \tan\Phi_2) - W_G(A_\mu) - \frac{A_\mu\cos\psi(A_\mu)}{A_o\cos\psi(A_o)}\frac{B}{\cos\frac{\Sigma\Phi}{2}} \tag{50}$$

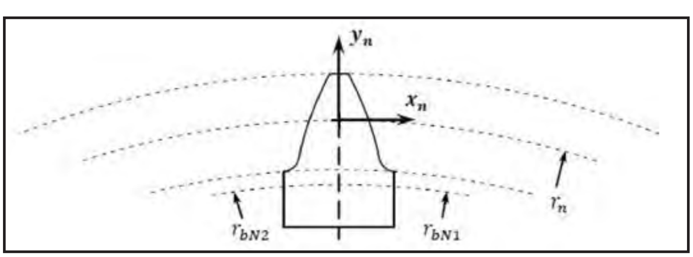

Figure 7 Definition of the geometry of the virtual spur gear in the normal plane.

Normal gear circular tooth thickness at pitch line with respect to cone distance,

$$t_{NG}(A_\mu) = b_P(A_\mu)(\tan\Phi_1 - \tan\Phi_2) + W_G(A_\mu) - \frac{A_\mu \cos\psi(A_\mu)}{A_o \cos\psi(A_o)} \frac{B}{\cos\frac{\Sigma\Phi}{2}} \tag{51}$$

Normal working radius with respect to cone distance,

$$r_{wN}(A_\mu) = r_N(A_\mu) + w \tag{52}$$

Where

w is a range variable for calculating the working radius. The valid range for w is,

$$-b(A_\mu) \le w \le a(A_\mu) \tag{53}$$

Pressure angle at working radius with respect to cone distance, concave,

$$\Phi_{1w}(A_\mu) = \cos^{-1}\frac{r_{bN1}(A_\mu)}{r_{wN}(A_\mu)} \tag{54}$$

Pressure angle at working radius with respect to cone distance, convex,

$$\Phi_{2w}(A_\mu) = \cos^{-1}\frac{r_{bN2}(A_\mu)}{r_{wN}(A_\mu)} \tag{55}$$

Normal circular tooth thickness for pinion at working radius with respect to cone distance,

$$t_{wNP}(A_\mu) = \left[\frac{t_{NP}(A_\mu)}{r_N(A_\mu)} + \operatorname{inv}\Phi_1 - \operatorname{inv}\Phi_{1w} + \operatorname{inv}(-\Phi_2) - \operatorname{inv}\Phi_{2w}\right] r_{wN}(A_\mu) \tag{56}$$

Normal circular tooth thickness for gear at working radius with respect to cone distance,

$$t_{wNG}(A_\mu) = \left[\frac{t_{NG}(A_\mu)}{r_N(A_\mu)} + \operatorname{inv}\Phi_1 - \operatorname{inv}\Phi_{1w} + \operatorname{inv}(-\Phi_2) - \operatorname{inv}\Phi_{2w}\right] r_{wN}(A_\mu) \tag{57}$$

Certain designs have the dedendum plunge below the virtual gear's base radius; when this occurs, the normal circular tooth thickness will become a complex number. Only the real portion of this value should be used when recording the answers.

Converting thicknesses to coordinates. The tooth thickness calculations shown earlier in *Generalizing AGMA 929-A06* is a circular tooth thickness positioned at a specified working radius. The local coordinate system has the origin located where the pitch radius crosses the center of the tooth thickness (Fig. 7). For each working radius used the calculated circular tooth thicknesses need to be converted to chordal thicknesses before they can be recorded as Cartesian coordinates.

Normal chordal tooth thickness for pinion at working radius with respect to cone distance,

$$t_{wcNP}(A_\mu) = 2r_{wN}(A_\mu)\sin\frac{t_{wNP}(A_\mu)}{2r_{wN}(A_\mu)} \tag{58}$$

Normal chordal tooth thickness for gear at working radius with respect to cone distance,

$$t_{wcNG}(A_\mu) = 2r_{wN}(A_\mu)\sin\frac{t_{wNG}(A_\mu)}{2r_{wN}(A_\mu)} \tag{59}$$

Now that the circular thickness has been converted to a chordal thickness, a small correction is needed to the location of the thickness in the profile direction (along y_n). Figure 8 depicts this correction and provides a visual explanation why this correction is required. The working radius is equal to the pitch radius in the figure, and its relative radius has been decreased to exaggerate the size of the correction in the figure.

Pinion shift factor at working distance with respect to cone distance,

$$y_{wsP}(A_\mu) = r_{wN}(A_\mu)\left[1 - \cos\frac{t_{wNP}(A_\mu)}{2r_{wN}(A_\mu)}\right] \tag{60}$$

Gear shift factor at working distance with respect to cone distance,

$$y_{wsG}(A_\mu) = r_{wN}(A_\mu)\left[1 - \cos\frac{t_{wNG}(A_\mu)}{2r_{wN}(A_\mu)}\right] \tag{61}$$

Local Cartesian coordinates for the pinion with respect to cone distance,

$$pt_{1P} = \left(\frac{t_{wcNP}(A_\mu)}{2}, w - y_{wsP}(A_\mu)\right) \tag{62}$$

$$pt_{2P} = \left(\frac{t_{wcNP}(A_\mu)}{2}, w - y_{wsG}(A_\mu)\right) \tag{63}$$

Local Cartesian coordinates for the gear with respect to cone distance,

$$pt_{1G} = \left(\frac{t_{wcNG}(A_\mu)}{2}, w - y_{wsG}(A_\mu)\right) \tag{64}$$

$$pt_{2G} = \left(-\frac{t_{wcNG}(A_\mu)}{2}, w - y_{wsG}(A_\mu)\right) \tag{65}$$

Transform the Local Normal Tooth Thicknesses to Global

To this point all the tooth thickness points are defined relative to a local coordinate system. The global location for each one of these local coordinate systems are known, but to complete the model, all points describing the tooth flanks must be known relative to the global coordinate system. This is accomplished using a coordinate transformation matrix, C_T:

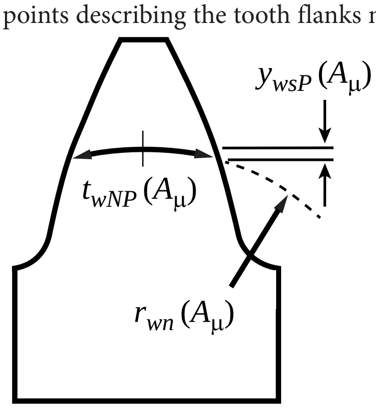

Figure 8 Shift factor when converting circular to chordal thicknesses (pinion shown).

$$C_T = C_n C_G \tag{66}$$

Where,

C_G is a 3×3 identity matrix that describes the global coordinate system. See Coordinate System Definition for a more detailed explanation. Once a vector, V_p, relative to the local coordinate system, C_n, is constructed that passes through a calculated tooth flank point, the transformation can be calculated:

$$V_G = C_T V_P \tag{67}$$

Where,

V_G is a vector that passes through the exact same flank point, but is described relative to the global coordinate system.

Results

Now that the method is complete, the next logical step is to determine just how accurate this model is when compared to the theoretical geometry of a spiral bevel gear. This method is strictly approximate; many caveats have been discussed in the previous sections. To accomplish a comparison between this method and a theoretical part there must be a reliable standard by which to compare it. Comparing the calculated points from this method with a physical, cut part would introduce potential variations from the manufacturing process. For this reason alone it was decided to compare the calculated points to a different, yet trusted, mathematical model. Gleason Works has developed a commercial software package—*T900*—that generates an accurate point cloud describing the geometry of the tooth flank and fillet condition of bevel gears and pinions. While the purpose of this software is far greater than just the generation of a point cloud, the other functionality is beyond the scope of this document. The point cloud produced from *T900* can be imported into a CAD package to assist in the generation of the exact geometry produced by the machine settings for a particular design. The point cloud represents the standard as to which this method is compared.

Table 1 Basic spiral geometry of model

	Pinion	Gear
Number of teeth	11	57
Face width	2.0	2.0
Diametral pitch	4.0	
Shaft angle	Non 90°	

The member chosen for this analysis is a left-hand spiral bevel gear generated by face mill completing.

Some of the basic geometry has been provided in Table 1, but the exact details of the geometry are relatively unimportant. An angular set was chosen as this method has no shaft angle restrictions.

The output from *T900* is a point cloud that describes the flanks of a spiral bevel or hypoid gear set. A gear tooth is divided into a 13- (profile) by-10 (length) grid for each flank; therefore 260 unique points describe each tooth. For this analysis these discrete points were bridged together using Siemens *NX 8.5* CAD software. The point cloud was connected in the profile and lengthwise direction with curves generated by a cubic, polynomial regression. Once the lattice of curves is generated the curves are used as ribs to create a bi-cubic surface. Figure 9 shows the tooth surface generated from the *T900* point cloud in gray.

The face width of the part is broken into 10 segments for the calculation; addendum and dedendum are also broken into 10 segments. The part being modeled has a short addendum and long dedendum. Figure 10 shows the calculated points and solid model sectioned through the normal plane (Fig. 9) of a tooth. The calculated points go beyond the root line of the model because the calculated points were generated to the base circle radius of the virtual spur gear. When doing the comparison the last four points of each profile will be omitted, as they fall below the root fillet tangency point.

A linear measurement normal to the *T900* surface to each calculated point is used to measure the deviation between the calculated points and the surface. The normal tooth thicknesses at the toe and heel will be omitted in the comparison, as these points are beyond the bounds of the *T900* surface. The absolute values of the measured deviations for each flank are given (Tables 2 and 3).

The red values are measured deviations that exceed one one-thousandth of an inch. Overall, the results depict a model that very closely approximates the flanks predicted by the Gleason Works *T900* software. The average deviation for each normal cross-section in the lengthwise direction is displayed in Table 4.

Conclusion

The purpose of this presentation is to describe a procedure for calculating a very close approximation of the geometry of a spiral bevel gear tooth.

This method is built upon the techniques and formulas described in AGMA 929-A06.

The second portion of the document compared the results of this method with the results from a proven Gleason software package.

The results are extremely close.

Many models have been generated since this original case study, and the subsequent models correlate well with the geometry predicted by Gleason software.

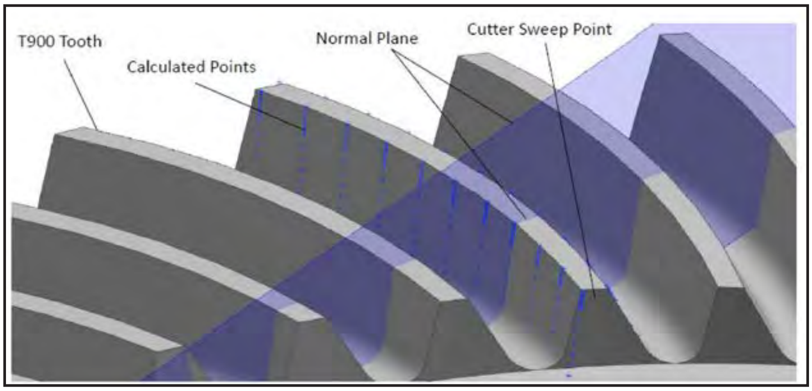

Figure 9 Calculated points overlaid on a tooth modeled using Gleason T900.

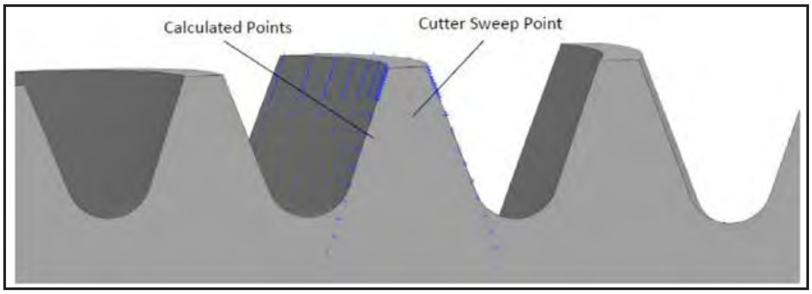

Figure 10 Calculated points in the normal plane.

The model described throughout this document should not be used for advanced analysis (i.e., finite element or the like), as the models created from this method do not have any modifications to the tooth flanks to adjust or optimize the tooth contact pattern.

At present AGMA's Bevel Gear Committee is working on revising the formulas in AGMA 929-A06 to adopt the generalized formulas described here. The technique of utilizing generalized formulas will expand the capabilities of AGMA 929.

References

1. Baxter, Jr., M.L. *Spiral Bevel Gear Theory*, Unpublished. 1963.
2. AGMA 929-A06. *Calculation of Bevel Gear Top Land and Guidance on Cutter Edge Radius.*
3. Colbourne, J.R. *The Geometry of Involute Gears*, Springer-Verlag, New York, 1987.
4. ANSI/AGMA 2005-D03. *Design Manual for Bevel Gears.*
5. Grant, G.B. *A Treatise on Gear Wheels*, 21st Edition. Philadelphia Gear Works Inc., Philadelphia, 1980.
6. Khiralla, T.W. *On the Geometry of External Involute Spur Gears*, C/I Leaming, North Hollywood, California, 1976.
7. Krenzer, T. *The Bevel Gear*, 2007.
8. Litvin, F.L. *Theory of Gearing*, NASA Reference Publication; 1212 (AVSCOM Technical Report; 88-C-035), 1989.
9. *NX 8.5 Help Documentation*. Siemens Product Lifecycle Management Software Inc., 2012.
10. Shtipelman, B.A. *Design and Manufacture of Hypoid Gears*, John Wiley and Sons, Inc. 1978.
11. *T900 User's Manual.* Gleason Works.

Table 2 Concave flank measured deviations, thousandths of an inch

		Heel									Toe
		0	1	2	3	4	5	6	7	8	9	10
Topland	0		0.927	0.938	0.949	0.963	0.969	0.956	0.927	0.899		
	1		0.249	0.214	0.188	0.174	0.154	0.109	0.035	0.046		
	2		0.305	0.258	0.223	0.201	0.173	0.121	0.042	0.047		
	3		0.358	0.302	0.257	0.226	0.189	0.130	0.045	0.049		
	4		0.411	0.343	0.289	0.249	0.205	0.138	0.045	0.054		
	5		0.461	0.384	0.319	0.270	0.218	0.143	0.043	0.061	0.158	
	6		0.051	0.422	0.348	0.289	0.230	0.146	0.038	0.070	0.171	
	7		0.558	0.459	0.375	0.307	0.241	0.148	0.032	0.080	0.186	
	8		0.603	0.494	0.401	0.323	0.249	0.148	0.025	0.092	0.201	
	9		0.647	0.528	0.425	0.337	0.257	0.147	0.018	0.104	0.218	
Pitch	10		0.689	0.559	0.447	0.350	0.262	0.146	0.010	0.116	0.235	
	11		0.839	0.671	0.522	0.396	0.268	0.125	0.039	0.205	0.360	
	12		0.952	0.744	0.555	0.381	0.215	0.024	0.186	0.387	0.575	
	13		1.023	0.077	0.526	0.299	0.113	0.098	0.324	0.546	0.765	
	14		1.049	0.759	0.523	0.350	0.015	0.291	0.644	1.046	1.345	
	15		1.024	0.423	0.298	0.190	0.418	0.754	0.950	0.467	1.259	
	16		0.913	0.000	0.052	0.103	0.539					
	17											
	18											
	19											
Root	20											

Table 3 Convex flank measured deviations, thousandths of an inch

		Heel									Toe
		0	1	2	3	4	5	6	7	8	9	10
Topland	**0**			0.342	0.344	0.326	0.307	0.313	0.373	0.377		
	1		0.296	0.327	0.340	0.332	0.320	0.334	0.371	0.405		
	2		0.268	0.311	0.334	0.335	0.331	0.353	0.397	0.436		
	3		0.238	0.292	0.325	0.336	0.341	0.370	0.421	0.465		
	4		0.206	0.271	0.315	0.335	0.348	0.385	0.442	0.493	0.538	
	5		0.171	0.248	0.302	0.332	0.354	0.398	0.462	0.518	0.566	
	6		0.135	0.222	0.288	0.328	0.358	0.409	0.479	0.542	0.593	
	7		0.096	0.195	0.271	0.321	0.360	0.419	0.495	0.565	0.619	
	8		0.056	0.166	0.252	0.312	0.360	0.427	0.510	0.586	0.643	
	9		0.013	0.135	0.232	0.302	0.359	0.433	0.523	0.605	0.667	
Pitch	**10**		0.031	0.102	0.210	0.289	0.356	0.438	0.534	0.623	0.690	
	11		0.231	0.055	0.094	0.212	0.318	0.442	0.581	0.702	0.817	
	12		0.460	0.243	0.054	0.102	0.246	0.402	0.562	0.729	0.864	
	13		0.710	0.467	0.254	0.042	0.140	0.328	0.542	0.746	0.938	
	14		0.983	0.690	0.416	0.186	0.230	0.281	0.566	0.705	0.840	
	15		1.285	0.911	0.615	0.389	0.158	0.008	0.101	0.526	1.220	
	16		1.559	1.321	1.114	0.765	0.403					
	17											
	18											
	19											
Root	**20**											

Table 4 Average deviation, thousandths of an inch

Flank	Heel									Toe
	0	1	2	3	4	5	6	7	8	9	10
Concave		0.695	0.486	0.394	0.318	0.277	0.277	0.213	0.267	0.498	
Convex		0.510	0.370	0.339	0.308	0.299	0.359	0.458	0.564	0.750	

After graduating from Northern Illinois University in 2010 with a bachelors' in mechanical engineering, **Brendan Bijonowski** has pursued a career in design. In 2011 he joined the engineering ranks of Arrow Gear Company, located in Downers Grove, IL as a design engineer. His passion for the geometry of gearing and attention to detail can clearly be seen in all of his work. Bijonowski is a member of the AGMA Bevel Gear Committee, where he works on defining geometry and improving rating methods. He is also a member of the AGMA Computer Programming Committee, where he applies his experience and knowledge as a gear engineer to an ever-growing collection of technical software.

Gleason

LAUNCHES NEW MANUFACTURING FACILITY IN INDIA

Gleason Corporation recently announced that it broke ground for a new manufacturing facility in the Bengalaru Aerospace Park Industrial Area located in Bangalore, India to accommodate Gleason's expanding product offerings and capabilities in India.

Gleason has long had a presence in the Indian market, first through representatives and then through Gleason Works (India) Private Limited, established in 1995. Gleason Works India has machine and cutting tool manufacturing operations in Bangalore, a cutting tools service center in Chennai, and sales and service offices in Delhi, Jamshedpur, Mumbai and Pune.

"We continue our belief that the Indian market offers significant near-term and long-term growth opportunities, and we are pleased and excited to take the next step to position Gleason to better serve the Indian market," said John J. Perrotti, president and chief executive officer of Gleason Corporation.

The Bengalaru Aerospace Park is home to many companies serving the aerospace industry. The Gleason facility will produce products and services for aerospace customers as well as markets including automotive, heavy truck, construction, agricultural equipment, energy and others. Phase 1 of the new Gleason Works India facility is planned for completion in the second half of 2016, and includes 50,000 square feet (4,650 SQM) of space for manufacturing, sales, service and administration. The facility will continue the manufacture of Gleason Genesis Gear Hobbing machines, gear cutting tools, workholding equipment, and aftermarket products and services, and will provide the space needed for continued expansion for other products.

ITAMCO

NAMED 2014 AUTODESK INVENTOR OF THE YEAR

The votes are in, and Autodesk customer ITAMCO has been named the Autodesk Inventor of the Year for 2014.

Members from the Autodesk Manufacturing community worldwide selected ITAMCO from among the dozen companies featured as 2014 monthly Autodesk Inventing the Future honorees. For more than eight years, Autodesk has identified innovative customers from among hundreds of thousands of designers and engineers that create using Autodesk manufacturing tools and featured their work via this monthly recognition.

Based in Plymouth, IN, ITAMCO delivers precision-machined components to original equipment manufacturers that serve a wide array of industries — ranging from oil and gas and renewable energy, to mining and construction and aerospace and defense. Autodesk Inventor 3D design software, as part of Autodesk Product Design Suite and Autodesk Factory Design Suite, are among the many tools ITAMCO leverages to better serve its customers.

"We are thrilled and honored to be recognized by the Autodesk Manufacturing community for this award.

It was certainly a team effort." said Joel Neidig, technology manager at ITAMCO.

For ITAMCO, the more precisely a gear is manufactured, the better it will perform, and using Inventor software for design and manufacturing processes makes it possible for the company to manufacture gears to precise sub-micron tolerances at .00004 inches.

This level of precision satisfies even the most demanding customers — such as NASA, which used ITAMCO's gears on the mechanical arm that built the international space station.

Additionally, ITAMCO recently designed, manufactured and built a new gearbox for construction vehicles in record time using Inventor and Autodesk Inventor HSM Pro. The software allowed ITAMCO to verify the assembly for any interference issues prior to manufacturing and to utilize the advanced computer aided manufacturing (CAM) capabilities within Inventor HSM Pro for machining and manufacturing the components.

ITAMCO's operations have also been enhanced by Factory Design Suite, which allows users to digitally optimize a factory layout before it's completed. This digital exploration came in handy when the company ordered a piece of machinery that can produce gears up to 13 feet in diameter and that weigh as much as 80,000 pounds.

The gear grinder arrived in 11 different crates, each weighing more than 20,000 pounds. With Factory Design Suite, the company was able to conduct careful analysis and simulation of the entire machine virtually before physically assembling and installing it on site, preventing costly mistakes and factory layout revisions.

As ITAMCO has continued to expand, the company has used Factory Design Suite to lay out new cells and equipment and make sure it meets industry standards of organization and efficiency across the factory floor.

Drake

RECEIVES AWARDS FROM WEATHERHEAD, NEXTEER

Drake Manufacturing Services Co., LLC of Warren, OH, was recently honored as a first-time recipient of the Weatherhead 100 award by the Weatherhead School of Management at Case Western Reserve University in Northeast Ohio.

For more than 25 years, the Weatherhead School of Management has recognized Northeast Ohio's fastest-growing companies. This award celebrates the spirit of entrepreneurship and recognizes companies that exemplify innovative success. With sales growth at over 200% during the 5-year period, Drake was ranked 36th in this elite group.

"Drake's commitment to technology, innovation, and a global presence has kept us strong while expanding our market share," said Drake CEO Jim Vosmik.

Drake Manufacturing Services Co., LLC is a global designer and builder of production systems for manufacturers of parts with threads. Founded in 1972, Drake helps maximize productivity, improve quality and reduce production costs for a variety of applications in the steering systems, power transmission, speed reducer, cutting tool, ball screw, linear motion, and aerospace industries.

Drake was also recently recognized during an awards presentation at the Nexteer 2014 Indirect Supplier Conference in Saginaw, MI.

The award was presented to Drake for their part played in the successful launch of Nexteer Automotive's K2XX product line for General Motors. A series of Drake GS:TI Internal Thread Grinders were installed at Nexteer's Saginaw facility as dedicated work cells to thread grind EPS ball nuts for this steering program.

Drake has developed a range of machines, software, grinding and milling processes for manufacturers of hydraulic and electric steering components (ball screws, ball nuts, steering racks, and worms). The company offers internal and external grinders as well as rack and thread milling machines to produce each major component in modern steering systems. Drake has also developed special grinding processes for licensees of its proprietary internal return ball nut technology. The patented Drake Internal Return Ball Nut, in use in EPS systems currently, is available for license.

Each Drake machine is delivered with Part Smart programs. Drake provides all software required to make good parts from day one. The operator needs only to input part specific variables into the control to run parts. No customer programming is required and the customer can change from one part to another in minutes.

Drake is a global designer and builder of production systems for manufacturers of parts with threads. Founded in 1972, Drake helps maximize productivity, improve quality and reduce production costs for a variety of applications in the steering systems, power transmission, speed reducer, cutting tool, ball screw, linear motion, and aerospace industries.

Star SU

NAMES RICK FALGIATANO AS VICE PRESIDENT OF CUTTING TOOL SALES

Star SU (Hoffman Estates, IL) recently appointed **Rick Falgiatano** as vice president of sales for its cutting tool division.

Rick brings 35 years of experience in the cutting tool industry, including 20 in sales management roles — most recently as district sales manager for Kennametal (Latrobe, PA). Falgiatano has gained expertise in milling and drilling, as well as managing channel partner distribution, integration and integrated programs.

Falgiatano attended the University of Phoenix in Warrenville, IL, and served as past president and charter board member of the Society of Carbide and Tool Engineers (SCTE) Rockford and Chicago chapters.

Paul Andruszko

PROMOTED TO GENERAL MANAGER OF GEAR MOTIONS NIAGARA

Gear Motions recently promoted Paul Andruszko to general manager of its Niagara Gear division. The division has also earned an International Organization for Standardization (ISO) 9001-2008 Registration.

"The goal of our company has always been to be one of the best precision gear manufacturers," said Bob Barden, former vice president and general manager of Gear Motions Niagara Gear division. "My efforts over the last 35 years have been geared toward maintaining that goal. Paul Andruszko has the talent to drive the company forward. We worked together closely for 26 years, and I'm confident that he will take the company to the next level."

"Over the past few years, Bob Barden and I have been working closely together so that the transition of leadership would be as smooth and seamless as possible," Andruszko said. "I have the knowledge, experience and passion to move this company in a direction that will allow it to reach its fullest potential. My vision for this company is to not only maintain but greatly improve upon the level of growth and success we have experienced in the past. Additionally, the ISO registration will help open doors to new potential customers domestic and abroad."

Niagara Gear's ISO registration demonstrates Gear Motions' commitment to delivering products that meet world-class specifications for quality, safety and efficiency. It ensures that all processes are repeatable and predictable.

"We are very proud to accomplish something not all manufacturers are able to do," Andruszko said. "For us to do it in less than nine months demonstrates the hard work, dedication and commitment of each employee. This certification validates our Quality Management System and procedures, and ensures that every person within the organization is performing his or her role consistently every day."

AMT

REPORTS U.S. CUTTING TOOL CONSUMPTION TOTALS $181.9 MILLION FOR JANUARY

January U.S. cutting tool consumption totaled $181.9 million, according to the U.S. Cutting Tool Institute (USCTI) and The Association for Manufacturing Technology (AMT). This total, as reported by companies participating in the Cutting Tool Market Report (CTMR) collaboration, was down 1.7% from December's total and up 1.9% from January 2014.

These numbers and all data in this report are based on the totals actually reported by the companies participating in the CTMR program. The totals here represent about 80% of the U.S. market for cutting tools.

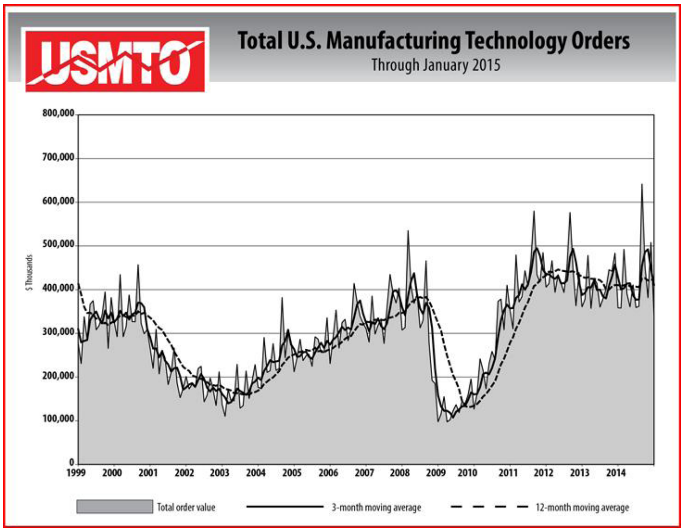

"The industrial production index for manufacturing typically leads cutting tool production by one or two months," said Pat McGibbon, vice president of AMT's strategic analytics department. "January's 1.7% decrease in shipments mirrors December's decline in industrial production. The short lived fall reflected by January's increase in industrial production leaves us optimistic to see positive cutting tool shipment growth in February and March."

The CTMR is jointly compiled by AMT and USCTI, two trade associations representing the development, production and distribution of cutting tool technology and products. It provides a monthly statement on U.S. manufacturers' consumption of the primary consumable in the manufacturing process — the cutting tool. Analysis of cutting tool consumption is a leading indicator of both upturns and downturns in U.S. manufacturing activity, as it is a true measure of actual production levels.

The AMT also reported that January U.S. manufacturing technology orders totaled $341.17 million. This total, as reported by companies participating in the USMTO program, was down 32.9% from December's $508.57 million and down 4.8% when compared with the total of $358.45 million reported for January 2014.

"To understand why we saw this drop in orders for January, December 2014 saw a sharp increase in sales," said Douglas K. Woods, AMT president. "This was driven by many end-of-year orders that had been rushed through in order to qualify for tax rebate provisions that were enacted at the last minute for 2014. This is evidenced by the comparatively lower average order value seen in December vs. January, meaning that most end-of-year orders were for less expensive, in-stock machines that could be shipped quickly. The decline wasn't unexpected, and we still foresee the manufacturing economy keeping on a stable path."

Hydraulic Institute

APPOINTS MICHAEL B. MICHAUD EXECUTIVE DIRECTOR

The Hydraulic Institute recently announced the appointment of **Michael B. Michaud** as the Institute's next executive director, effective May 1.

"On behalf of the entire Board I am very pleased to welcome Michael Michaud as HI's new executive director," said George Harris, chairman of the Hydraulic Institute board and president and CEO of Hydro Inc. "As we approach our 100th anniversary in 2017, this is a very exciting time to be a part of HI and our vision for global growth. Michael's talent and international experience will be invaluable to us as we develop and implement strategies to realize this vision and to continue the growth that we have experienced under the leadership of Bob Asdal and the HI staff."

For the past 19 years, Michaud has held various leadership roles at the American Society of Mechanical Engineers (ASME) where he currently is managing director of global alliances, responsible for ASME's global strategy execution and international business development, primarily by growing a network of global partners. Prior assignments included managing several business areas including ASME's training and professional development portfolio, ASME's gas turbine and petroleum technology institutes as well as outreach and support for ASME's international membership.

"We are fortunate to have found someone like Mike," said John H. White, Hydraulic Institute president and CEO of Taco, Inc. "He brings a unique blend of strategic vision and a solid operational experience and a track record of sustained, global growth. With a relatively new Board-approved policy to admit pump and supplier OEMs outside North America as members, serving the global marketplace will become a bigger focus area for the Institute." Responsible for ASME's global strategy since 2008, Michaud has successfully translated this strategy into a 12% annual growth rate outside the US for ASME."

"This is a fantastic time to join the Hydraulic Institute and I am extremely honored to have been chosen to lead it" said Michaud. "As HI approaches its 100 year anniversary, we are reminded of the past success, creating standards, developing resources for the industry and working to improve pump and pump system efficiency, ultimately producing energy and cost savings for pump users and society at large. I plan to continue to build on this lasting legacy of successful programs and work to position the Hydraulic Institute for its next 100 years."

Michaud will replace Robert Asdal, who will retire on June 30, 2015 after 20 years at the Hyrdraulic Institue.

Junker

ACQUIRES MAJORITY SHARE IN BRAZILIAN GRINDING MACHINE MANUFACTURER

The Junker Group recently added Brazilian grinding machine manufacturer ZEMA to its corporate group.

ZEMA was founded back in 1953, has more than 80 employees and manufactures CNC grinding machines with conventional grinding wheels – up until now mainly for the Brazilian market.

"Now we can fulfill any customer needs, open up additional markets and supply combined production lines (CBN, corundum)." said Junker CEO Rochus Mayer.

Paresh Shah

NAMED OPERATIONS MANAGER OF SCHAFER INDUSTRIES

Schafer Industries recently announced the appointment of **Paresh Shah** as operations manager of the company's gear unit, Schafer Gear Works, in South Bend, IN

Schafer Gear Works has plants in South Bend as well as in Fort Wayne, IN, and Rockford, IL. The company's 108,000-square-foot South Bend location produces high-volume gears for a variety of industrial applications.

Shah came to Schafer Gear Works in 1993 as a gear engineer. In 1995 he was promoted to engineering manager where he managed the engineering group in South Bend and also served as a liaison between both domestic and overseas vendors.

Prior to joining Schafer Gear Works, Shah was senior process engineer for International Gear Corporation in Cleveland, OH.

Shah has a bachelor's degree in mechanical engineering from Birla Vishwakarma Mahavidyalaya in Gujarat, India and a master's in mechanical engineering from New Jersey Institute of Technology.

Edward McTernan

NAMED VICE PRESIDENT OF SALES AND MARKETING AT CLEVELAND GEAR

Cleveland Gear recently named **Edward McTernan** the vice president of sales and marketing.

McTernan was formally product manager for the modular enclosed drives division overseeing all efforts of Modular Gearing Group. He has over 30 years of experience in the power transmission industry and a bachelor of business from John Carroll University.

April 7-9 – Ipsen U Cherry Valley, IL. Ipsen U is a practical course for building and refreshing knowledge of thermal processing equipment. Ipsen U addresses all levels of experience in a casual open-forum environment that encourages attendees to ask questions about specific equipment and processes. The class follows a modular format that allows participants to interact with several Ipsen experts and have their specific questions answered. Ipsen U allows customers direct access to information that transfers furnace maintenance and upkeep into their own hands. Cost of course is $950 per student. Class starts every day at 8:30 a.m. and ends at 4:30 p.m. Breakfast and lunch are provided each day, along with one group dinner. Participants receive an Ipsen U certificate and an Ipsen polo shirt. Reservations are required, as class size is limited. Attendees are responsible for transportation and hotel costs. Reservations are due two weeks prior to start date. For more information, visit *www.ipsenusa.com*.

April 13-17 – Motion, Drive & Automation (MDA) at Hannover Messe Hannover, Germany. MDA showcases the latest power transmission, fluid power and drive technology. Attendees to Hannover Messe 2015 – the world's largest industrial technology event with 10 concurrent trade fairs – will have the opportunity to network, pursue business and see the latest solutions on the international stage. For more information, visit *www.hannovermesse.de* or call (773) 796-4250.

April 20-23 – AeroDef Manufacturing Hilton Anatole, Dallas, TX. New in 2015, AeroDef Manufacturing will take place in Texas, one of the top manufacturing states in the country. The new location offers opportunities to reach a promising new audience for any company. The leading aerospace and defense OEMs have come together to provide direction for AeroDef have and lend insight on what they need from suppliers, discuss their current and future technology investments and plan for developing a skilled workforce. AeroDef attracts high-level attendees with exclusive content developed – and presented – by the leading aerospace and defense OEMs. Speakers, panel discussions and the technical conference are carefully selected to address issues and technologies of strategic importance to the industry. Networking events are held on the floor to encourage meaningful collaboration among presenters, attendees and exhibitors. For more information, visit *www.aerodefevent.com*.

April 29-May 1 – 2015 AGMA/ABMA Annual Meeting The Meritage Resort and Spa, Napa Valley, CA. This year's annual meeting will address the key issues facing manufacturing and offer opportunities to network, make memories, forge relationships and build on future partnerships. Napa Valley provides much to explore and many attendees will bring a spouse or guest. In lieu of the golf tournament, the planning committee opted to keep open the second afternoon for exploration of this unique location. For more information, visit *www.agma.org*.

May 6-7 – Design-2-Part Show Schaumburg Convention Center, Schaumburg, IL. Manufacturers nationwide rely on Design-2-Part Shows as the most efficient place to meet high-quality, reliable American job shops and contract manufacturers. In just a few hours you can find cost effective, quality suppliers, learn about new technologies and materials, see and compare parts and components, and quote jobs and evaluate quality price while getting delivery on the spot. Finding trustworthy contract manufacturers who can provide flexible, cost-effective solutions and scale up growing organizations is critical. There is no better way to identify new outsourcing partners than spending even one half-day at this show. For more information, visit *www.d2p.com*.

May 12-14 - EASTEC Eastern States Exposition, West Springfield, MA. With more than 500 exhibitors, complimentary conference sessions, industry keynotes and much more, EASTEC is an event dedicated to keeping northeast manufacturers competitive. It's where manufacturing ideas, processes and products that make an impact in the northeast region are highlighted through exhibits, education and networking events. The event offers a unique chance to connect with resources that can solve any company's most pressing problems, improve productivity and increase profits. It's clear why so many business owners, engineers, designers, production managers and purchasing executives attend EASTEC to keep their operations current. EASTEC brings human ingenuity and manufacturing brilliance together. For more information, visit *www.easteconline.com*.

May 18-21 – AWEA Windpower 2015 Conference & Exhibition Orange County Convention Center, Orland, FL. Wind energy's premiere industry gathering is a concentration of expertise and innovation that draws thousands of professionals from around the world to trade knowledge, experience and best practices across all industry segments. And in 2015, Windpower will address what you can do now to meet the challenges of today, while preparing for tomorrow. The Windpower 2015 cutting-edge program presents and examines the technical developments and evolving issues that are transforming the industry and increasing the competitiveness of wind power. AWEA has assembled top industry experts for this conference who will present deep-dive sessions on a variety of relevant topics. Targeted tracks provide the opportunity to network, collaborate and advance your tactical understanding in areas that impact you most. For more information, visit *www.windpowerexpo.org*.

June 15-17 – Western Manufacturing Technology Show Edmonton EXPO Centre, Edmonton, Alberta, Canada. True to its name, WMTS targets the specific needs of manufacturers in Western Canada. Ever-evolving technology, unique economic challenges, and the heavy influence of the oil and gas industry present a diverse mix of circumstances—and WMTS is up to the task of meeting them. A showcase of top solution providers, the WMTS has the answers attendees are searching for. Walk the show floor and meet face-to-face with the experts who can explain how applying new methods and advanced technology can improve operations and margins. Leading-edge machine tools, tooling and accessories, fabrication, design, automation, process control, and plant maintenance equipment—it's everything businesses need all under one-roof. Combined with an industry keynote, an interactive town hall panel and limitless opportunities to network and share ideas with like-minded colleagues, WMTS is a complete manufacturing experience that will give attendees the practical knowledge needed to stay competitive in Western Canada. For more information, visit *www.wmts.ca*.

gear TECHNOLOGY

FREE SUBSCRIPTION

You have been selected to receive this FREE sample copy of *Gear Technology,* the world's leading publication on gear design, engineering and manufacturing. Please read through it, and if you like what you see, sign up for a **FREE SUBSCRIPTION** using the form below.

FIND THE EXACT SUBJECTS YOU ARE LOOKING FOR: Subscribers now get access to the 30 years of searchable articles in our online archive.

1

☐ **YES** I want to receive/continue to receive ***Gear Technology*** FREE!

☐ No thank you.

Name:________________________ (print) JobTitle/Position: ____________________

Signature ________________________ (required) Date: ________________

2 E-mail ______________________________

(So we can notify you when the online edition is available)

SAVE a TREE!

☐ I ONLY want the digital edition (e-mail required)

3 Please update your contact information or attach you business card here. (No Staples)

Company Name: ________________________

Address: ________________________

City: ________________________

State/Province: ____________ ZIP+4/Postal Code: ____________

Country: ________________________

Telephone: ____________ Fax:____________

E-mail: ________________________

Website: ________________________

4 What is your primary JOB FUNCTION (check ONLY one)

- ❏ Corporate Executive (B)
- ❏ Manufacturing Production Management (C)
- ❏ Manufacturing Production Department (D)
- ❏ Manufacturing Engineering Management (E)
- ❏ Manufacturing Engineering Department (F)
- ❏ Product Design, R&D Management (H)
- ❏ Product Design, R&D Department (I)
- ❏ Purchasing (L)
- ❏ Marketing, Sales or Communications (M)
- ❏ Quality Control Management (P)
- ❏ Quality Control Department (Q)
- ❏ Other (Please describe) (N) ____________

5 My company's principal product or service is:____________

6 How are YOU involved with gears (check all that apply)?

- ☐ My company MAKES gears (20)
- ☐ My company BUYS gears (22)
- ☐ I DESIGN gears (23)
- ☐ I am a SUPPLIER to the GEAR INDUSTRY (please specify product or service) (24) ____________

Is there a colleague within your company that might benefit from having their own copy of ***Gear Technology*** magazine?

Name: ________________________

Title: ________________________

DIGITAL SUBSCRIPTIONS

- ❏ **YES,** I want to be notified each issue when ***Gear Technology*** is available online
- ❏ **YES,** I would like to receive ***Gear Technology's*** monthly e-mail newsletter
- ❏ **YES,** I would like to receive ***Gear Technology's*** twice monthly e-mail Product Alerts
- ❏ **YES,** I would like to receive 3rd-party e-mails from ***Gear Technology's*** advertisers and partners
- ❏ **YES,** I would like to receive subscription renewal notices by e-mail
- ❏ **No,** I do not wish to be contacted by e-mail.

FAX TO 1-847-437-6618 or VISIT US ONLINE AT ***www.geartechnology.com/subscribe.htm***

How Do You Say 'Gears' in Italian?

Erik Schmidt, Assistant Editor

It was late November in Northern Italy, and everything was coming up vinegar oil and high-performance cars for Cory Sanderson and the 11 other members of his Yankee armada.

They sat around a rustic table in scenic Tuscany (or was it Emilia-Romagna? Or Lombardy? Any which way, it was a breathtaking and bountiful land), enjoying heaping plates of antipasto and primo and secondo and contorno…

Sanderson, Koepfer America's VP of marketing and sales, doesn't recall the exact name of the ristorante — all those elegant, fine dining establishments in *Settentrione* look alike, anyway — but he does know what it wasn't called.

"It was a lot better than going to a Maggiano's, that's for sure," he said.

And, for the better part of a week, so went Koepfer America's Italian Gear Tour, which roared back to life on Nov. 16, 2014 after a roughly seven-year dormancy for what Sanderson blamed on "economic issues."

The trip's return was not met with as much fanfare as, let's say, Michael Jordan reappearing at the United Center wearing that anomalous No. 45 jersey after his ill-fated baseball sabbatical, but it was still a welcome breath of fresh air in an industry that occasionally gets stuffy — a rare chance to mix in a tiny bit of pleasure with the overabundance of business.

"It's always been the concept of this trip to expose people to the culture of the country," Sanderson said. "We try to visit a major landmark or a major city. We try to do a couple museums that are significant in some way. And then we always try to do something that you can only do in that part of the world.

"So, for Italy, there are a lot of unique things, actually. They've got a lot going on for them."

For starters, they have gears.

The collection of industry professionals on the tour — which included members from C.L.C. S.r.l., Gear Machinery Resources, Forest City Gear, New World Technology, Ontario Drive & Gear and Timron Precision Gear, Inc. — visited several renowned gear manufactures, including Corradini Giacomo Gears and OMIG Ingranaggi, to get briefed on the latest Italian products primed to hit the North American market.

Once they got the meat and potatoes of the trip out of the way, the group got to enjoy the vast luxuries and spoils of the Italian ethos, which included sightseeing in Florence, wine tasting in the Tuscany countryside and a special visit to one of Italy's largest producers of balsamic vinegar. After all, you can't put a bevel gear on a slab of Parmigiano Reggiano.

As Sanderson described the three different levels of balsamic they tried:

"Good, better and mind blowing."

Then, since "it was kind of on the way," the group stopped by the Museo Ferrari, because anytime you get the chance to test-drive a $200,000 supercar you have to throw your trip itinerary right out the window.

Norbert Benik (Ontario Drive & Gear), Roberto Cervi (C.L.C. S.r.l.), Claudio Montanari (C.L.C. S.r.l.), Warren MacRae (New World Technologies), Richard Reenan (Gear Machinery Resources), Gene Fann (Forest City Gear), Jared Lyford (Forest City Gear), Jim Fritz (Timron Precision Gear, Inc.), Cory Sanderson (Koepfer America, LLC), Kevin Corpe (Koepfer America, LLC).

"Just to be in the city of [Maranello, Enzo Ferrari's hometown] was incredible," Sanderson said. "As we're coming into the city we're on the bus and we're just getting passed left and right by Ferraris. Obviously they have a very distinct sound, especially when they're passing you.

"They had a stand next to the museum where you could rent a vehicle for different increments of time, and we had a couple people do that. So that was fun and everyone came back with gigantic smiles on their faces, as you might imagine.

"And then we hit Lamborghini, because if you're going to do one you might as well do the other."

Oh, sure. *When in Rome, right*? Well, at least when you're 350 kilometers north of Rome.

Though Sanderson — the trip's organizer and host — said he was fairly stressed out making sure nobody in his party wandered off the Matterhorn or got attacked by a bent-winged bat, it would also seem he took a rather laissez faire (pardon my French, *lasciare*) approach to tour guiding.

To Sanderson's credit, this is precisely the right way to travel, especially when flanked by hard working, clock-punching industry executives who rarely have the time or opportunity to venture outside of the office.

He was also able to answer an age-old riddle: How do you turn a group of American sophisticates into fun-loving, Ferrari-driving Italians?

Just land in Florence and add balsamic.

"It could have been a little bit more relaxed if it was pure pleasure, but I think the balance we ended up with was really good," Sanderson said. "We saw a lot of different things and ultimately nobody complained. As soon as we got back to Chicago and parted ways everyone was gracious and thankful.

"They were happy they could be a part of it."

Apparently the trip was such a hit that Koepfer is going to do it again in the fall of 2015, this time traveling to Italy *and* Germany.

Oh Dio.

Wait until Sanderson gets a load of a Ferrari on the Autobahn.